Neural Oscillations Underlying Behavior:

Adjustments after Commission Errors and

Temporal Judgements

by

Tara van Viegen

A thesis submitted to the University of Birmingham

for the degree of

DOCTOR OF PHILOSOPHY

School of Psychology
College of Life and Environmental Sciences
University of Birmingham
November 2018

Abstract

The current thesis aimed to: 1) explore whether alpha peak frequency (APF) as measured with electroencephalography (EEG) might be indicative of an internal clock. No systematic relationship between APF and temporal decision making was found, which suggests that a straightforward interpretation of APF reflecting the brain's internal clock is too simplistic. 2) examine the role of oscillatory power on performance monitoring and temporal decision making. We found no evidence that medial frontal cortex used oscillatory power to influence subsequent processing in down-stream regions after an error was committed. Instead, we found phase-based connectivity after an error although the implications on behavioral adjustments remain unexplored. In the temporal decision making experiments we found increased theta power in correct compared to incorrect judgements after the short time interval had elapsed, which might suggest that theta power reflects evidence accumulation of temporal information. 3) examine the role of climbing neural activity in temporal decision making as reflected by slow evoked potentials (SEPs) in the EEG. No consistent evidence across the different experiments was observed, which suggests that SEPs do not reflect temporal evidence accumulation in the current time estimation task and differences are instead reflected in theta power differences.

DEDICATION

This thesis is dedicated to my grandparents:

Judith & Piet Nelissen and Joke van Doornik.

I wish you could see me now.

ACKNOWLEDGEMENTS

therefore would like to thank everyone at Creation Climbing Centre, especially James. And some of my climbing buddies: Giulio Degano, Isotta Rigoni, Cory Knapp, Matt & Steve.

I would also like to thank everyone in Birmingham and Amsterdam that helped my thesis into existence through friendship and support. I am thinking of Jorrit Makkinga, Sterre Boerkamp, Myrte Beltman, Sam Prinssen. And Sourour & Wesley Trevelyan, Natalie Kelly & Dagmar Fraser. Special thanks to Leo for help and support.

I would like to thank my parents, Ronald and Monique van Viegen. Thank you for believing in me. Thank you for your unwavering support. Thank you for understanding. Thank you.

Finally, I would like to thank Steffen Bürgers and Judo van Viegen. Your support has meant so much to me. I look forward to our many (climbing) adventures together. You are my chosen family and you make me very proud. Judo, ik hoop dat je ooit kunt begrijpen hoe belangrijk je voor me bent en hoe je mijn leven zin hebt gegeven. Steffen, it is an honour to go through life with you by my side. You make me feel incredibly happy and lucky. Ik hou heel veel van jullie allebei.

TABLE OF CONTENTS

LIST OF FIGURES

LIST OF TABLES

CHAPTER 1

GENERAL INTRODUCTION

Our every day is filled with decisions and evidence-accumulation. Sometimes, decisions are made about time intervals, and evidence is accumulated on passing time, for example when waiting for a traffic light to switch from red to green. Decision making is thought to rely on the accumulation of noisy sensory evidence. After enough noisy evidence has accumulated a decision boundary is reached and motor behavior might ensue as a result of the decision-making process. In this thesis I aim to examine whether similar neural mechanisms underlie temporal and non-temporal decision making. More specifically, I will explore the role of neural oscillations and event related potentials as measured with electroencephalography (EEG) in temporal evidence accumulation and in the termination of automated behavior.

Drift diffusion models have extensively been used to explain decision making processes (Ratcliff, 1978; 2001; Ratcliff & McKoon, 2008; Ratcliff & Rouder, 1998; Ratcliff et al., 2016; Smith & Ratcliff, 2004). More recently, these models have been used to explain temporal decision making (Balci & Simen, 2016; Simen et al., 2011, Simen et al., 2013). These modelling approaches suggest there might be shared neural mechanisms between temporal and non-temporal decision making, but research in this field is lacking. Interestingly, the medial prefrontal cortex has been linked to inhibitory and cognitive control (e.g. Ridderinkhof et al., 2004) and the same region might play a role in temporal evidence accumulation (Petter et al., 2016). Especially theta (4-7 Hz) oscillations have been hypothesized to play an important role in inhibitory and cognitive control (Cavanagh &

Frank, 2014) as well as in interval timing (Parker et al., 2014; Heskje et al., 2019). I aim to further establish the role of theta activity from the medial prefrontal cortex in terminating automated behavior by examining the relationship between single-trial activity from this region and behavioral adjustments that followed when automated behavior was not properly terminated. Next, I ask whether this termination process is related to the termination of temporal evidence accumulation. To do this, I will examine how temporal evidence accumulation differs when participants reach different response boundaries (i.e. correct and incorrect responses) in a temporal discrimination task.

To introduce the topics of this thesis to the reader, the general introduction is divided into three overarching topics: 1) time estimation, 2) decision making and 3) neural signatures. The general introduction starts with a historical overview of computational models that aim to explain time perception. This overview is followed by a brief discussion of different experimental designs to study time perception. Then, I discuss computational models of decision making. Next, I hone in on drift diffusion models and how these computational models might be related to temporal and non-temporal decision making. After discussing the computational models I move on to discuss neural implementations of these computational models. To this end, I first discuss evidence for decision making based on ramping neural activity and then oscillatory activity. Finally, I briefly discuss how the evidence from oscillatory activity has inspired new computational models of time perception, which brings me back to the discussion of (recent) computational models of time perception. Finally, I conclude the introduction with the aims of the different empirical chapters.

Historic overview of timing models

Pacemaker-accumulator models

Pacemaker-accumulator models are the first attempt of a mathematical model to describe participants' behavior at discriminating intervals of slightly different duration (Merchant & delaFuente, 2014, chapter 3 by Hass & Durstewitz). In these models, pulses are emitted at short intervals such that the pacemaker has a regular average frequency and the pulses are accumulated to represent a value for the time that has passed (Creelman, 1960). In Creelman's study participants performed a forced choice paradigm, where on each trial two intervals were presented in sequence and participants reported which interval was longer. The original paper of Creelman uses signal detection theory (SDT) to explain how errors arise: a time interval T is compared to T+ΔT and both intervals are represented by the number of pulses accumulated after their respective intervals (Figure 1.1). The representation can only be perfect if an observer is capable of detecting the exact on- and offset of the different intervals and if they accurately store the amount of pulses in working memory, which they can retrieve again after they have accumulated the pulses of the second interval (Creelman, 1960). Creelman acknowledged that an observer is unlikely to do this perfectly and therefore, the representations of both intervals will overlap, especially with smaller values of ΔT (Figure 1.1).
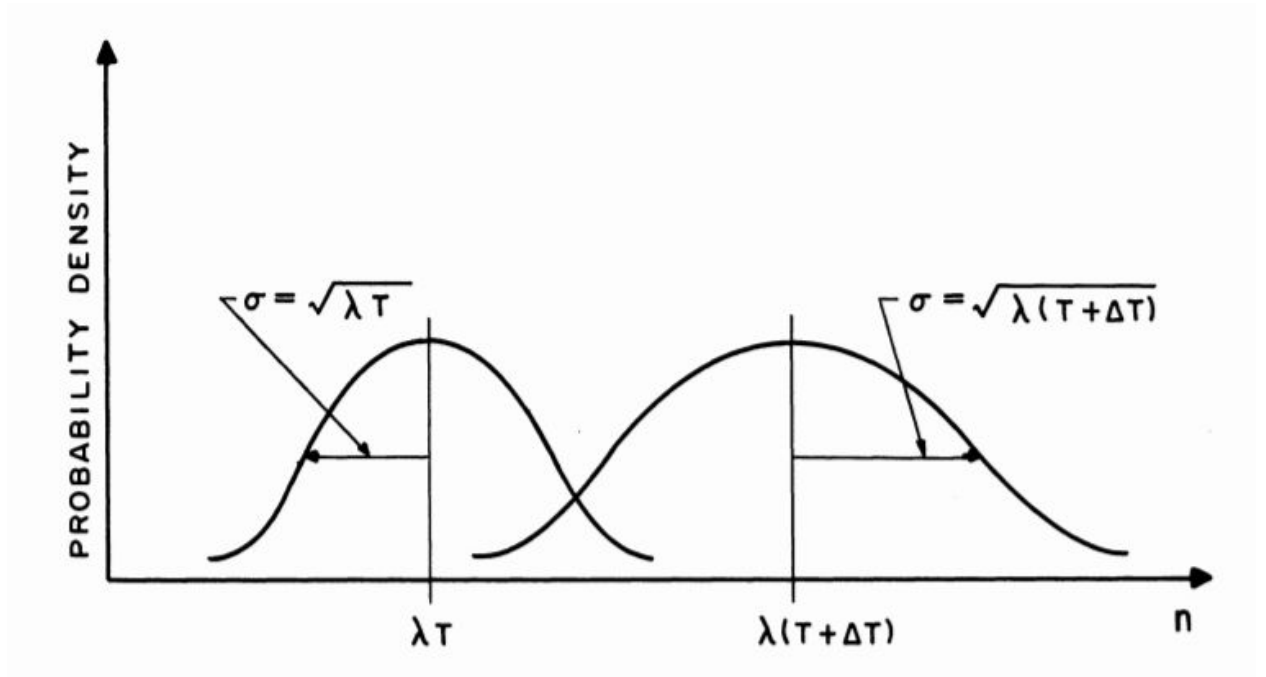
Figure 1.1. Signal detection theoretic explanation for forced choice time interval discrimination by Creelman (1960). Time interval T and T+ΔT are compared by the participants, who needs to report which of the intervals is longer. The intervals are represented by a normal distribution with a mean and variance equal to λT. λ represents the rate of the pacemaker. Taken from Creelman, 1960.

Mathematically, Creelman explained that an interval of j ms can be represented as a normal distribution with mean and variance of λj. λ is a constant that represents the frequency of the pacemaker. Longer intervals, T+ΔT, also have larger means and variance and the larger variance contributes to a wider normal distribution. For each trial the difference between the representations can be calculated:

$$d'_{1,2} = \sqrt{2\lambda} \frac{\Delta T}{\sqrt{2T+\Delta T}} \qquad (1)$$

The pacemaker in the model proposed by Creelman described above was hypothesized to function at a mean frequency following a Poisson process (this Poisson process is approximated by a normal distribution when λT is large).

An alternative model was proposed by Treisman (1963) that contained a pacemaker that was deterministic, an oscillator, where the frequency of the pacemaker was thought to represent arousal. Treisman argued that it would be easier to keep track of time with a deterministic accumulator (Treisman, 2013). Moreover, he noted that neural pacemakers had been described. He also noted that oscillations of various frequencies could be observed in the electroencephalogram (EEG) and that heartbeat and respiration were inherently rhythmic as well. Treisman provided his pacemaker-accumulator with a hierarchical structure that consisted of a counter, comparator and store (Figure 1.2). The comparator of Treisman's model is a decision process that, just as Creelman's model, follows signal detection theory (Treisman, 2013). Therefore, the most important difference between Creelman's and Treisman's models discussed thus far is the stochastic vs. deterministic functioning of the pacemaker, and, to some extent, the flexibility of the pacemaker.
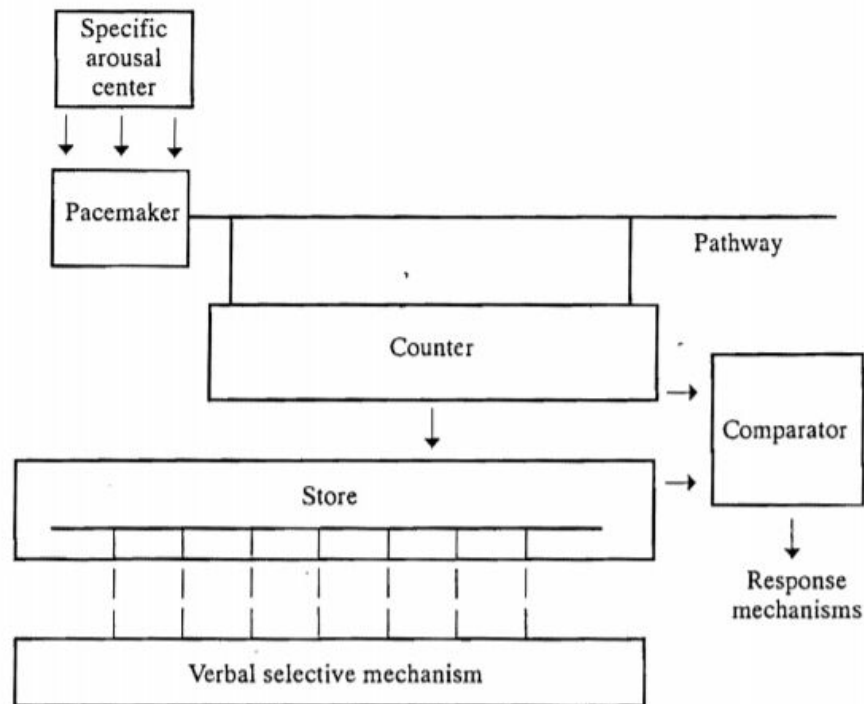
Figure 1.2. Treisman's model of the internal clock. Taken from Treisman, 1963 and Block & Zakay, 1996.

Scalar Expectancy Theory

One influential variant of the pacemaker-accumulator models is the Scalar Expectancy Theory (SET, Gibbon, 1977). SET has gained a lot of traction, because it explains the scalar property of time perception, i.e. Weber's law (Hass & Durstewitz, 2014). Weber's law is well known in psychophysics and sensory perception and it suggests that the discriminability between two events is linearly related to the magnitude of the standard stimulus (Getty, 1975; Grondin, 2001). Mathematically, this can be written as: $\Delta\phi = K\phi$, where $\Delta\phi$ is the difference threshold, ϕ is the standard stimulus and K is the Weber fraction (Grondin, 2001). The generalized form of Weber's law, $\Delta\phi = K\phi + a$, also takes into account a as a source of sensory noise, which interferes with the temporal

discrimination. Weber's law can also be represented by a constant coefficient of variation (σ/μ), where variability is proportional to the mean (Allan, 1998). Another law that applies to time perception is the Psychophysical Law, which states that there is a power relationship between real, elapsed time and subjectively, experienced time (Allan, 1998; Grondin, 2001). The exponent of this power law has been calculated for many different experiments and has been found to vary between 0.9 and 1.1 (Grondin, 2001; Allan, 1998). Note that a power law with an exponent of 1 would lead to linear time, where the physical time would correspond directly with psychological time. One important observation that time is experienced nonlinearly comes from time bisection tasks (Staddon & Higa, 1999). In time bisection tasks, participants are trained on two standard intervals, one short and one long in duration. When participants are well able to distinguish between the standard intervals, participants are presented with intermediate intervals and participants decide for each interval whether it is more similar to the short (T_s) or the long (T_l) standard. This method allows the experimenter to find the indifference interval (T_p, i.e. bisection point) for a participant. When the indifference interval is presented, the participant is equally likely to report that the interval is similar to the short and the long interval. Participants often have their indifference interval close to the geometric mean of the short and long interval: $T_p = (T_s \cdot T_l)^{1/2}$. Interestingly, scalar timing would predict the indifference interval at the harmonic mean: $T_p = \frac{2T_s \cdot T_l}{T_s + T_l}$. Finally, linear time would predict the indifference interval at the arithmetic mean.

SET is hypothesized to consist of three modules in the form of a clock, memory and decision process. The clock functions in a similar fashion to the pacemaker-accumulator proposed by Treisman: a Poisson process of successive pulses forms the pacemaker

(Grondin, 2001). In addition to the pacemaker the clock consists of a switch, which is flipped by external information to start the interval timer (the pacemaker), and an accumulator, which sums the pulses of the pacemaker. After the clock module, the memory module is reached. This memory module consists of working memory and reference memory. The output from the accumulator is temporarily stored in working memory and the value is compared to the reference memory. The reference module contains long term stores of several, different (interval) lengths. The output of the memory module is fed into the decision module. The decision module is thought to apply a decision rule based on a ratio comparison of the pulses in working memory and the pulses in reference memory. However, which decision rule is applied depends on the task (Allan, 1998). It is the decision module where overt behavior is produced based on the outcome of the decision rule (Wearden, 1999). Wearden formulated the decision rule for comparing a standard or reference tone to tones that could be short, longer or of the same length as the reference tone as follows:

$$|s^* - t|/t < b^* \qquad (2)$$

where s^* is the sample from the reference memory, t is the presented tone and b^* is the threshold value, which varies from trial to trial.

Experiments to study time perception

A lot of different experiments have been designed to study human time perception, starting with the difference between prospective and retrospective time estimation. In prospective

interval timing tasks participants are aware that they have to report durations of time before exposure to the time interval. Previous work has found that these tasks are better explained by attentional processes (Block & Zakay, 1997; Zakay & Block, 2004). Retrospective timing tasks are tasks where participants do not beforehand know that they have to report the time interval. These tasks have been found to rely on working memory processes (Block & Zakay, 1997; Zakay & Block, 2004). In both retro- and prospective timing tasks duration estimation and reproduction of the time interval can be used. Prospective timing tasks are much more common in the time estimation literature (Grondin, 2014), partially because these tasks can also use production tasks and interval comparison tasks.

In temporal production tasks, participants are instructed to produce intervals of a certain length (e.g. 0.5 or 8 s). The interval can be delineated by the participant with two button presses (at the start and end of the time interval), or the interval starts with a sound or the display of a visual stimulus and the participant only uses a button press to end the elapsed time interval. In synchronization tasks participants need to synchronize their response to a second stimulus that delineates a time interval, or participants need to produce a response in the same frequency (i.e. if the interstimulus interval —the time between the first and second stimulus— is 0.8 s participants should press the button 0.8 s after the second stimulus). A special case of a synchronization task is the rhythmic tapping task where participants tap in beat with e.g. a metronome and participants continue the beat after the metronome has stopped.

In temporal discrimination tasks participants discriminate between intervals. The comparison method presents two durations sequentially and participants decide whether

the intervals are the same or different. The experimenter can keep one interval duration fixed, i.e. the standard, or she can vary both intervals. In the single stimulus task, participants are presented with an interval that is either the short or the long standard duration and participants respond by judging the stimulus as short or long. Especially interval comparison tasks, such as time bisection tasks which I introduced earlier, are powerful tools as they allow two alternative forced choice designs and estimation of psychometric functions. The experimenter can plot the probability the participant responded long as a function of the presented time intervals. This procedure leads to an S-shaped curve and the bisection point is the point where 50% of intervals are classified as long.

Models of decision making

Irrespective of the timing task used, participants make a decision to e.g. classify a time interval as long or short, or to end a production trial by pressing or releasing a button. When the decision is made between two response options, sequential sampling models allow integration of both accuracy and response times into a single theoretical framework (Ratcliff & Smith, 2004). Note that this differs from SDT discusses earlier, because SDT only takes accuracy into account (Green & Swets, 1966; Ratcliff & Smith, 2004). Sequential sampling models assume that the decision process consists of sequential samples of the stimulus, because the stimulus is presented in a noisy fashion by the brain. To reach a decision, a critical amount of evidence needs to be accumulated. This decision bound determines which of the two possible decisions are made and the time it takes to reach the decision is reflected in the response time (Ratcliff & Smith, 2004). Sequential

sampling models predict that response times are longer and accuracy is lower for stimuli that are more difficult to distinguish (Ratcliff & Smith, 2004). Different sequential sampling models exists and they distinguish themselves (among other ways) in the application of the stopping rule. The stopping rule can be absolute, where one response option needs to reach a certain threshold, or relative, where one response option needs to accrue more evidence than the other.

Sequential Sampling Models

- Relative Stopping Rule: Random Walk Models
  - Discrete Time & Varying Amounts of Evidence: Random Walk Models
  - Continuous Time & Varying Amounts of Evidence: Diffusion Models
    - Decay in Drift as a Function of Distance from Starting Point: Ornstein Uhlenbeck Model
    - Drift is Constant as a Function of Time and Distance from Starting Point: Wiener Diffusion Model
- Absolute Stopping Rule: Recruitment Models
  - Discrete Time & Varying Amounts of Evidence: Accumulator Model
  - Continuous Time & Varying Amounts of Evidence: Poisson Counter Model

Figure 1.3. Taxonomy of sequential sampling models. Reproduced from Ratcliff & Smith, 2004.

Random Walk Models

Random walk models fall under the class of models that apply a relative stopping rule (Ratcliff & Smith, 2004), such that evidence in favor of one response option is evidence against the other response option. In its simplest form, signal accumulation would be completely random, e.g. like white noise, where all evidence sampling would be independent: $X_t = \varepsilon_t$, where X_t captures the value of the evidence at time t and ε

captures a random value from e.g. a Gaussian distribution. However, it is more likely that biological systems are represented by models that take into account the accrued evidence, i.e. a random walk, a running sum of independent observations such that: $X_t = \sum\limits_{s=1}^{t} \varepsilon_s$, which can be written as: $X_t = X_{t-1} + \varepsilon_t$ (Wagenmakers et al., 2004). These decision models are often compared to a drunkard that has an equal probability of walking (or swaying) left or right. This comparison can be further extended by adding drift to the drunkard's behavior, e.g. when he is missing his right shoe. An important limitation of random walk models is that they cannot explain the often-observed response time effect for error responses: errors have shorter response times than correct responses.

Drift Diffusion Models

Diffusion models are a type of sequential sampling model that stems from the class of random walk models. Earlier I pointed out that sequential sampling models and SDT differ, because SDT only takes accuracy and not response time into account. However, diffusion models can be seen as an extension of SDT, where a step in the accumulation process can be seen as a sample from one of the distributions that are described in SDT (the bell shaped curves in Figure 1.1; Mulder et al., 2014). In diffusion models evidence is accrued continuously over time (Ratcliff, 1978; Ratcliff & Smith, 2004), rather than in discrete time steps. Evidence is accumulated from a starting point, z, and the accumulation will continue until a response boundary is reached (Figure 1.4). The starting point reflects the participant's preference for one response option over the other (Forstmann et al., 2016). The response boundary can be negative or positive (Ratcliff & Rouder, 1998). The total

time needed to come to a response consists of some fixed encoding time, plus the time it takes to reach one of the response boundaries from the starting point, plus a fixed response execution time (Forstmann et al., 2016). The slope of the evidence accumulation, i.e. the amount of evidence that is accumulated per unit time is known as the drift rate, ξ (Ratcliff & Smith, 2004) also known as v (Ratcliff & Rouder, 1998). The drift rate is dependent on the quality of the information coming from the stimulus (Philiastides et al., 2006), on attention (Bogacz et al., 2006) or on subject abilities (Forstmann et al., 2016). Figure 1.4 shows that the drift rate is not fixed over time, but instead varies. Importantly, both SDT and DDM aim to separate which parts of the decision making process are under strategic control, i.e. the criterion in SDT and the distance between the boundaries and where the starting point is in drift diffusion models, versus parts of the decision making process which are not under strategic control, i.e. d' in SDT and drift rate in DDM (Forstmann et al., 2016). The variability of the drift is assumed to be normally distributed (Ratcliff & Rouder, 1998). The within-trial variance in drift rate is known as the diffusion coefficient, s^2 (Ratcliff & Smith, 2004) and is a model parameter in the form of the standard deviation, s (Ratcliff & Rouder, 1998). If the variability is large enough, the accumulated evidence can cross the response boundary of the other stimulus, leading to an erroneous response. Drift rate also varies over trials, captured by another model parameter, η, represents variability, which is hypothesized to be normally distributed (Ratcliff & Rouder, 1998). For example, identical stimuli might be better attended on one trial than on another, which changes the drift rate over trials.
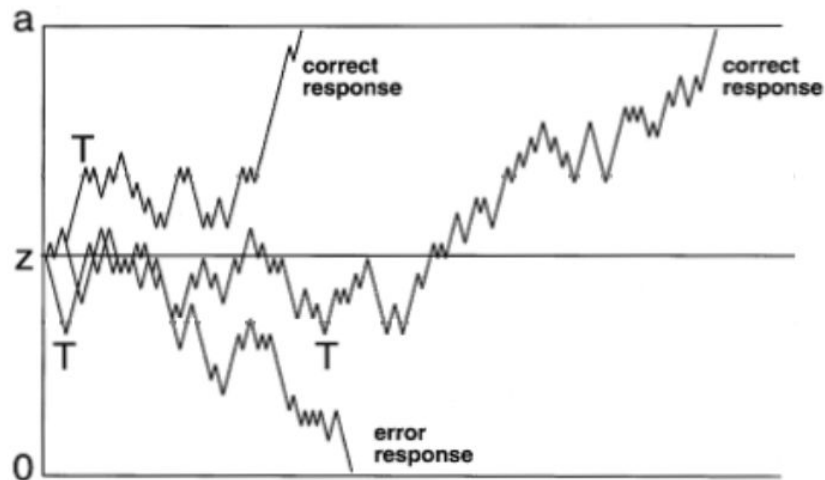
Figure 1.4. Drift diffusion model. Evidence accumulation starts at z and follows a random walk with evidence being updated continuously. The accumulated evidence can reach the response boundary at a, yielding a correct response, or the response boundary at 0, yielding an error response. Three different observations are illustrated by T. Adapted from Ratcliff & Rouder, 1998.

If participants move their response boundaries away from their starting points, they will be more accurate, because the accumulated evidence is less likely to cross the response threshold of the opposite response boundary by chance. But this strategy will also increase response times (Ratcliff & Smith, 2004; Forstmann et al., 2016). As such, boundary separation reflects the speed-accuracy trade-off the participant is currently performing at (Forstmann et al., 2016). It is important to note that stimuli that have a large, positive drift rate are less likely to reach the opposite decision boundary, whereas stimuli that have an intermediate drift rate are more likely to reach the opposite decision boundary by mistake (Ratcliff & Rouder, 1998). Stimuli with large, positive drift rates are easy to detect and these stimuli lead to relatively short response times and a lot of accurate responses,

whereas stimuli with intermediate drift rates are difficult and they will have longer response times and more error responses (Ratcliff & Rouder, 1998). Examples might be where the different intensities of a visual stimulus are presented – the more intense stimulus provides more evidence, and the drift is more rapid towards the detection boundary. Note that different drift rates also bias the model to predict slower response times for erroneous responses. Therefore, in order to account for erroneous response times that are shorter than correct response times, the starting point of the model needs to be able to vary on a trial-by-trial basis or as a function of strategy (Ratcliff & Rouder, 1998; Ratcliff & Smith, 2004).

Ornstein-Uhlenbeck model

The Ornstein-Uhlenbeck (OU) model is similar to the drift diffusion model described above (see Figure 1.3). However, the OU model has an extra parameter β, or λ, which represents the decay of evidence accumulation over time where the accumulation is falling back to the starting point (Ratcliff & Smith, 2004). Bogacz et al. (2006) showed that for the drift diffusion model:

$$dx = Adt + cdW \qquad (3)$$

where $x(0) = x_0$ and dx denotes the change in x for a small time interval dt. In this case the drift rate is represented by A and W represents white noise. Whereas for the OU model: $dx = (\lambda x + A)dt + cdW$, where λ is a parameter that accelerates or decelerates x to a response boundary depending on its sign (Bogacz et al., 2006). When λ is set to 0, the

OU model and the Wiener drift diffusion model, where the rate of accumulated evidence is constant, become interchangeable (Ratcliff & Smith, 2004). Champions of the OU model have argued that this model is superior over the Wiener drift diffusion model, because the decay term might be more neurally plausible (Usher & McClelland, 2001). Neural firing rates of single cells saturate as a function of stimulus intensity and when the stimulus is removed the firing rate decreases (Ratcliff & Smith, 2004).

Accumulator model

The accumulator model has a long history in the sequential sampling models, but it was shown in 2004 by Ratcliff & Smith that the accumulator model cannot account for very fast errors that are sometimes observed in decision making tasks (Brown & Heathcote, 2008). The linear ballistic accumulator uses linear, independent response accumulators to explain patterns in response time distributions (Brown & Heathcote, 2008). The "leaky competing accumulator" model was proposed by Usher & McClelland (2001), which consisted of an accumulator process that fluctuated from trial-to-trial due to random variability in both the starting point and drift rate (Brown & Heathcote, 2008). In addition to these two sources of random variability, Usher & McClelland also added two non-linear processes to the evidence accumulation, namely passive decay of evidence as a function of time and response competition, such that evidence for one response boundary is negative evidence for the other response boundary (Brown & Heathcote, 2008). More recently, these additions to evidence accumulation were further simplified when Brown & Heathcote (2008) suggested that they could explain response times on perceptual decision making tasks without the non-linear processes.

Drift diffusion model for interval timing

Thus far, I have explored the models historically bound to time estimation, such as pacemaker-accumulator models and SET. But time estimation, and interval timing in particular, has been linked to drift diffusion models that were designed to explain decision making. In 2011 Rivest & Bengio extended the drift diffusion model with a learning rule, which allowed rapid learning to generalize to new time intervals. The authors hypothesized that ramping neural activity is used to predict when a reward will be received in time, such that the animal will respond (e.g. start licking) when it has accumulated enough evidence that a reward is about to occur (Rivest & Bengio, 2011).

In the same year, another group independently linked drift diffusion models to time estimation (Simen et al., 2011). To account for time scale invariance of time estimation time-related DDMs assume that the drift-diffusion process consists of the sum of two opposing Poisson processes (Balci & Simen, 2016). The time-related DDM assumes that: i) interspike intervals are exponentially distributed with rate parameter λ, ii) the spike times of different pacemaker neurons are independent, iii) neural integrators sum spikes over time and iv) inhibitory and excitatory input to the accumulator are proportional (i.e. the opposing Poisson processes; Balci & Simen, 2016; Simen et al., 2011). The general DDM equation in 3 can be rewritten to (Balci & Simen, 2016; Simen et al., 2011, Simen et al., 2013):

$$dx = (1 - \gamma)\lambda \cdot dt + \sqrt{((1 + \gamma)\lambda)} \cdot dW$$

To explain interval timing with the drift diffusion model a two-stage model is proposed (see also Morita et al., 2019): the first stage uses evidence accumulation to explain time estimation and the second stage uses the traditional drift diffusion process to explain the decision process (Balci & Simen, 2016; Simen et al., 2011, Simen et al., 2013). The first stage might be implemented by ramping neural activity as measured with the contingent negative variation (CNV; see below), which should scale with the length of the to-be-timed interval. The second stage might be implemented through ramping activity that is related to the decision process as measured with the centroparietal positivity (CPP; see below).

Drift diffusion models and Go/No-go tasks

The models of decision making discussed so far are applicable to typical tasks of decision making, which use a two-choice procedure. In these tasks a stimulus is presented and the participant decides whether this stimulus belongs to category A or B. In other decision making tasks participants respond to a Go stimulus and withhold responses to a No-go stimulus. These so-called Go/No-go tasks exist in different variants. Interestingly, participants sometimes perform better on Go responses (i.e. shorter response times and higher accuracy) than on corresponding responses on the two-choice task (Gomez et al., 2007). Donders (1868/1969) first tried to explain the difference between these responses through a simple additive formula: the response time of the two-choice procedure is longer than the go/no-go procedure due to response selection. However, many researchers have since argued that the go/no-go procedure also includes a response selection when participants decide to respond or rather to withhold that response (e.g. Ulrich et al., 1999).

Participant's performance is often measured as the amount of commission errors made, i.e. when participants responded to a No-go stimulus where they should have withheld their response. Commission errors are thought to provide a handle on inhibitory control and as such, Go/No-go tasks have been used in clinical settings to assess inhibitory control in patient populations (e.g. in ADHD, autism, bipolar disorder, schizophrenia and mild traumatic brain injury; Ratcliff et al., 2018). However, response times and accuracy alone do not always provide a satisfactory explanation of behavior. Fast responses on Go stimuli are indicative of efficient processing (Ratcliff et al., 2018), but this behavior is often seen in combination with higher rates for commission errors. High accuracy on No-go stimuli, on the other hand, is often seen together with slow response times to Go stimuli. Sequential sampling models can combine response times and accuracy into a single decision process (Ratcliff et al., 2018), which might make it easier to identify optimal performance on a go/no-go task.

When modeling Go/No-go data with a DDM the withhold response threshold is best modelled with an implicit boundary, i.e. the DDM only has an explicit boundary for Go responses and an implicit boundary for No-go responses (Gomez et al., 2007). Gomez and colleagues (2007) found that the DDM with an implicit boundary was a better fit to the data than the single decision boundary DDM. Because participants should not respond to the No-go stimulus (and because participants sometimes fail to respond to go stimuli, i.e. misses), the choice probability data is fit without the response time distributions of the no-go responses. Gomez et al. (2007) used a combination of two-choice and go/no-go procedures with lexical decision making to examine the claim that the go/no-go task is more suited to study cognitive processes than two-choice tasks in the context of lexical

decision making. If anything, Gomez et al. (2007) found evidence for the opposite: two-choice tasks provide richer data, because of the response time distributions for both decision boundaries. However, Gomez et al. (2007) did find that go/no-go data can be fitted with DDM.

More recently, Ratcliff et al. (2018) showed that accuracy and response time distributions of go/no-go procedures can also be approximated with DDMs without collecting data on a two-choice procedure in the same participants (as Gomez and colleagues did in 2007). As in Gomez et al. (2007), Ratcliff and colleagues (2018) used only the choice probabilities and not the response times for no-go responses (i.e. correct rejections and misses). Both studies found similar results: the Go/No-go data was better explained by an implicit No-go boundary than by a single boundary model (Ractliff et al., 2018; Gomez et al., 2007). This suggests that Go/No-go data is more complex than the simple additive formula Donders proposed.

SART and sequential sampling models

A special case of the Go/No-go task is the sustained attention to response task (SART). In the standard version of this task participants need to press a button in response to the presentation of non-target numbers (Robertson et al., 1997). When the target number "3" is presented participants need to withhold their response. Different versions of the task exist, such as the $SART_{FIXED}$ where the trials are constantly presented in the same order (cycling through 1-9) and the upcoming target can be easily predicted. Or the $SART_{RANDOM}$ where presentation of the digits is random. Other variations concern the length of the inter-trial interval, which can be fixed or random. Finally, the task may use different stimuli

rather than digits. Regardless of these task differences, a typical response pattern can be observed where participants typically respond with: i) a fast button press on trials where a go stimulus (1-9, but not 3) was presented, ii) participants make a high number of commission errors by pressing the response button on the presentation of the no-go stimulus (3) and iii) participants miss few trials (i.e. they almost never omit a response to a Go stimulus). The SART is thought to induce a speed-accuracy tradeoff (Robertson et al., 1997; Hawkins et al., 2019), such that participants with faster response times make more commission errors.

One important limitation of evidence accumulation models, such as the sequential sampling models discussed above, is that the underlying assumption of the model is that each decision is reached through a process of evidence accumulation (Hawkins et al., 2019). The qualitative description of commission errors in the SART are often ascribed to an automated response bias. Participants commit false alarms, because they are biased to respond with a button press (Robertson et al., 1997). One way of dealing with modeling of the response time data is to include contaminant responses by drawing a subset of trials with response times from a uniform distribution between the minimally and maximally observed response times (Ratcliff & Tuerlinckx, 2002).

Hawkins and colleagues (2019) recently tried to fit the go/no-go DDM from Gomez et al. (2007) and Ratcliff et al. (2018) to SART data. They collected behavioral data in humans with the $SART_{RANDOM}$ and found that the go/no-go DDM does not accurately explain the entire RT distribution. The RT distributions showed that participants quite often show responses that are quicker (<150 ms) than what is typically observed in decision making paradigms. This finding suggests that participants might not truly rely on evidence

accumulation processes from the stimulus during a SART, instead participants are relying on guesses without processing the stimulus. It also highlights the importance of examining full RT distributions. Interestingly, earlier modelling attempts of go/no-go data excluded responses with response times shorter than 300 ms (Gomez et al., 2007; Ratcliff et al., 2018).

Climbing neural activity for decision making and temporal estimation

We have discussed modeling approaches of response time and accuracy in perceptual decision making. Here, I will discuss different perceptual decision making tasks and the neural mechanisms that underlie the different stages of the decision process. Sensory information about an external stimulus is initially encoded by neurons in primary sensory cortex, whereas calculations on — or comparisons of this information with information form (e.g.) working memory — takes place in higher-order regions, such as association cortex (Gold & Shadlen, 2001).

Vibrotactile frequency discrimination and random dot motion tasks

Single-cell recordings from non-human primates have provided the earliest evidence discriminating the short-lived representation of stimulus features in primary sensory regions and sustained representations in association cortex (Gold & Shadlen, 2001; Heekeren et al., 2004). In vibrotactile frequency discrimination tasks monkeys need to decide whether the frequency of the first tactile stimulus (f1) is lower or higher than the frequency of the second tactile stimulus (f2). Neurons in primary somatosensory cortex (S1) often: i) increase their firing rate with increased stimulation frequency and ii) modulate

their activity according to the periodicity of the stimulus (Gold & Shadlen, 2001). This strongly suggests that S1 activity reflects information about the stimuli, but not about the comparison or the decision. Activity of the neurons in medial and ventral premotor cortex has been found to persist throughout the interval between the first and second physical stimulation (i.e. the delay period). In addition, some of the neurons' activity has been found to reflect a comparison between f1 and f2 (Gold & Shadlen, 2001).

The Random Dot Motion (RDM) task sets itself apart from the vibrotactile frequency discrimination task by eliminating the need for working memory, because it allows decision making processes to take place with the presentation of a single visual stimulus (Gold & Shadlen, 2001). The visual stimulus consists of dots with some proportion that move in one direction or another (sometimes the opposing direction) and task difficulty was manipulated by altering the percentage of dots that move coherently. Monkeys indicate their response through an eye movement to the left or right of the dot pattern. Sensory information is processed in area MT/V5, while neurons in the lateral intraparietal area (LIP) are thought to track the decision variable (Gold & Shadlen, 2001; Roitman & Shadlen, 2002).

A pattern that is typically observed in tasks like the RDM is that activity in LIP and frontal-eye fields (FEF) dips upon stimulus presentation (Gold & Shadlen, 2007). After this initial dip, activity ramps up or tapers further down depending on whether evidence is accumulating for a response towards or away from the receptive field of the neuron. Moreover, the speed with which the activity ramps up is related to the quality of the sensory information (Hanks & Summerfield, 2017). Finally, it has been shown that activity in FEF and LIP reaches a threshold if monkeys have to wait before they are allowed to

respond (Hanks & Summerfield, 2017). Taken together these findings suggest that some oculomotor neurons represent the drift rate as modelled in the DDM.

Human neuroimaging and electrophysiology

Non-human primate (NHP) research is well suited for invasive recordings, but it is challenging to teach complex decision-making tasks to NHPs. Moreover, single-cell recordings often span only a limited range of brain regions. Heekeren and colleagues (2004) therefore extended the single-cell recordings in non-human primates to whole brain neuroimaging with fMRI in humans by using a more complex perceptual decision making task with faces and houses. The face and house images were masked with noise. Activity of the posterior portion of the left dorsolateral prefrontal cortex (DLPFC) positively correlated with performance (Heekeren et al., 2004). Moreover, activity in this region was higher for easier than for hard decisions and activity in this region was correlated with the absolute difference in activity for house- and face-selective regions (Heekeren et al., 2004). Research from the same group showed involvement of the same DLPFC when the task was more similar to the RDM task used in monkey electrophysiology (Heekeren et al., 2006). In line with the experiments in NHP, Heekeren and colleagues showed that blood oxygenation level-dependent (BOLD) amplitude was higher when stimulus evidence was stronger (Heekeren et al., 2008). Although the fMRI experiments discussed here provide an important link between non-human primate electrophysiology and human decision making processes, the low temporal resolution of fMRI cannot readily separate evidence accumulation and decision variable processes (Gold & Shadlen, 2001).

Electroencephalography (EEG) has higher temporal resolution and has been used to examine the distinct processing stages in perceptual decision making. VanRullen & Thorpe (2001) used event related potentials (ERPs) and a version of a Go/no-go task to tease apart the distinct stages of the decision process. Participants were instructed to release a button if participants saw an animal in a naturalistic scene. In a second task, participants were instructed to release a button if they saw a means of transportation. Crucially, the distractors in the first task (means of transportation) were the targets in the second task and vice versa. This task design afforded disentangling of ERP responses to low-level visual stimulation and ERP responses to higher-level cognitive decisions. VanRullen & Thorpe (2001) found that differences in the ERP could be observed 75-80 ms after stimulus onset that were related to stimulus category, which were independent of the task instructions. The early ERP was followed by a slower ERP at ~150 ms that correlated with task instruction, which was independent of stimulus category and correlated with participants' decision.

In 2006 Philiastides et al. used a task that was more similar to the task of Heekeren et al. (2004) discussed above, but Philiastides and colleagues used EEG to look at the relative timing of decision making. Participants performed two experiments: In the first task participants judged whether a stimulus that was embedded in noise contained a car or a face (similar to Heekeren et al.). In the second task, participants were presented with a cue that instructed participants to discriminate cars and faces or the color of the stimulus (green or red). Different noise levels manipulated the task difficulty of the car/face discrimination. Differentiating cars from faces and green from red stimuli both showed a N170, a negative ERP component that peaks ~170 ms. A later component dubbed the

D220, an ERP component related to task difficulty that peaks ~220 ms, was only present when comparing more and less difficult car/face discrimination trials. And there was no difference in the D220 when discriminating red and green stimuli, because this task was easy. These findings suggest that the D220 is inversely related to stimulus evidence (Philiastides et al., 2006). The researchers also observed a late component after the D220, at ~300 ms. This late component was highly correlated with the mean drift rate and it shifted backwards in time for more difficult stimuli (Philiastides et al., 2006). The same group of researchers used a similar analysis on single-trial data by applying a data-split based on the amplitude of the late component (Ratcliff et al., 2009). The group of trials with a more positive late component had a higher drift rate than trials with less positive late components.

The late component described by Philiastides et al. (2006) was corroborated by a study from Bode and colleagues (2012). Bode et al. used a support vector machine learning approach to link single-trial EEG activity to perceptual decision making. They used inanimate object categories, rather than faces to show that EEG can still be used to decode decisions even when processing is less focal (i.e. inanimate objects are processed less focally than faces). In line with the findings of Philiastides and colleagues (2006), Bode et al. (2012) also observed choice encoding ~300 ms post-stimulus. In addition, when participants were presented with pure noise trials, upcoming decisions could be reliably decoded from the EEG (Bode et al., 2012). Modelling different versions of the DDM to these noise trials indicated that the DDM with variable starting point best explained these trials. Interestingly, the starting point on these noise trials was shifted in the direction of the choice on the previous trial (Bode et al., 2012).

In summary, the EEG papers discussed so far showed that combining sequential sampling models like the DDM with macroscopic brain activity measured with EEG yields valuable insights. Activity ~300 ms post-stimulus was shown to covary with the amount of sensory evidence. Recent research with EEG even suggests there is an event related potential that directly reflects the drift rate. To show this, O'Connell and colleagues (2012) used a paradigm where the stimulus underwent gradual changes and participants responded with a button press when they noticed the target dimmed. The stimulus flickered at 21.25Hz as to evoke a steady-state visual-evoked potential (SSVEP), which allowed the researchers to examine sensory encoding of contrast over time (O'Connell et al., 2012). The researchers divided the data of each participant into fast, medium and slow responses and showed that the centro-parietal positivity (CPP) was closely related to response times. First, O'Connell and colleagues showed that the CPP builds up over time differently for the different response bins. Second, they showed that action execution takes place when the CPP reaches a criterion level (O'Connell et al., 2012). Finally, they showed that the CPP also closely tracked integration of evidence in an auditory variant of the task and when participants were asked to count the number of targets rather than responding with a button press on each trial. These task changes suggest that this CPP reflects a domain general mechanism. Interestingly, O'Connell et al. (2012) showed that the CPP is closely related to the P300, a positive ERP component at ~300 ms, when the target stimulus had a sudden onset (see also Twomey et al., 2015). Recently, van Vugt et al. (2019) showed that the build-up of the CPP correlates with the drift rate and that this link extends beyond perceptual decision making to memory based decision, which further highlights the general involvement of the CPP during evidence accumulation.

CNV and perception of time

Now that we have reviewed the relationship between climbing neural activity and perceptual decision making I will move on to discuss the contested relationship of climbing neural activity in the form of the CNV and its role in time estimation.

A classic study by Walter and colleagues (1964) first linked the CNV to temporal expectations. In this seminal study, two stimuli (S1-S2) were presented with a time interval in the second range between them. Walter et al. (1964) showed that a sustained negative potential appeared over midfrontal electrodes when participants had to respond to the presentation of the second stimulus. The CNV peaked just before the presentation of the second stimulus. However, if participants were instructed not to respond to the second stimulus, the CNV disappeared. Interestingly, the CNV remained present when participants responded to the second stimulus and hence learned the stimulus contingency between S1-S2, but were later in the experiment instructed to stop responding to the second stimulus, for about 30 trials. After those 30 trials the CNV was extinguished (Walter et al., 1964).

Macar and colleagues (1999) have linked the CNV not only to temporal expectation, but to timing in temporal discrimination and production tasks. The CNV was evoked when participants were instructed to discriminate or produce time intervals in the second range (~2.5s), but there was no CNV when participants performed a control task that was devoid of time judgements (Macar et al., 1999). It has been proposed that the CNV reflects the accumulator of the pacemaker-accumulator models discussed earlier (Macar & Vidal, 2004; 2009). However, Kononowicz & van Rijn (2011) failed to confirm important

predictions of this idea: if the CNV represents the temporal accumulator, participants' CNV amplitude and slope should predict temporal discrimination abilities and the CNV should not show any habituation effects.

Regardless, recent findings suggest that the CNV plays a role in duration judgements. Wiener and colleagues (2012) used repetitive transcranial magnetic stimulation (rTMS) and showed that stimulation induced changes in CNV amplitude correlated with an increased tendency to judge a comparison interval as long. This effect was only present for rTMS of the right supramarginal gyrus (rSMG) but not for midline occipital/parietal junction stimulation (Wiener et al., 2012). Subjective bias in responding was measured as the constant error term of the psychometric curve (i.e. the difference between the bisection point and the standard interval). For participants with larger positive bias (i.e. those participants with a tendency to judge the second duration as short irrespective of its physical length) rSMG stimulation had less effect on CNV amplitude. Interestingly, rSMG stimulation affected both the CNV and the N1 — an early component associated with attentional orienting — but only the CNV correlated with bias. Taken together, these findings suggest that bias is related to changes in drift rate rather than starting point (Wiener et al., 2012).

In summary, evidence accumulation (i.e. drift rate) might be represented by ramping neural activity. There is some evidence that suggests that the CPP might reflect drift rate for decision making processes in general and that the CNV might reflect similar aspects of temporal evidence accumulation. It is important to note that single-cell recordings showed increases and decreases in ramping activity depending on whether the evidence was accumulating to a saccade toward or away from the neuron's receptive field. When

measured at the scalp, as with EEG, these neuronal populations might cancel each other out (Philiastides et al., 2006).

Oscillations during perceptual decision making/evidence accumulation

Above we have reviewed the data on event related potentials related to temporal and perceptual decision making, but when we collect EEG data we do not only possess information about phase-locked or evoked activity. We also have information about the power, phase and frequency of oscillations in the EEG.

Van Vugt et al. (2012) related decreasing activity in the theta (4-9 Hz) band with evidence accumulation when participants performed a random dot motion task. When participants performed a decision-making task on very similar stimuli that did not need continuous evidence accumulation, this relationship was absent (van Vugt et al., 2012). In addition, Van Vugt and colleagues showed that the slopes of the decreasing theta band activity over parietal regions correlated with drift rates estimated from the behavioral data of individual participants.

Polonía et al. (2014) compared value- and perception-based decision making and found that gamma (30-90 Hz) oscillations over parietal regions play an important role in evidence accumulation for both value-based and perceptual decision making. This finding was in line with previous research that showed that enhancement in the gamma (64-100 Hz) band as measured with magnetoencephalography (MEG) predicted participants' choices (Donner et al., 2009). In addition, Donner and colleagues found that beta (12-36 Hz) band suppression over contralateral motor region was predictive of participants' choices.

The involvement of the beta band in evidence accumulation remains controversial, because it has been suggested that the lateralized beta activity over motor cortex does not represent evidence accumulation in and of itself, but instead reflects the translation of an evidence accumulation signal from downstream regions into a response preparation signal (Wyart et al., 2012). Wyart and colleagues (2012) found that the beta (10-30 Hz) activity had more properties of a response preparation signal, that implemented decisions based on evidence accumulated in the delta (1-3 Hz) band instead. Specifically, Wyart et al. (2012) showed that sensory evidence is not accumulated in a purely linear fashion but instead fluctuates rhythmically such that evidence presented at a preferred phase of the delta oscillation is weighted more heavily than evidence presented at the non-preferred phase.

Oscillations in perceptual resolution

Recent research suggests that alpha oscillations dictate the temporal resolution of the visual system (VanRullen, 2016; VanRullen & Koch, 2003), adding to the idea that alpha oscillations are important for temporal relationships in the brain. The relationship between alpha oscillations and the temporal resolution of the visual system was "revamped" by the discovery that visual perception correlates with alpha phase (Dubois et al, 2009; Mathewson et al., 2009; Busch et al., 2009; but see Ruzzoli et al., 2019 for a failure to replicate these effects). Participants were more likely to perceive a stimulus at certain phases of the alpha oscillation than others. Behavioral oscillations at ~7 Hz were also described such that the time between an orienting stimulus and a task relevant stimulus influenced perception (VanRullen & Dubois, 2011, see also Fiebelkorn et al., 2013 and

Landau & Fries, 2012 for behavioral oscillations at different frequencies). Certain parts of the alpha oscillation are deemed more excitable than others and this idea was supported by neural firing probabilities that matched these more and less excitable phases (Haegens et al., 2011; Bollimunta et al., 2011). Moreover, gamma power related to alpha phase in a similar fashion (Osipova et al., 2008). Taken together, these findings suggest that oscillations in neural activity are tightly linked to perception.

Relatedly, earlier studies of alpha frequency and decision making showed that alpha frequency negatively correlated with response times, such that higher alpha frequency (indicative of more effective processing) correlates with faster responses (Surwillo, 1961; 1966a and b). However, this relationship might possibly be explained by confounds such as age, intelligence or brain anatomy (Klimesch et al., 1996; VanRullen, 2018). Recent studies more convincingly suggested that the frequency of alpha oscillations play a role in visual perception and temporal binding (Samaha & Postle, 2015; Cecere et al., 2015). Samaha & Postle (2015) used within-subject analysis, which discounts possible explanations due to inter-subject variability.

The working hypothesis that relates alpha frequency to perception is that when two stimuli fall on the same alpha cycle, the stimuli are more likely to bind together into a single percept, but when alpha frequency is lower and the two stimuli fall on different alpha waves, the stimuli are more likely to be perceived as two separate events (Samaha & Postle, 2015; VanRullen et al., 2016; White, 2018). The internal clock hypothesis of alpha oscillations from Treisman (1963) is somewhat comparable to the idea that alpha oscillations dictate the temporal resolution of the visual system. When alpha frequency is high, we sample our environment more often than when alpha frequency is low. As a

consequence, participants would be more likely to overestimate the time that has passed when alpha frequency is high (because they accumulate more cycles). When alpha frequency is low, participants would be more likely to underestimate the same time interval.

Oscillations in time estimation

Historically, alpha oscillations have been implicated in time estimation. Specifically, the frequency of alpha oscillations (see previous paragraph). Here, I will first discuss the influential idea of Treisman (1963) that alpha frequency might serve as the brain's pacemaker. Then, I will discuss more recent findings that ascribe a role to other frequency bands in different timing tasks.

Alpha frequency as pacemaker

The suggestion that alpha oscillations serve as a pacemaker finds its origin in a study that first linked body temperature to time estimation. Hoagland showed that increased body temperature led to both temporal underestimation (Hoagland, 1933) and increased alpha frequency (Hoagland, 1936a, 1936b and 1936c). Werboff directly examined the relationship between alpha oscillations and time estimation in 1962. Participants timed temporal intervals of 2 and 8s by pressing a button at the on- and offset of the timed interval. Participants that had higher alpha power at rest (eye-closed) were more likely to overestimate time compared to participants with low alpha power at rest (Werboff, 1962). In addition, Werboff found that a relative change in overall frequency (i.e. not specific to the alpha range) correlated with temporal estimations such that higher overall frequencies

correlated with temporal underestimation (Werboff, 1962). It is important to note that this relationship goes in the opposite direction of the working hypothesis laid out in the previous paragraph. However, as stated, Werboff used a measure of overall frequency changes. Next, Anliker (1963) found that when participants became drowsy, their alpha power decreased and their 3s tapping intervals lengthened. This finding has been interpreted to suggest that synchronized alpha oscillations represent the pacemaker in temporal accumulation (e.g. Herbst & Landau, 2016; Matell & Meck, 2004; Oprisan & Buhusi, 2011).

And finally, Surwillo (1966) reported a case study of a participant that had a visible alpha rhythm in their EEG 99% of the time, which allowed the researcher to estimate the length of individual alpha cycles. Surwillo showed that in this participant longer alpha cycles (i.e. lower alpha frequency) correlated with longer produced time intervals (10 s). However, this was only a case study. Treisman (1984) tried to replicate and extend these effects in more participants, but was unable to do so. He found that the variability in temporal estimation was much higher than the variability in alpha frequency.

Beta power and time estimation

A recent interval production timing task looked at the relationship between oscillatory activity in different frequency bands and the length of the produced interval (Kononowicz & van Rijn, 2015). Beta oscillations were first linked to temporal estimation in monkeys (Bartolo et al., 2014). LFP recordings in the striatum showed that beta (12-30 Hz) oscillations were prominently present during the continuation phase of a synchronization-continuation task. In this task macaque monkeys synchronize their tapping

in beat with a metronome during the synchronization phase and the monkeys continue their tapping after the metronome has stopped in the continuation phase (Bartolo et al., 2014). Moreover, the same group of researchers later showed that both regular and irregular sequences of taps evoked a transient beta burst, but that only the internally paced regular sequence evoked sustained beta oscillations (Bartolo & Merchant, 2015). Kononowicz & van Rijn (2015) asked whether beta oscillations played a similar role in human participants and in longer interval durations. Participants timed ~2.5 s intervals by pressing a button at the on- and offset of the interval. Kononowicz & van Rijn (2015) subdivided the trials in short and long durations based on trial-to-trial variability. Pre- and post-first key press beta power positively correlated with produced time intervals (Kononowicz & van Rijn, 2015). In addition, they found that theta power was negatively correlated with produced time intervals (Kononowicz & van Rijn, 2015).

Kulashekhar and colleagues (2016) used a different paradigm to study the contribution of different frequency bands to time estimation. In their task, participants were instructed to either keep color information or temporal information in working memory. This time/color paradigm was developed by Coull (2004) and allows the examination of temporal estimations in the absence of motor confounds (Wiener et al., 2018). When participants kept temporal information in working memory stronger beta power was recorded with MEG than when participants kept color information in working memory (Kulashekhar et al., 2016). Source reconstruction indicated that the supplementary motor area (SMA), posterior parietal cortex (PPC), dorso- and ventrolateral PFC represent the neural correlate of duration estimation (Kulashekhar et al., 2016).

The studies discussed so far linked beta power as recorded with M/EEG to time estimation, but a recent study went beyond the correlational relationship by trying to induce enhanced beta power with transcranial alternating current stimulation (tACS). Wiener and colleagues (2018) stimulated at alpha (10 Hz) and beta (20 Hz) frequencies over frontocentral electrodes and found that the beta stimulation led to increased reports of long durations. Moreover, they used the drift diffusion model for interval timing discussed above to relate beta power changes with behavioral changes. Interestingly, Wiener et al. (2018) found that beta power was related to changes in the starting point of the drift diffusion process and not to the drift rate or the decision boundaries.

Multiple oscillator models of time perception

I have mostly discussed time perception models that have a long history, e.g. pacemaker-accumulator model and scalar expectancy theory, but here I want to discuss more recent models that ascribe important roles to oscillatory activity. In its simplest form, the models discussed below are extensions of pacemaker-accumulator models with several pacemakers (i.e. oscillators; Ivry & Richardson, 2002).

Multiple-oscillator model

One behavioral observation that is poorly explained by pacemaker-accumulator models is that certain intervals are more readily discriminated than others, i.e. the nonlinearity[1]

---

[1] Collyer et al. (1992) used an experiment where participants were instructed to tap along to a beat (synchronized tapping). After 50 beats, the beat stopped and participants were instructed to keep tapping their finger in the same rhythm for 50 additional taps (continuation tapping). Collyer and colleagues found that in general the data for the continuation tapping was well approximated by an identity function, because the continuation tapping was comparable to the interstimulus intervals. However, they also

between physical time and temporal representations (Crystal et al., 1997; Crystal, 1999). Moreover, single oscillators might not be reliable for the timing of longer time intervals, since the exact spike time of a neuron depends on the neuron's membrane potential. The membrane potential will fluctuate more over longer periods of time than over short periods of time and as such will influence the exact spike time of the neuron (Miall, 1996). Multiple oscillators have been proposed to overcome both issues (Miall, 1989; Church & Broadbent, 1990). Church & Broadbent proposed different oscillator periods, which increase in powers of two (i.e. 200, 400, 800, 1600 ms etc.). Instead of an accumulator as in the pacemaker-accumulator models discussed earlier, the multiple oscillator model contains a status indicator (Church & Broadbent, 1990). These status indicators read the phase of the oscillation across a population of oscillators, rather than counting the cycles (i.e. beats) of the oscillation. As such, the output is binary, detecting when the oscillators (or some proportion of them) are all in phase (Miall, 1996) and both working memory and reference memory consist of matrices of connection weights rather than sample distributions (Church & Broadbent, 1990).

Striatal beat frequency model

The striatal beat frequency (SBF) model incorporates the beat frequency model of Miall (1989) and links to the neurobiology of the basal ganglia (Matell & Meck, 2004). In the SBF distributed, cortical regions contain neural populations that oscillate in different intrinsic frequencies (1-15 Hz; Petter et al., 2016) and the medium spiny neurons, which are

---

observed some residual variance that fluctuated in an oscillatory fashion as a function of interstimulus time (Collyer et al., 1992). In 1994 Collyer and colleagues replicated their earlier results and provided an explanation in the form of the multiple-oscillator model (Collyer et al. 1994; Church & Broadbent 1990, 1991).

located in the striatum, act as coincidence detectors (Paton & Buonomano, 2018). Striatal involvement in interval timing is supported by the firing behavior of striatal neurons (Buhusi & Oprisan, 2014). Phasic dopaminergic activity of the ventral tegmental area and the substantia nigra are hypothesized to reset cortical oscillations and medium spiny neurons (Petter et al., 2016), and as such serve as a start-gun to signal the interval time (Buhusi & Meck, 2005). The role of dopamine in interval timing will be discussed in more detail in the paragraph after exploring the role of the medial frontal cortex in performance monitoring and interval timing.

Medial frontal cortex

The medial prefrontal cortex is thought to play an important role in decision making, including conflict monitoring, error detection and inhibitory control (Carter et al., 1998; Ridderinkhof et al., 2004). It is important to note though that inhibitory control has also been interpreted as a form of conflict monitoring (Donkers & van Boxtel, 2004; Nieuwenhuis et al., 2003). The medial frontal cortex is thought to be activated when unfavorable outcomes are achieved (Ridderinkhof et al., 2004). Part of the medial frontal cortex, the anterior cingulate cortex, is thought to generate the error-related negativity (ERN; Herrmann et al., 2004). In addition to phase-locked activity as captured in the ERN, the medial frontal cortex is also thought to be the source of non-phase-locked theta (~4-7 Hz) oscillations (Tsujimoto et al., 2006). As such, the ACC is seen as an important hub in the performance monitoring system (Ridderinkhof et al., 2004; Rushworth et al., 2004; Rushworth et al., 2007).

In addition to the role that the medial frontal cortex plays in error processing, which is largely fulfilled by the ACC, the medial frontal cortex in the primate brain encompasses the pre-supplementary motor area (pre-SMA), the supplementary motor area (SMA) and the supplementary eye fields (SEF; Rushworth et al., 2004; Rushworth et al., 2007). The pre-SMA and SMA play a crucial role in the planning, execution and control of actions, especially movements with temporal structure (Schwartze et al., 2012). Functionally, the pre-SMA and SMA can be distinguished due to their roles in internally and externally generated movement, respectively (Schwartze et al,. 2012). Recent intracranial recordings actually identified the pre-SMA as the generator of the ERN by showing that the intracranial variant of the ERN occurred earlier and had a larger amplitude in the pre-SMA than in the ACC (Fu et al., 2019).

The medial frontal cortex also plays an important role in interval timing. Matell and colleagues (2003) showed that some ACC neurons in rats modulate their firing as a function of interval length. Recently, this role was further substantiated when Kim et al. (2013) found similar results in rats in the absence of any possible motor confounds. Taken together, these findings suggest that the medial frontal cortex might be part of an internal clock (Kim et al., 2013). A neuroimaging study that contrasted brain activity in timing tasks with and without an explicit motor component also showed consistent activation of (a.o.) the medial frontal cortex in the ACC and SMA (Pouthas et al., 2005; Stevens et al., 2006). In addition, electrophysiological recordings in monkeys showed that neurons in the pre-SMA were involved in interval timing (Mita et al., 2009). All in all, some regions of the medial frontal cortex, namely the ACC, SMA and pre-SMA, seem involved in performance monitoring and interval timing.

The role of dopamine in interval timing and performance monitoring

Previous research showed that the internal clock can be influenced through the administration of dopamine agonists and antagonists (Meck, 2006), such that dopamine agonists speed up and antagonists slow down the internal clock. In contrast, cholinergic manipulations affect the memory stage of interval timing tasks (Buhusi & Meck, 2005). In addition, patients with Parkinson's Disease (Parker et al., 2014), Huntington's disease (Paulsen et al., 2004) and schizophrenia (Rammsayer et al., 1990; Tracy et al., 1998), which are all diseases thought to affect the dopamine system, have impaired timing abilities (Buhusi & Meck, 2005). In interval timing, the interval is thought to be timed through the firing of a start-gun at the onset of the interval in the form of a dopaminergic burst, which phase resets and synchronizes cortical oscillations (Buhusi & Meck, 2005; Matell & Meck, 2004). In addition to interval timing dopamine is also thought to play a key role in performance monitoring (Holroyd & Coles, 2002; Ullsperger, 2010; Ulsperger et al., 2014). Moreover, Mueller and colleagues (2011) recently showed that low and high versus medium dopamine levels were related to behavioral adjustments after errors.

Theta oscillations

Theta oscillations (~4-7 Hz) from medial frontal cortex are thought to reflect cognitive control (Cavanagh & Frank, 2014). More specifically, theta power is thought to play an important role in performance monitoring, as theta oscillations in the medial frontal cortex have larger amplitudes after an error was committed compared to correct button presses (Debener et al., 2005; Luu et al., 2004). In addition, theta oscillations have been linked to

interval timing. Parker and colleagues (2015) showed that theta power increased upon cue presentation when human participants and rats were instructed to perform an interval timing task. Importantly, this oscillatory pattern was not present in dopamine depleted rats or in patients with Parkinson's Disease (Parker et al,. 2015).

Current thesis

The aim of the current thesis was three-fold. First, the aim was to explore whether EEG activity might be indicative of an internal clock. From the literature overview in the general introduction, it has become clear that the frequency of alpha oscillations are thought to play an important role in the speed of information processing (Treisman, 1963; Kononowicz & van Wassenhove, 2016) through: i) the hypothesized relationship between alpha frequency and the temporal resolution of the visual system (vanRullen, 2016) and ii) the relationship between response time and alpha frequency (Surwillo, 1961). To this end, EEG data was collected in two experiments where participants judged whether the elapsed time between a tone and a visual stimulus was short or long. The different experiments examined slightly different temporal intervals to assess whether any difference in correct and incorrect temporal judgements were general to timing mechanisms, or whether these differences were specific to the time intervals tested in the different experiments. The relationship between alpha frequency and interval timing has been examined before, but advances in the methodological estimation of alpha frequency justify renewed interest in this question. In this first empirical chapter an automated measure of alpha peak frequency was used and instantaneous frequency was calculated to increase the temporal sensitivity. If alpha frequency represents the internal clock, alpha peak frequency (APF) is expected to

be higher on overestimated short interval trials compared to correct short interval trials, whereas APF is expected to be lower on underestimated long interval trials compared to correct long interval trials.

Second, the aim of the current thesis was to further the understanding of theta oscillations from midfrontal electrodes in performance monitoring and in temporal decision making. From the general introduction it has become clear that the medial frontal cortex is thought to play an important role in performance monitoring and in interval timing. Specifically, the power of theta oscillations has been related to both behaviors, as enhanced theta power is observed directly after errors and in interval timing tasks (Parker et al., 2014). In this thesis the aim was to examine how medial frontal cortex exerts control over downstream regions after an error is committed. To this end, participants performed a go/no-go task while their EEG was collected. Post-error slowing (PES) was used as a behavioral measure of adjustments after errors. If medial frontal cortex exerts its influence on behavioral adjustments directly, we would predict a correlation between midfrontal theta power and PES. Alternatively, medial frontal cortex might exert its influence on downstream regions through functional connectivity with sensory regions (e.g. through amplitude-amplitude coupling as found by Mazaheri et al., 2009). In that case, we would expect a correlation between the strength of the functional connectivity and behavioral adjustments.

In addition, power changes in the time estimation task from the first empirical chapter were examined. This third empirical chapter examined whether theta band power was related to temporal judgments. Theta power in medial frontal cortex increased when a cue was presented that instructed participants to perform an interval timing task (Parker et al., 2014). However, it remains to be elucidated whether theta power reflects activity of the

internal clock (possibly pre-SMA) over the duration of the timed interval, reflecting the accumulation of temporal evidence. From the general introduction, it has become clear that previous literature has also implicated beta power in the indexing of interval timing (Kononowicz & van Rijn, 2015). Beta power measured before the reproduced interval correlated with longer reproductions. This suggests that higher beta power might reflect a slowly running internal clock, as participants let more time pass by before their threshold is reached to close the reproduced interval (Kononowicz & van Rijn, 2015). In this chapter power in different frequency bands was compared between correct and incorrect temporal judgments.

Third, the role of climbing neural activity in temporal decision making was examined. In perceptual (non-temporal) decision making, the centro-parietal positivity (CPP) has been found to track the accumulation of noisy sensory evidence (Kelly & O'Connell, 2013). In temporal decision making, the contingent negative variation (CNV) has been implicated (Macar et al., 1999) and contested (Kononowicz & Penney, 2016; Kononowicz & van Rijn, 2011; Kononowicz & van Rijn, 2014; van Rijn et al., 2011). However, these slow potentials have never been studies simultaneously in a temporal decision making study that shares many characteristics with non-temporal decision making studies as used in the study of the CPP. In the last empirical chapter, the time estimation experiments are analysed to study the contribution of the CPP and CNV in temporal decision making. In addition, error-related potentials are examined within the realm of temporal decision-making. If temporal errors are processed similarly to non-temporal errors, we would expect a larger error-related negativity for incorrect compared to correct responses.

CHAPTER 2

Alpha frequency and temporal judgements

The paradigm of Chapters 2, 4 and 5 has been used for a manuscript that is currently on biorxiv (https://doi.org/10.1101/224386). However, the manuscript on biorxiv is written about Experiment 1 and only focuses on time-frequency power. It is important to note that the same preprocessing pipeline and paradigm is used in Chapters 2, 4 and 5 as in the manuscript on biorxiv.

ABSTRACT

It remains to be elucidated how humans are capable of keeping track of time on short (1-2 s) time scales. Already in the sixties it was hypothesized that alpha frequency might reflect the internal clock, mostly fuelled by findings that correlated alpha peak frequency and response times. Recently, alpha frequency has been linked to the resolution of the visual system and recent methodological advances beg a re-evaluation of the relationship between alpha frequency and the internal clock. Here, we used a temporal discrimination task where participants judged 1 vs. 1.5 s intervals in Experiment 1 and 1.5 vs 2 s intervals in Experiment 2. If alpha peak frequency reflects the internal clock higher alpha frequency should correspond to overestimation of physical time, whereas lower alpha frequency should correspond to underestimation of physical time. In long interval (2 s) trials of Experiment 2 participants were found to have higher instantaneous alpha frequency for correct compared to incorrect judgments, but this effect flipped after the short interval had

elapsed. Moreover, the relationship between alpha frequency and subjective experience of time did not replicate in any of the other conditions. In addition, if alpha frequency represents the speed of information processing a negative correlation between alpha frequency and response times should emerge. Instead, higher alpha frequency was consistently correlated with slower responses. Finally, we analyzed aggregate datasets to substantiate null-findings in our data. Higher alpha frequency was observed in correct compared to incorrect responses to the long (1.5 s) interval in Experiment 1.

2.1 INTRODUCTION

Scientific research has contributed immensely to our understanding of how mammailians are capable of keeping track of 24-hour rhythms. The suprachiasmatic nucleus is thought to play a crucial role in time-keeping of these time intervals (Reppert & Moore, 1991). However, how humans are able to keep track of time on shorter time scales (seconds to minutes), remains poorly understood (Kononowicz & Van Wassenhove, 2016). An influential theory that was developed in the 60ies and gained traction in recent years is that the brain contains an accumulator that collects pulses to estimate time (Treisman, 1963; Surwillo, 1966; Kononowicz & Van Wassenhove, 2016). More specifically, it has been proposed that alpha oscillations might provide the beat or the pulses of this internal clock mechanism (Treisman, 1963; Treisman, 1984; Glicksohn et al,. 2009).

Even though this hypothesis has been around for over 60 years empirical evidence supporting this idea seems sparse. Previous research however has related alpha (~10 Hz) activity to perceptual accuracy and reaction times (Dustman & Beck, 1965; Callaway & Yeager, 1960), which might indicate some relationship between the speed of the

information processing system and alpha activity (but see Klimesch et al., 1996 for an alternative explanation of the earlier findings). Alpha oscillations are a suited candidate for such a mechanism, because pacemakers of the alpha rhythm have been described in the thalamus (Andersen et al., 1968). Moreover, the thalamus is well-known for its interconnectedness with other brain regions (Jones, 2001). As such, pacemaker cells in the thalamus that function at an alpha rhythm might enslave cortical regions and underlie a cortical, distributed pacemaker (Hughes and Crunelli, 2005; Klimesch, 2012).

Indirect evidence that information processing in the brain undergoes a rhythmic process stems from recent research, which has identified behavioral oscillations where stimulus detection was better at certain time points than others (~7 Hz; Busch & VanRullen, 2010; Fiebelkorn et al., 2013; Landau & Fries, 2012; Landau et al., 2015; VanRullen et al., 2007). It is important to note that the exact frequencies in these studies range from ~4-8 Hz. Moreover, these behavioral oscillations have been described mostly in spatial attention paradigms. Although a recent study extended these findings to feature-based attention (Re et al., 2019). Taken together, these studies might suggest that information processing in the brain is bound by an alpha rhythm (VanRullen, 2016).

In addition to behavioral oscillations, the influence of alpha phase as recorded with MEG or EEG, has been studied extensively. Several studies have supported the idea that stimulus detection and alpha phase are coupled (Ai & Ro, 2014; Busch et al., 2009; Mathewson et al., 2009; Milton & Pleydell-Pearce, 2016). This suggests that alpha oscillations might be related to more and less excitable cortical states and this idea was further substantiated by findings relating local field-potentials in the alpha band to neural firing probability (Haegens et al., 2011), where neurons were found to be more likely to fire in the trough compared to

the peak of the alpha oscillation. However, a recent registered report failed to replicate the relationship between alpha phase and stimulus detection (Ruzzoli et al., 2019).

Top-down control over the excitable phases of the alpha oscillations would suggest timekeeping mechanisms that might rely on alpha activity. Although there are some inconsistencies in the literature with regards to top-down control of alpha phase (van Diepen et al., 2015), recent research suggests that when task difficulty is sufficiently high, top-down control of alpha phase adjustments can be observed (Samaha et al., 2015; Solís-Vivanco et al., 2018). Another line of research investigated the role of alpha frequency in separating and integrating multisensory information. Cecere and colleagues (2015) showed that individual alpha frequency (IAF) correlated with the sound-induced double-flash illusion, where participants with a lower IAF, and hence longer alpha cycles, experienced the sound-induced double-flash illusion across a longer inter-beep interval (i.e. longer inflection point). Moreover, application of tACS to speed up or slow down IAF with 2 Hz affected the sound-induced double-flash illusion such that speeding up of IAF led to shorter inflection points and slowing down of IAF led to longer inflection points (Cecere et al., 2015). In addition, Samaha & Postle (2015) showed that IAF correlated with two-flash fusion thresholds, such that faster IAF yielded more accurate two-flash discrimination behavior.

Ronconi & Melcher (2017) used rapid presentation of sensory stimuli, also referred to as entrainment, to influence IAF to examine the causal relationship between IAF and integration and segregation of visual information. Importantly, they showed that stimuli that were presented within the same phase of the theta/alpha oscillation were more likely to be integrated into a single percept, whereas stimuli that were presented at opposing phases

of the theta/alpha cycle were more likely to be segregated into two separate percepts (Ronconi & Melcher, 2017). However, Ronconi & Melcher (2017) found only partial support for the idea that speeding up of the IAF through entrainment would lead to better discrimination performance (in fact, the findings from their first experiment were in the opposite direction such that speeding of the IAF was correlated with poorer discrimination performance). All in all, these findings hint at a possible relationship between alpha frequency and the resolution of the visual system. Although it is important to note that the original findings of both Samaha & Postle (2015) and Cecere et al. (2015) were not replicated in a recent attempt to combine these studies in a full parametric design (Bürgers & Noppeney, in prep). Moreover, Bayes factors consistently supported the null, suggesting that the relationship between IAF and the integration or segregation of audio-visual information is less straightforward than previously thought (Bürgers & Noppeney, in prep).

For the hypothesis that alpha frequency serves as the temporal pacemaker of the brain, the findings discussed so far need to be extended beyond the (audio-)visual system. Surwillo (1961) showed that lower IAF correlated with longer response times (RT) and that higher IAF correlated with shorter RT (see also Jin et al., 2006). Again, these findings were later found not to replicate by Boddy (1971). However, when participants learned to speed up or slow down their IAF based on biofeedback, participants were faster or slower depending on their IAF such that when participants sped up their IAF, response times became faster (Woodruff, 1975). Previous research showed that the alpha frequency differs between participants and is relatively stable within a participant (Haegens et al., 2014), which supports the idea that IAF reflects a general timing mechanism. Moreover, Haegens and colleagues (2014) found that alpha peak frequency scaled with cognitive

load in a working memory task, such that higher load corresponded to higher peak frequency. In addition, Moran et al. (2010) showed that alpha peak frequency correlated with working memory performance such that participants with higher working memory performance had higher peak frequency. Taken together, these findings suggest that higher IAF might be indicative of faster or more efficient information processing.

Limited research has directly examined the link between IAF and temporal decision making. Treisman (1984) found no direct relationship between temporal production intervals and IAF (but see Treisman et al., 1994). However, Glickson et al. (2009) found that taking interhemispheric differences in IAF into account led to a correlation between a left-right interhemispheric IAF index and produced durations. To shed light onto these contradictory findings, the current EEG study examined the relationship between alpha frequency and interval discrimination. To this end, an automated procedure was used to estimate IAF to exclude effects due to the large amount of researcher-degrees of freedom researchers typically encounter when estimating IAF (Corcoran et al., 2018). In addition, instantaneous frequency was used to track moment-to-moment changes in alpha peak frequency (Cohen, 2014; Mierau et al., 2017). If alpha frequency represents an internal clock we expect to see higher alpha frequency for overestimated time intervals and lower alpha frequency for underestimated time intervals. Moreover, if alpha frequency represents the general speed of the operating system, we would expect higher alpha frequency to be associated with shorter response times and lower alpha frequency with longer response times.

2.2 MATERIALS & METHODS

2.2.1 Participants

Twenty-three healthy adults participated in Experiment 1. Data from five participants were excluded (three participants made too few, i.e. <20, errors in the short interval, one participant made too few errors in the long interval and one participant made too few errors in both intervals). Eighteen datasets were therefore used for further analyses (13 females, mean age: 26 years, range: 19-40 years, 3 left handed). Sixteen adults (all right handed) participated in Experiment 2; none had participated in Experiment 1. Data from 3 participants was excluded (two participants made too many errors, >75%, on the short interval and one participant made too few errors, i.e. <20, on the long interval). Thirteen datasets were used for further analyses (10 females, mean age: 19 years, range: 18-21 years, all right handed).

Participants had normal or corrected-to-normal vision and hearing and they had no known history of neurological disorders. In concordance with university guidelines, participants were paid £6 or 1 participation credit per hour. Participants gave written informed consent before data collection. Ethical approval was provided by the Ethics Committee of the University of Birmingham.

2.2.2 Paradigm

We utilized a novel two-forced-choice temporal judgement paradigm where the participant's task was to estimate whether the time between an auditory stimulus and a visual stimulus was short or long (1 s versus 1.5 s in Experiment 1 and 1.5 s versus 2 s in

Experiment 2), via a button press (Figure 2.1). The paradigm was programmed in Matlab (Natick, MA) using Psychophysics Toolbox extension (Brainard, 1997; Kleiner et al, 2007; psychtoolbox.org). The auditory stimulus was a pure tone of 1000 Hz, which was administered through headphones (Sennheiser, HD 280 PRO) and lasted for 50 ms (including a 5 ms rise and fall shaped by a Blackman window). The tone signified the start of the interval, which was followed by a visual stimulus that indicated the end of the interval. The visual stimulus was a Gabor patch (angle 5° clockwise, contrast 80%, spatial frequency 10 Hz, phase 0°), which lasted for 50 ms. Short and long intervals were randomly interspersed.
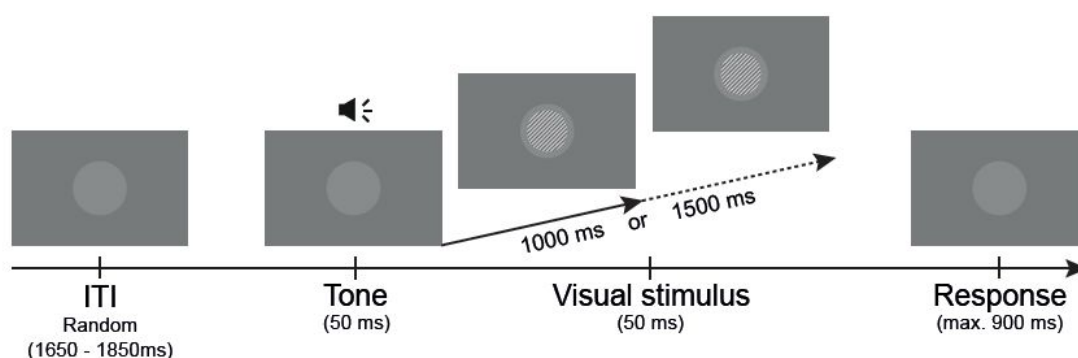
Figure 2.1 Experimental paradigm for Experiment 1. Participants performed a discrimination task estimating the time interval between the tone and the visual stimulus. Trials were initiated with the presentation of a 1000 Hz pure tone for 50 ms. The tone was followed by a Gabor patch, which lasted for 50 ms, at 1 or 1.5 s after the tone was presented in Experiment 1 and at 1.5 or 2 s for Experiment 2. Participants judged whether the interval between the tone and the visual stimulus was short or long by pressing a button. Participants had 900ms to respond. After the response (or after 900 ms) a new trial was initiated. A light grey placeholder was always on the screen to minimize eye movements. ITI = inter-trial interval.

After the visual stimulus participants responded with a button press, using the index (left button) or middle (right button) finger of their right hand to indicate long or short intervals. Response buttons were randomly counterbalanced across participants. If participants did not respond within 900 ms, a screen was displayed that read "Too slow! Please respond faster." Participants were pushed to respond fast to enhance the likelihood that they would make errors. The dataset of Experiment 1 presented here contains data of 9 participants that pressed the left mouse button for the long interval and 9 participants that pressed the right mouse button for the long interval. The dataset of Experiment 2 presented here contains data of 7 participants that pressed the left mouse button for the long interval and 6 participants that pressed the right mouse button for the long interval.

Participants were seated in front of a computer screen and the distance from the monitor to the participants' eyes was passed onto the stimulus computer, such that the visual stimulus was always presented at a visual angle of ~4°. To assure participants kept their eyes on the screen a light grey placeholder was presented centrally on the grey background (Figure 2.1). The placeholder was 5% larger than the Gabor patch, so the Gabor patch fell inside the placeholder.

Participants practiced for 3 blocks that consisted of 12 trials each. Participants received feedback after each block. The EEG recording started by collecting resting state data with eyes open and eyes closed for 30 s each. This procedure was performed twice, randomly starting with either eyes closed or eyes open data collection. The resting state EEG data was not used for the purpose of this study. Following this, participants performed 16 blocks of 60 trials, yielding a total of 960 trials per participant. Each block lasted ~3 min and participants were instructed to rest their eyes in between blocks. The refresh rate of the

screen was 60 Hz and all timings of the experiment were set as multiples of this refresh rate.

2.2.3 Behavior

Behavioral measures consisted of response times and error rates. Response times were calculated from visual stimulus onset until response. Errors were calculated for each interval condition separately by calculating the percentage of errors relative to the total number of trials in that condition. Statistical analyses were performed on response times and errors, where the subject-specific averages were subjected to repeated-measures ANOVA. For response time the factors were interval (short or long) and response (correct or incorrect). Post-hoc analyses were performed through dependent samples t-tests. For error rates we also used dependent samples t-tests to compare error rates of the short and long interval.

In addition to response times and error rates, I examined signal detection theory measures of behavior. I examined a measure of participants' performance as indicated by d' (Green & Swets, 1966; Macmillan & Creelman, 2004), where d' is a measure of sensitivity or the ability to separate the long and short time intervals:

$$d' = z(H) - z(FA) \quad (1)$$

When intervals are easy to discriminate, d' will be high and when task difficulty is high and intervals are difficult to distinguish d' will be low. Bias (β) is a measure of a participant's inclination to prefer one response option over another:

$$\beta = -\frac{|z(H) + z(FA)|}{2} \quad (2)$$

When β is close to 0, participants don't show a preference for one response over the other. A negative β indicates a bias towards the long interval response and a positive β indicates a bias towards the short interval response.

Finally, the response time distributions of correct and incorrect responses to short and long intervals were compared through visual inspection for the different experiments. An exemplar participant for each experiment is shown in the results section. To assess whether there were differences in the overlap between RT distributions of correct responses to the short and long interval the Bhattacharyya coefficients were calculated (Bhattacharyya, 1943). To this end, the response time distribution of the long intervals was moved by 500 ms such that the response times aligned with interval onset time for both short and long intervals (i.e. response time relative to the offset of the short time interval). The overlap term was scaled for differences in trial counts. The different experiments were compared by applying an independent samples t-test to assess whether there were differences in overlap between the experiments.

2.2.4 Temporal jitter in experimental paradigm

Testing of the timing of the stimuli showed an off-set of the presentation of the visual stimulus (i.e. the offset of the time interval). The visual stimulus was presented with a random jitter of ~40 ms, meaning it could be presented between 980 and 1020 ms after the tone onset, where the visual stimulus onset should have been 1000 ms. The error was discovered before the data collection of Experiment 2. However, it was decided not to change the paradigm for data collection of the second experiment. A remaining open

question is how much this temporal jitter affects the estimation of supra-second time intervals.

2.2.5 Alpha peak frequency and instantaneous frequency

To estimate alpha peak frequency we used an automated approach (Corcoran et al., 2018) that smooths the power spectral density (PSD) and estimates the alpha peak frequency. PSD were computed in the post-tone interval (500-1000 ms after tone onset for short interval trials in Experiment 1, 500-1500 ms after tone onset for long interval trials in Experiment 1, 500-1500 ms after tone onset for short intervals in Experiment 2 and 500-2000 ms after tone onset for long intervals in Experiment 2) and averaged over trials separately for short and long intervals and response outcomes (correct, incorrect). It remains to be elucidated how many alpha sources exist and where there are located in the brain. Here, two different sets of electrodes were used to estimate alpha peak frequency. One region of interest was frontocentral: Fpz, Fp2, F7, F3, Fz, F4, F8, FC5, FC1, FC2, FC6, C3, Cz, C4, F5, F1, F2, F6, FC3, FCz, FC4, C5, C1, C2, C6 and the other was parieto-occipital: POz, O1, O2, PO5, PO3, PO4, PO6, PO7, PO8, Oz, Pz, P1, P3, P5, P2, P4, P6.

Power estimates were normalized by dividing power at each frequency with the average power in the 3-30 Hz range (Corcoran et al., 2018; Cross et al., 2018 biorxiv). The alpha band was defined from 6-14 Hz. The normalized PSD was smoothed by applying a Savitzky-Golay filter (SGF; Benwell et al., 2019; Corcoran et al., 2018; Keitel et al., 2018; Savitzky and Golay, 1964), which uses a least-squares polynomial fitting procedure. The parameters of the automated fitting procedure related to the SGF were set according to the

default settings used in Corcoran et al. (2018): F_w represents the filter width of the SGF and was set to 11, the polynomial degree k of the SGF was set to 5. Savitzky & Golay (1964) showed that their procedure smooths noisy data, while maintaining the shape and height of the waveform peaks (Schafer, 2011). The polynomial family is described by:

$$p(n) = \sum_{k=0}^{N} a_k n^k \quad (3)$$

A subset of samples of $2M + 1$ are centered around $n = 0$ (Schafer, 2011). The mean-squared error for the subset of samples are given by:

$$E_N = \sum_{n=-M}^{M} (p(n) - x[n])^2 \quad (4)$$

$$= \sum_{n=-M}^{M} \left(\sum_{k=0}^{N} a_k n^k - x[n] \right)^2 \quad (5)$$

The output for the next subset of samples is obtained by moving one sample to the right (Schafer, 2011).

For a given polynomial with degree N the output can be calculated through discrete convolution (Schafer, 2011):

$$y[n] = \sum_{m=-M}^{M} h[m]x[n-m] \quad (6)$$

$$= \sum_{m=n-M}^{n+M} h[n-m]x[m] \quad (7)$$

Differentiation of E_N in (2) and setting this derivative for each of the $N + 1$ coefficients to 0 allows the determination of the optimal coefficients for the polynomial in (1):

$$\frac{\partial E_N}{\partial a_i} = \sum_{n=-M}^{M} 2n^i \left(\sum_{k=0}^{N} a_k n^k - x[n] \right) = 0 \quad (8)$$

After applying the SGF the first and second derivatives from the filtered data are obtained to locate local minima and maxima in the PSD. The first derivative $g'(x)$ describes the slope of a tangent line to a function $g(x)$, such that:

$$g'(x) = \lim_{\Delta x \to 0} \frac{\Delta g(x)}{\Delta x} \qquad (9)$$

and when this slope is 0, the function $g(x)$ is at a peak or trough. Moreover, a peak in $g(x)$ will be preceded by positive values of $g'(x)$ before 0 and followed by negative values of $g'(x)$ after 0. And vice versa for a trough in $g(x)$.

Inflection points in $g(x)$ can be described by the same zero-crossings approach in the second derivative. The second derivative describes whether $g(x)$ is concave up or concave down. The second derivative is simply the derivative of the first derivative:

$$g''(x) = \lim_{\Delta x \to 0} \frac{\Delta g'(x)}{\Delta x} \qquad (10)$$

and when $g''(x)$ is 0, the slope of $g(x)$ is constant, indicating an inflection point. Taken together, the first and second derivatives are used to identify peaks and their boundaries in the PSD.

The peaks and boundaries obtained were compared to the background noise, which was estimated with a first order polynomial (regression line) to the normalized, log-transformed PSD (i.e. before SGF application). If the peaks were >1 standard deviation away from the regression line (default setting of *minP*, Corcoran et al., 2018), the peak was determined a true peak, as it was far enough removed from the background noise. In addition, the peak needed to be 20% higher than other peak candidates (default setting of *pDiff*, Corcoran et al., 2018). Before combining the peaks of different channels, the peaks at each channel were scaled according to Q, which was defined as:

$$Q = \frac{\int_{i_1}^{i_2} PSD(f)\, df}{i_2 - i_1} \qquad (11)$$

Where Q is the scaled average power within the peak interval bounded by $[i_1, i_2]$. Note that this is different from the bounds of the frequency range of interest as the peak interval bounds can be much narrower, and does not take into account secondary peaks. Higher values of Q are indicative of narrower peaks. Finally, the within subject channel estimates are scaled according to their Q values and a weighted average is obtained. The minimum number of channels used for cross-channel average, *cMin*, was set to 2 (the default setting used in Corcoran et al., 2018).

As explained in the introduction of this chapter, a higher temporal resolution of the frequency of the oscillation might be obtained by estimating instantaneous frequency (Cohen, 2014; Mierau et al., 2017). To this end the data was bandpass filtered in the frequency range of interest between 7-14 Hz with transition zones of 15%. A Hilbert transform was applied to obtain the analytic signal over the entire epoch (from -1 s before tone onset until +3.5 s after tone onset). Then, the phase angle time series were extracted and the temporal derivative was calculated (Cohen, 2014):

$$f(t) = \frac{1}{2\pi}\frac{d}{dt} arg\{H\{s(t)\}\} \qquad (12)$$

where H{s(t)} is the Hilbert transform of the EEG signal s(t) filtered in the alpha band and arg{H{s(t)}} is the unwrapped instantaneous phase angle time series. Finally, 10 median filters (linearly spaced between 10-400 ms as recommended by Cohen, 2014) were applied to filter out artefacts that are produced by taking the temporal derivative of the phase angle time series.

2.2.6 Statistics

Non-parametric cluster-based permutation statistics were applied to the instantaneous frequency when comparing correct and incorrect responses to correct for multiple comparisons across electrodes and time points (Maris and Oostenveld, 2007). The time window of interest spanned from 500 ms after tone onset until the presentation of the visual stimulus. Clusters were obtained when more than two neighbouring electrodes exceeded a threshold of $p < .025$ from a two-tailed dependent samples t-test. Instantaneous alpha frequency comparisons of correct and incorrect responses were tested two-tailed ($p < .025$). The Monte Carlo p-values of each cluster were obtained by randomly swapping condition labels within participants 2500 times. This randomization procedure is used to create a null distribution, which is subsequently used for comparison to the observed effect. For correlation analyses, we compared Fisher's z-transformed correlation values to 0.

For alpha peak frequency correct and incorrect responses to short and long intervals were compared separately through dependent samples t-tests. This statistical analysis was performed separately for the different experiments and the different regions of interest (fronto-central and posterior-occipital, see above). A mixed effects ANOVA was applied when combining the alpha peak frequency measures across both experiments to increase the power of the analysis. The mixed effects ANOVA had a 2 × 2 design, with experiment as between-subjects factor (Experiment 1 vs. Experiment 2) and interval length as the within-subjects factor (short vs. long interval). The difference in alpha peak frequency between correct and incorrect responses was used as input to the mixed effects ANOVA.

2.2.7 Instantaneous frequency and response time

Next, we asked whether fluctuations in instantaneous frequency were associated with response times. To this end, we calculated Spearman's ranked correlation between instantaneous frequency at each time point and electrode with response time. We z-transformed the rank correlation according to the formula in 2.2.5. We compared the z-scores for correct and incorrect responses and short and long intervals to 0 through a cluster based permutation test by collapsing over the time interval that was indicated by the previous analysis where we compared instantaneous frequency of correct and incorrect responses. If alpha frequency represents both the internal clock and the speed of the system we would expect shorter response times when the instantaneous frequency is higher and longer response times when the instantaneous frequency is lower.

2.2.8 Fixed effects analyses

To substantiate any null-findings a more sensitive analysis was performed by treating the data from all participants as coming from one single aggregate dataset. To this end, the epochs were cut from tone onset until visual stimulus onset and the trials were concatenated for each channel. The data was normalized through z-scoring:

$$z = \frac{x - \bar{x}}{\sigma} \qquad (13)$$

where x is the concatenated trial data at that channel, $\bar{x}$ is the averaged activity across the concatenated trial $\times$ time points, and σ is the standard deviation of that activity. After normalizing the individual participant data, the data is concatenated across participants in an aggregate dataset.

The covariance matrix of the aggregate dataset was obtained and eigenvalue decomposition was applied to the covariance matrix (i.e. principal component analysis). Next, the three eigenvectors (or eigenvariates) with the largest eigenvalues were used as the unmixing matrix, which were projected onto the aggregate dataset. Then the aggregate dataset was divided back into trials $\times$ time points and the trials were split into the conditions (short interval, correct response; short interval, incorrect response; long interval, correct response; long interval, incorrect response) they belonged to. Finally, instantaneous frequency was acquired from the data for each principal component separately. Cluster-based permutation statistics were used to correct for multiple comparisons over time (from 500 ms after tone onset until visual stimulus onset). Correct and incorrect responses for the short and long interval conditions were compared separately and the data were treated as coming from a single subject with independent samples t-test.

2.3 RESULTS

2.3.1 Behavior

Participants judged whether the time interval between a tone and a visual stimulus was short or long. For Experiment 1 (Figure 3.2A, left) we found that participants were faster on correct (μ = 354 ms) than incorrect (μ = 420 ms) responses, which came about as a main effect of response ($F(1,17) = 69.807$, $p < .001$, $\eta p^2 = .804$). We also found that participants were faster on long (1.5 s, μ = 360 ms) than short (1 s, μ = 415 ms) interval trials, as indicated by a main effect of interval length ($F(1,17) = 35.538$, $p < .001$, $\eta p^2 = .676$).

Finally, we found that participants were fastest on correctly perceived long trials, through a significant interaction effect of response x interval length ($F(1,17) = 40.882$, $p < .001$, $\eta p^2 = .706$). Post-hoc analyses showed that participants were faster ($t(17) = -11.45$, $p < .001$) on correct ($\mu = 291 \pm 11$ ms, mean ± SEM) compared to incorrect ($\mu = 429 \pm 16$ ms) trials for the long interval, but there was no significant difference ($t(17) = .3862$, $p < .7$) between correct ($\mu = 418 \pm 15$ ms) and incorrect ($\mu = 412 \pm 23$ ms) judgements on the short interval.
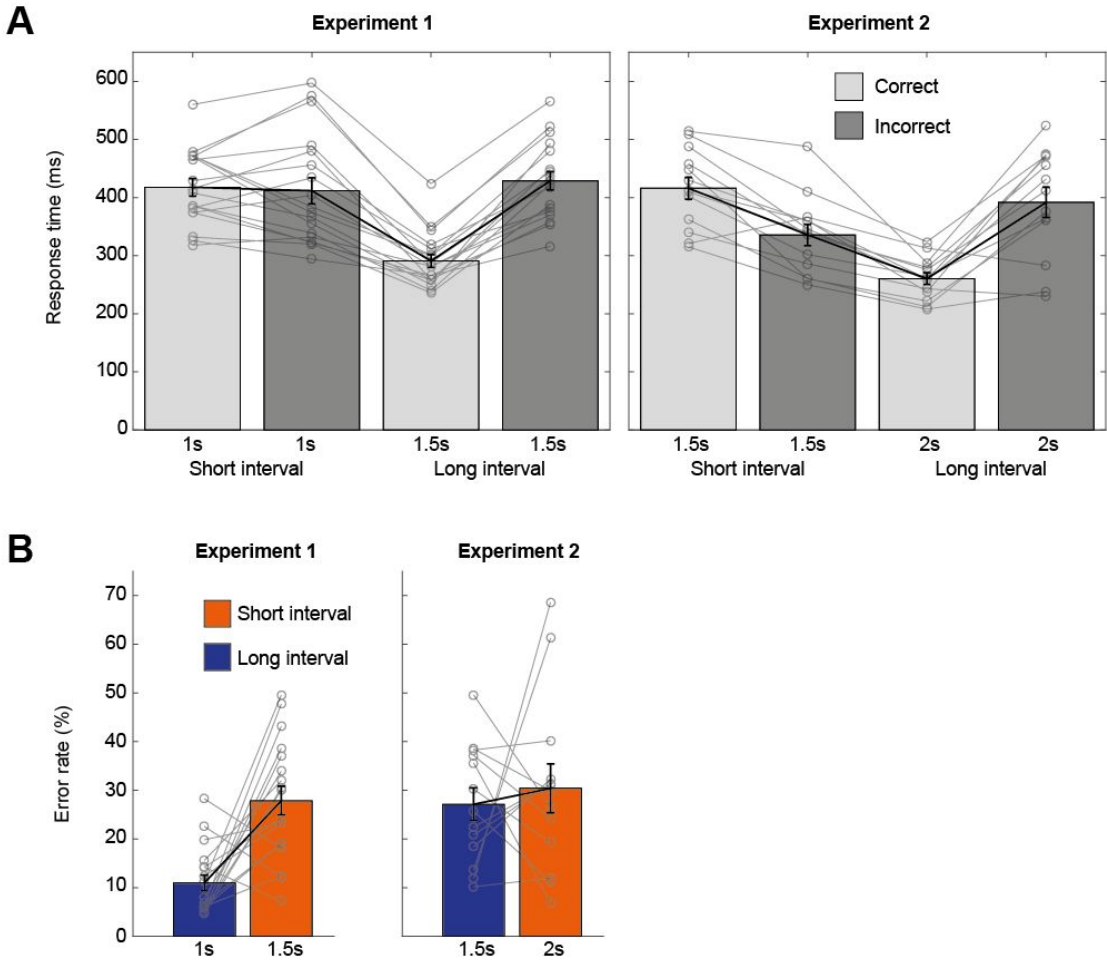
Figure 2.2 Response times and error rates for temporal discrimination of both experiments. Participants were fastest for correctly judged long interval trials in Experiment 1 (A; left). Participants were also fastest on

correctly judged long interval trials in Experiment 2 (A; right). Participants responded faster in correct (light grey) compared to incorrect judgements of the short interval in Experiment 2, but not in Experiment 1. For Experiment 1 (B; left) we found that participants made significantly more errors in the long (1.5 s) interval than in the short (1 s) interval. For Experiment 2 (B; right) we found no significant difference in error rates between long (2 s) and short (1.5 s) intervals. Error bars on all plots represent 1 standard error of the mean over participants, opaque lines and open dots represent single participant data, whereas the mean is represented in thick black lines. For response times the median was chosen to represent single participant's data.

For Experiment 2 (Figure 2.2A, right) we found roughly a similar pattern where participants responded fastest to correctly judged long interval trials, although participants now responded faster to short interval trials incorrectly judged as long compared to correctly judged as short. As a result, participants were not significantly faster on correct (μ = 338 ms) than incorrect (μ = 364 ms) responses, as shown by a trending main effect of response ($F(1,12)$ = 4.658, p = .052, ηp^2 = .280). As in Experiment 1, participants were faster (μ = 326 ms) on long interval trials compared to short (μ = 376 ms) interval trials, which came about as a main effect of interval length ($F(1,12)$ = 61.033, p <.001, ηp^2 = .836). Finally, we found that participants were fastest on correctly perceived long trials, through a significant interaction effect of response × interval length ($F(1,12)$ = 40.146, p <.001, ηp^2 = .770). Post-hoc analyses showed that participants were faster ($t(12)$ = -5.42, p <.001) on correct (μ = 260 ± 10 ms) compared to incorrect (μ = 392 ± 26 ms) trials for the long interval and we observed the opposite pattern for the short interval trials where participants were faster ($t(12)$ = 5.1, p <.001) for incorrect (μ = 336 ± 18 ms) compared to correct (μ = 416 ± 19 ms) responses.

Visual inspection of the full response time distributions of Experiment 1 showed an approximately normal distribution for response times to the short interval. Whereas responses to the long interval showed a clearer peak for earlier responses (Figure 2.3). The normally distributed response times for the short duration make it more difficult for a drift diffusion model to fit well to these data (Guy Hawkins, email communication, October 2019).
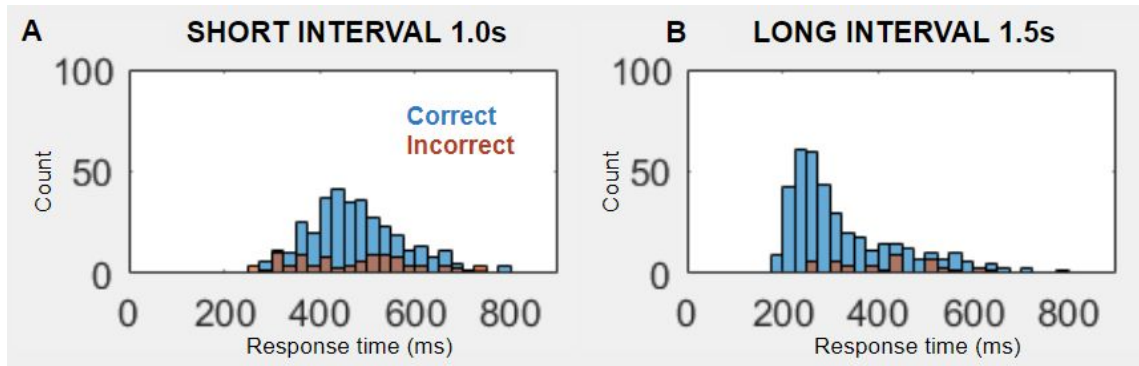
Figure 2.3 Response time distribution for an exemplar participant. Responses to the short interval presentation were approximately normally distributed (A), whereas responses to the long interval were more clustered around earlier response times (B). Correct responses in blue, incorrect responses in red.

Visual inspection of the response time distributions of Experiment 2 showed very similar dynamics to the response time distributions of Experiment 1, with the exception of a larger leading edge for the long interval choices. Note that it was more difficult to choose an exemplar participant as behavior was more variable in experiment 2 than in experiment 1 (see error rates in Figure 2.2). In the long (2s) interval of Experiment 2 participants showed more response times below 200 ms (Figure 2.4).
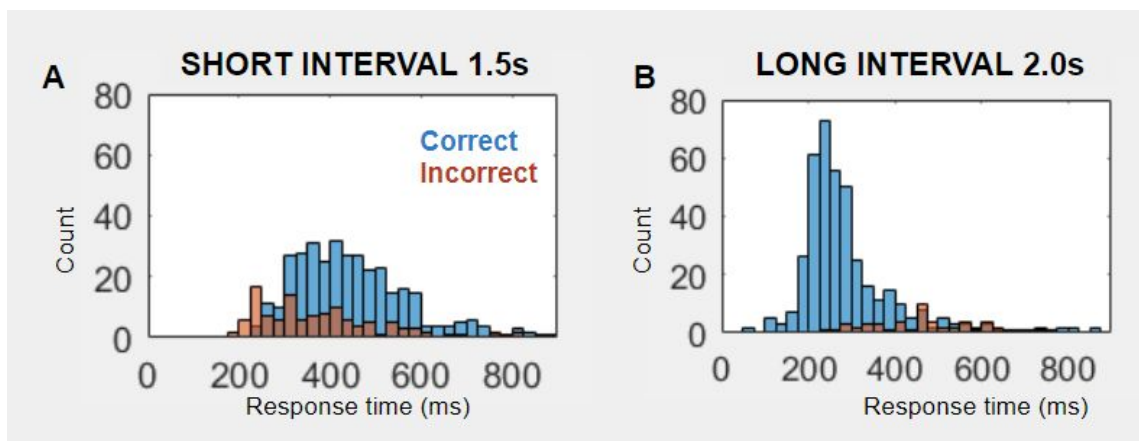
Figure 2.4 Response time distribution of an exemplar participant for Experiment 2. Responses to the short interval presentation were approximately normally distributed (A), whereas responses to the long interval were more clustered around earlier response times (B). When comparing these RT distributions to the distributions in Figure 2.3 the most striking difference is the leading edge in the correct long interval judgements. Correct responses in blue, incorrect responses in red.

To assess whether there were differences in response time distributions between the different experiments I calculated the Bhattacharyya coefficients for correct responses. These coefficients provide a measure of similarity of the response time distributions. Importantly, correct responses times were compared for short and long intervals by locking them to the real (short) or probable (long) presentation of the tone. Independent samples t-test showed that the coefficients were larger for experiment 2 (0.23 ± 0.1, mean ± standard deviation) than for experiment 1 (0.16 ± 0.08; t(29) = 2.1, p = .045; Figure 2.5), which means that the response time distributions were more similar in Experiment 2 than in Experiment 1.
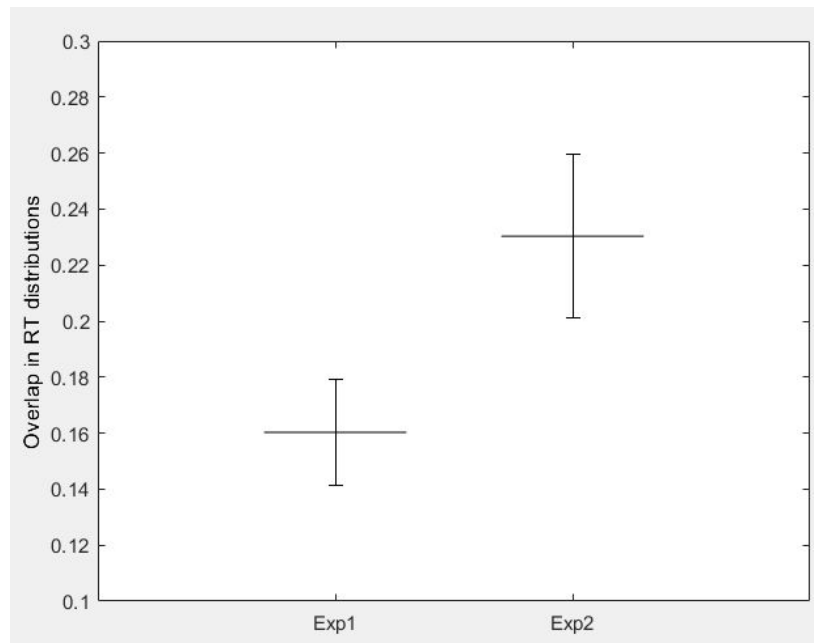
Figure 2.5 Overlap in correct response time distributions for short and long intervals was larger for Experiment 2 than 1. Error bars represent standard error of the mean.

Taken together, our response time data suggests that participants respond fastest to long interval trials that are experienced as long. Importantly, this effect is dependent on context given that we observed a different pattern for 1.5 s intervals in Experiment 1 (as the long interval) compared to Experiment 2 (as the short interval).

In addition to response times, we also looked at error rates. In Experiment 1 participants made more errors (Figure 2.2B, left; $t(17)$ = -4.32, p <.001) in the long (1.5 s, μ = 27.8 ± 2.9%) compared to the short (1 s, μ = 11.0 ± 1.6%) interval. In Experiment 2 participants did not make significantly (Figure 2.2B, right; $t(12)$ = -0.467, p >.6) more errors in the long (2 s, μ = 30.4 ± 5.0%) or in the short (1.5 s, μ = 27.1 ± 3.4%) interval. In summary, participants made ~23% errors on these tasks and participants made less errors on the 1 s interval than on longer intervals.

Finally, I examined signal detection theory measures of performance. d' values indicate whether participants are able to discriminate between short and long intervals (Figure 2.6 left plot of A and B). An independent samples t-test showed that participants obtained higher d' for Experiment 1 (μ = 1.9 ± 0.4, mean ± standard deviation) than Experiment 2 (μ = 1.2 ± 0.6; t(29) = 4.1, p < .001). Bias is a measure of participants' tendency to report one response over another (Figure 2.5 right plot of A and B). Participants showed a larger response bias in Experiment 1 (μ = 0.3 ± 0.3) than in Experiment 2 (μ = 0.0 ± 0.3; t(29) = 2.3, p = 0.023). Moreover, participants had a response bias to responding short in Experiment 1 as indicated by a dependent samples t-test that compared the bias to 0 (t(17) = 4.5, p < .001). The response bias did not differ from 0 in Experiment 2 (t(12) = 0.3, p > .05).
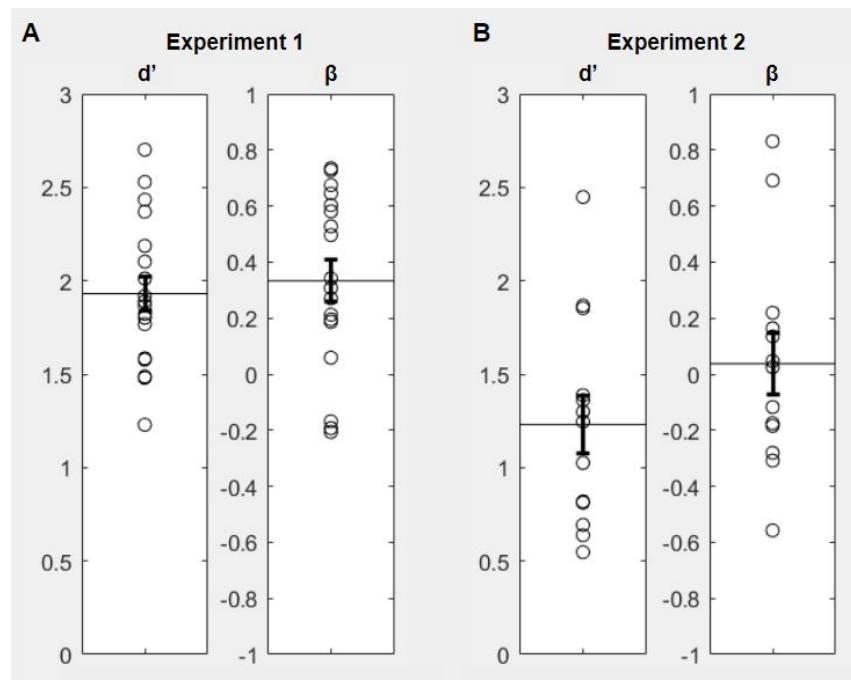
Figure 2.6 Signal detection theory measures of behavior. d' is a measure of participants ability to discriminate between long and short intervals (A and B, leftward plot) and . provides a measure of a participant's tendency to respond one response option over another (A and B, rightward plot). d' was significantly higher for Experiment 1 than Experiment 2 (compare leftward plot of A and B). ☐ was also significantly higher for Experiment 1 than Experiment 2 (compare rightward plot of A and B). ☐ was significantly different from 0 in Experiment 1 (rightward plot in A), indicating that participants had a bias to respond that they experienced a short interval.

2.3.2 Alpha frequency and the internal clock

We first calculated instantaneous frequency to examine whether the speed of alpha oscillations correlated with over- or underestimation of interval discrimination. If the speed of alpha oscillations relates to the speed of the internal clock, higher alpha frequencies should relate to temporal overestimation and lower alpha frequencies to underestimation. To this end, instantaneous frequency of correct and incorrect judgments to short and long interval trials were compared separately. In Experiment 1 no differences between correct and incorrect responses were observed in the short (1 s; one negative cluster with $p = .14$) or long (1.5 s; two negative cluster with smallest $p = 0.18$) interval (Figure 2.7A and B). In Experiment 2 the short (1.5 s) intervals showed no differences between correct and incorrect responses (Figure 2.7C; 5 positive clusters with smallest $p = .13$). The long (2 s) interval trials had instantaneous alpha frequency estimates that were higher for correct ($\mu = 10.13 \pm 0.10$ Hz) than for incorrect ($\mu = 10.03 \pm 0.095$ Hz) responses over a left-lateralized occipito-parietal cluster (Figure 2.7A; black/white inset). The difference in alpha frequency was significant ($p = .009$) and largest from 1122-1304 ms post-tone onset. This finding supports the hypothesis that lower alpha frequency is related to temporal

underestimation. However, contrary to this hypothesis, a significant cluster ($p = .006$) with the opposite effect over the same electrodes appeared from 1694-1902 ms, such that instantaneous frequency was higher in incorrect ($\mu = 10.13 \pm 0.086$ Hz) responses than correct ($\mu = 10.03 \pm 0.081$ Hz) responses (Figure 2.7D).
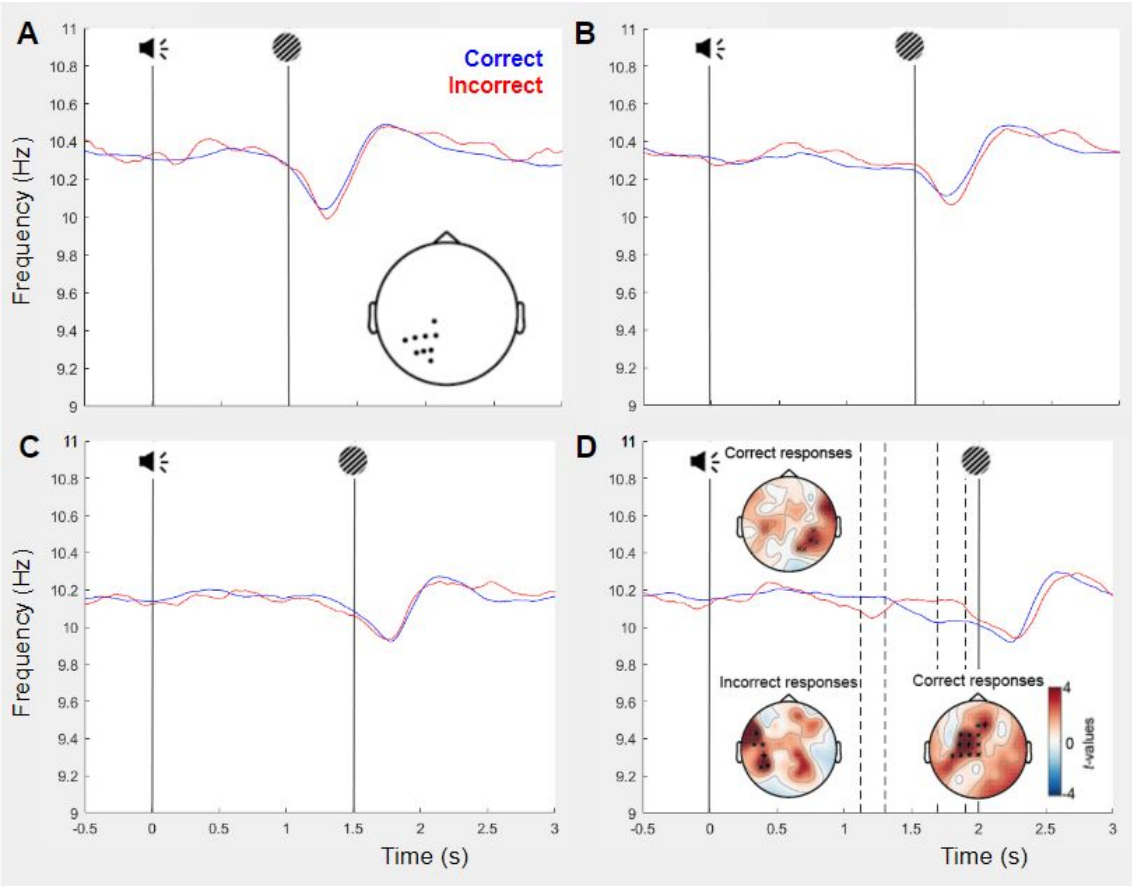
Figure 2.7 Instantaneous frequency for different interval lengths for Experiment 1 and 2. Participants discriminated trials of different lengths and instantaneous alpha frequency was estimated between 500 ms after tone onset (black line with speaker icon) until visual stimulus onset (black line with Gabor patch). Participants correctly (blue lines) or incorrectly (red lines) identified the interval length. In Experiment 1 there was no difference in instantaneous alpha frequency between correct and incorrect responses for the short (A) or the long interval (B). In Experiment 2 there was no difference in the short interval (C), but there was a

significant difference between correct and incorrect responses for the long interval (D). A positive cluster was identified, which was most pronounced from 1122-1304 ms after tone-onset. Instantaneous alpha frequency in this time window correlated positively with response times for correct and incorrect responses (see insets). In addition, a negative cluster was identified, which was most pronounced from 1694-1902 ms after tone-onset. Instantaneous alpha frequency in this time window correlated positively with response times for correct responses (see inset). This pattern was not observed for incorrect responses. * represent electrodes with significant correlation values, dotted lines represent significant time points.

Next, we asked whether the differences in instantaneous frequency we observed in the longer interval of Experiment 2 were associated with response times. If instantaneous alpha frequency reflects the speed of the internal clock, and as such is a reflection of the speed of information processing, we would expect shorter response times for trials with higher alpha frequency. However, if alpha frequency independently reflects the internal clock, and is not related to the speed of information processing, we would expect slower response times when less pulses are accumulated in the correct trials and longer response times when more pulses are accumulated in the incorrect trials. However, the results we obtained followed a mix of these predictions (Figure 2.7D; insets). For correct responses we found that in the early time window alpha frequency was positively associated (p = .01) with response times (z = 0.598 ± 0.146). For incorrect responses we found that in the early time window alpha frequency was positively associated (p = .004) with response times (z = 1.199 ± 0.245). In the later time window we found a positive association (p = .002) between correct responses and response times (z = 0.745 ± 0.124). We did not find a significant association between response times and alpha frequency for incorrect responses in the later time window.

After examining instantaneous alpha frequency we examined alpha peak frequency (APF) for task-related activity. Although APF does not have the temporal resolution instantaneous frequency has, the APF measure is easier to interpret. We examined the period after the evoked response to the tone has died out (500 ms after tone onset) until visual stimulus onset. Figure 2.8 shows the APF for occipito-parietal (top row) and fronto-central (bottom row) electrodes. We did not find any significant effects when we compared correct and incorrect responses on the long or short interval for either experiment or topographical region of interest (posterior-occipital or fronto-central; Table 2.1). Combining the data of both experiments in a mixed effects ANOVA on the difference in APF between correct and incorrect responses with interval length as a within-subjects factor (short and long intervals) and experiment as the between subjects factor also did not yield any significant effects for APF estimated at fronto-central ($p > .1$) or posterior-occipital ($p > .4$) electrodes.

Table 2.1 Alpha peak frequency for the different trial types in both experiments. FC = frontro-central, PO = posterior-occipital, C = correct, I = incorrect.

	Interval	Response	FC APF	Statistics	PO APF	Statistics
Exp 1	Short	C	9.20 ± 1.82	$t(14) = 1.74$ $p = .1$	9.80 ± 1.50	$t(13) = 0.20$ $p = .85$
		I	9.06 ± 1.98		9.65 ± 1.65	
	Long	C	9.14 ± 1.86	$t(15) = 0.83$ $p = .42$	9.52 ± 1.78	$t(16) = 1.32$ $p = .21$
		I	9.33 ± 2.17		9.20 ± 1.92	
Exp 2	Short	C	8.78 ± 1.60	$t(11) = -0.1$ $p = .92$	7.96 ± 1.27	$t(8) = 0 .09$ $p = .93$
		I	8.52 ± 1.03		7.84 ± 1.27	
	Long	C	9.51 ± 1.89	$t(11) = -0.8$ $p = .45$	7.73 ± 1.41	$t(8) = -0.08$ $p = .94$
		I	8.69 ± 1.83		8.01 ± 1.57	

Posterior-occipital electrodes

A EXPERIMENT 1

B EXPERIMENT 2

Fronto-central electrodes

C EXPERIMENT 1

D EXPERIMENT 2
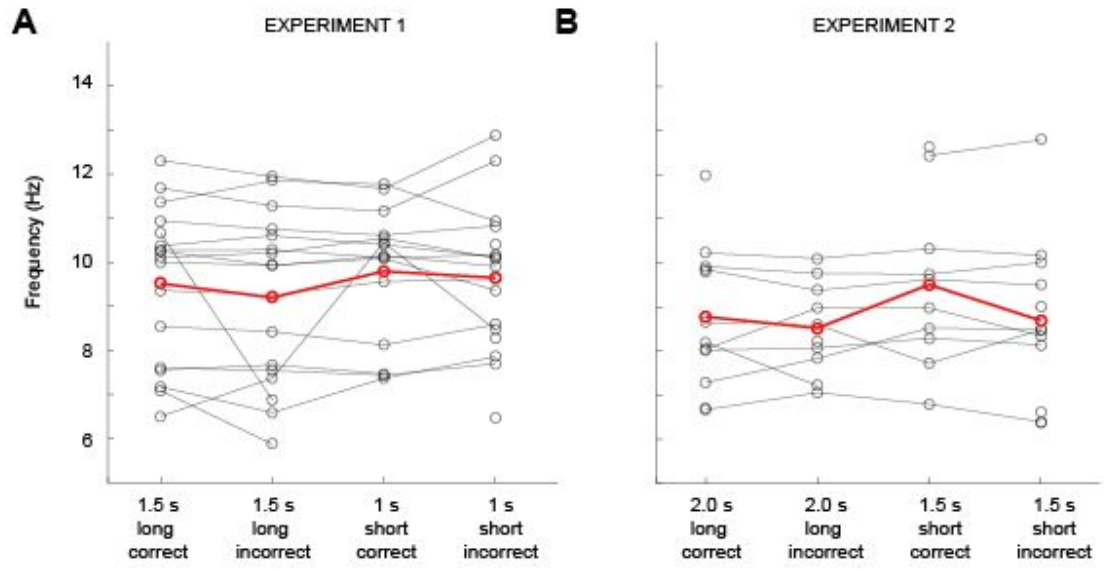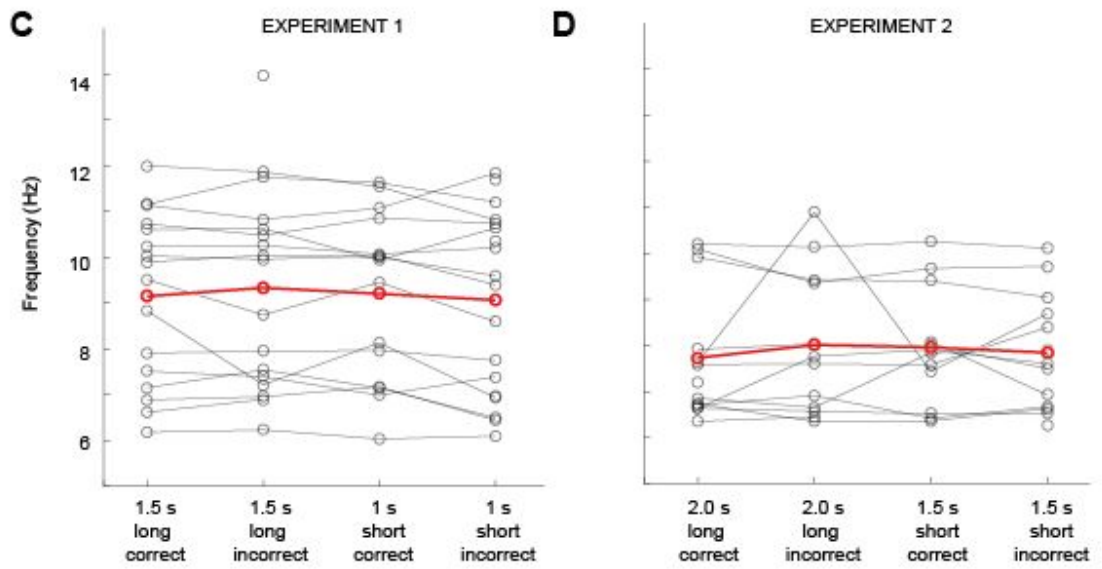
Figure 2.8 Alpha peak frequency for posterior-occipital and fronto-central electrodes. Red lines represent means without taking missing values into account. Black lines and open circles represent individual participant data.

2.3.3 Aggregate data analysis

To increase the sensitivity of the analyses and to substantiate the null-finding of the APF an aggregate dataset was created. To this end individual participant's data was normalized and all trials belonging to the same experiment were treated as belonging to one (aggregate) participant. The data dimensionality was reduced through principal component analysis and 3 eigenvectors with the highest eigenvalues were selected for further analyses. Instantaneous alpha frequency was calculated on each component separately. For Experiment 1 the 3 components explained 72.82% of the variance. Moreover, instantaneous alpha frequency of component 2 (variance explained: 18.09%) differed significantly for correct and incorrect responses for long interval trials (Figure 2.9A, bottom row, middle column, p = .008). The difference between correct and incorrect responses was most pronounced from 1272-1500 ms after tone-onset. Component 1 (Figure 2.9A, bottom row, left column; variance explained: 39.46%) and 3 (Figure 2.9A, bottom row, right column; variance explained: 15.27%) did not show differences for the long interval. Neither of the components showed any significant differences for the short interval (Figure 2.9A, top row).

For Experiment 2 the 3 components explained 63.51% of the variance. But there were no significant differences between correct and incorrect responses for the short or long

intervals for any of the components (Figure 2.9B; no clusters, variance explained per component: 34.10%, 15.17% and 14.23%).
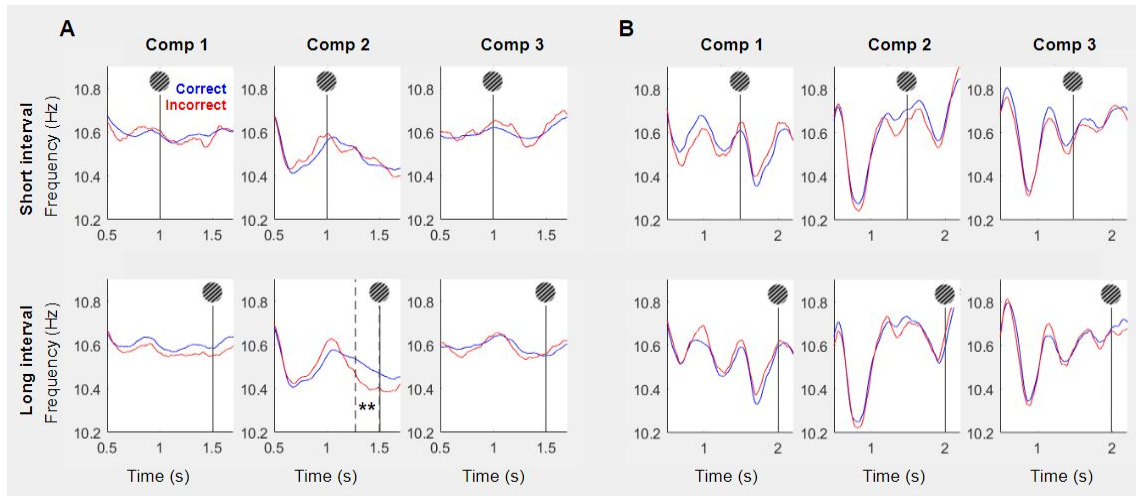
Figure 2.9 Instantaneous alpha frequency as calculated for aggregate dataset. An aggregate dataset was obtained by normalizing power for each participant and collapsing the data across participants. A PCA was applied to extract the three eigenvectors with the highest eigenvalues. Instantaneous frequency was extracted for each component separately. Data of Experiment 1 is shown in A, where the top row shows instantaneous frequency for the different components for the short interval, correct responses in blue and incorrect responses in red. No differences were found. Bottom row shows instantaneous frequency for the long interval trials. A significant difference was found for the second component, where alpha frequency was higher for correct than incorrect responses from 1272-1500 ms after tone onset (dotted lines). B shows the same analysis on the aggregate data of Experiment 2. No significant differences were found for any component or interval length. ** indicate significance, Gabor patch and black line indicate the end of the to-be-timed interval. Statistical analyses were performed from 500 ms after tone onset up until visual stimulus onset.

2.4 DISCUSSION

In line with previous results, we found that participants are capable of judging empty intervals in a temporal discrimination task (we found similar error rates to Gontier et al.,

2013, who used 450 and 550 ms time intervals). Importantly, we found that temporal discrimination depends on the context created by the task, because our experiments allowed us to compare how participants responded to 1.5 s intervals that functioned as the short or the long interval, in the two experiments. In Experiment 1 participants responded faster to 1.5 s (long) intervals if they correctly identified them as long, while in Experiment 2 participants responded faster to 1.5 s (short) intervals if they incorrectly identified them as long. This suggests that context is important for the subjective experience of elapsed time. Note though, that different participants participated in both Experiments, which might also explain differences in performance between the experiments. In addition to response time and error rate differences, signal detection theory analyses showed that participants performed better in Experiment 1 than 2, as indicated by higher d' from Experiment 1 than 2. In addition, participants showed a larger response bias in Experiment 1 than 2, where participants were more likely to respond they experienced a short interval irrespective of the physical stimulus.

Previous research has suggested that sub- and supra-second time intervals might rely on different processes, such that <1 s intervals might be processed in the motor circuitry, whereas >1 s intervals might rely on cognitively controlled processes through prefrontal and parietal brain regions (Lewis & Miall, 2003). Interestingly, we found in Experiment 1 that participants were much better at estimating time for 1 s intervals compared to 1.5 s intervals (lower error rates and higher d'). Previous research has shown that participants are better at time estimation for short intervals compared to longer ones (Gontier et al., 2013). However, in Experiment 2 we found no significant difference in error rates for 1.5 and 2 s intervals. In addition, participants were fastest to respond to long interval trials that

were correctly judged as long for both experiments. However, in Experiment 2 we found that participants were also faster on short intervals that were incorrectly judged as long. We did not observe this pattern for 1 s (short) intervals in Experiment 1, because here participants took the same amount of time to respond for correct and incorrect judgements. Taken together, these findings suggest that something special might be going on with 1 s intervals.

One potential explanation why participants are better at time estimation for 1 s time intervals in our paradigm might be that the relative difference between intervals is largest with the 1 s interval (i.e. the difference between the long and short interval in Experiment 1 is 500 ms, which is 50% of the 1 s interval, in Experiment 2 the difference between the short and long interval is also 500 ms, but that is only 33% of the 1.5 s interval). Alternatively, it might be that 1 s interval timing relies more on an automatic system, which largely depends on motor circuitry, whereas longer (>1 s) intervals rely on cognitively controlled systems, which are seated in prefrontal and parietal brain regions (Lewis & Miall, 2003). However, our response time data does not fully support this explanation. If participants were performing 1 s interval timing through a more automated system, we would expect response times for this interval to be shorter. We observed the opposite effect of response times in our data, where participants were slower for 1 s interval timing. Unless, the motor circuitry involvement in judging 1 s time intervals might hamper motor preparation and therefore might prevent any fast responses to 1 s intervals.

Time estimation as temporal evidence accumulation might explain our data better: Participants might have a template in working memory of the short interval and when the

short interval has elapsed, participants prepare a response for the long judgement. This explains why participants respond faster when they correctly judge a long interval as long. When participants incorrectly judge a long interval as short, they did not accumulate the noisy evidence of the elapsed time properly leading to the underestimation. In that case participants did not prepare the response, which makes them slower on incorrectly judged long interval trials. And the opposite is true for short intervals judged as long: participants accumulated evidence too quickly and therefore overestimated the elapsed time, but they did prepare their response. An open question is why, in line with the previous, participants respond faster on 1.5 s short intervals judged as long (incorrect) compared to short (correct) in Experiment 2, but do not speed up on 1 s short intervals judged as long (incorrect) compared to short (correct) in Experiment 1. Perhaps the 1 s interval in Experiment 1 is too short to allow for evidence accumulation and response preparation to afford any differences in response times. Or, as explained above, the 1 s interval timing might rely on motor circuitry which prevents motor preparation. But future research which controls for the relative difference between time intervals is necessary to draw a conclusion. Interestingly, the comparison of overlap of the response time distributions for correct responses to the short and long interval of both experiments showed that there was significantly more overlap in RT distributions for the second compared to the first experiment. This suggests, in line with the predictions of scalar timing theory (STT), that for longer intervals (i.e. Experiment 2) decisions have a wider distribution. It might be that participants make a probabilistic judgement in Experiment 2, instead of the categorical decision participants make in Experiment 1. However, an important limitation of the analysis and therefore the interpretation of this finding is that the analysis assumes a fixed

response latency, i.e. non-decision time, across participants. Although this does not explain why the RT distributions were found to be more similar in the second than in the first experiment.

In the current chapter we showed that instantaneous frequency differed for long (2 s) interval trials of Experiment 2. Contrary to our expectation that instantaneous frequency would be lower for long interval trials in which time was underestimated (i.e. judged as short) compared to trials that were judged correctly (as long), we found that instantaneous frequency first followed this expectation (note that this effect was marginally significant) and then flipped such that instantaneous frequency was higher for underestimated trials. Moreover, we expected that instantaneous frequency would show an inverse relationship with response time (but see for an alternative interpretation below), i.e. we expected faster response times when instantaneous alpha frequency was higher, but we only found support for a positive correlation between instantaneous frequency and response times. However, the differences in instantaneous frequency were not replicated in any of the other conditions, or experiments, or with the alpha peak frequency (APF) measure. When we repeated the instantaneous alpha frequency analyses on an aggregate dataset, we found that alpha frequency was higher for correct compared to incorrect responses in the long interval of Experiment 1. This finding was in line with our hypothesis where lower alpha frequency would be related to underestimation of time that passed by. However, these findings did not replicate for the short interval or for aggregate data of Experiment 2.

Previous research from the 60ies suggested that alpha frequency and response times should show an inverse relationship (Dustman & Beck, 1965; Callaway & Yeager, 1960).

From this, it was argued that alpha frequency might represent the speed of information processing. However, Klimesch and colleagues (1996) have argued that this relationship between APF and response times can be explained by power differences that occur during alpha desynchronization. As such, they showed that the relationship between APF and response times was spurious (Klimesch et al., 1996). Alpha frequency has also been hypothesized to reflect the internal clock (Treisman, 1963). In our data, we focused on the relationship between APF and temporal judgements, but we did not find an effect of APF. Previous research suggested that APF and time estimation might not show a one-to-one relationship (Treisman, 1984). However, more recent research suggested that it is the left-right asymmetry of APF that correlated with produced durations (Glicksohn et al., 2009). In our data we did not look at left-right APF asymmetry, but we did examine APF separately for fronto-central and posterior-occipital electrodes. However, our data do not support a direct relationship between APF and temporal decision making.

In addition to APF we also looked at instantaneous alpha frequency as this measure has a higher temporal sensitivity (Mierau et al., 2017; Cohen, 2014). We found a significant difference in instantaneous frequency for responses to long interval trials of Experiment 2. Interestingly, instantaneous alpha frequency was higher in correct responses before the short time interval had unfolded, followed by higher instantaneous alpha frequency for incorrect responses after the short interval was over. These effects make it hard to interpret the effect of instantaneous alpha frequency on time estimation. In addition, the effect was not replicated in any of the other time intervals. It might be that the shift in instantaneous alpha frequency came about through the expected onset of the visual stimulus in the short interval trials. In addition, we looked at instantaneous alpha frequency

of aggregate data and found higher instantaneous alpha frequency for correct compared to incorrect responses to long interval trials of Experiment 1. Taken together, there is some support for the idea that lower alpha frequency leads to underestimation of long time intervals. However, the support is limited since we did not observe consistent effects across intervals.

Interestingly, the limited effects observed in the current experiments were observed in long interval trials in both cases. A follow-up study should combine several (>2) interval lengths within an experiment, to see if the current findings are related to the hazard-rate that changes between short and long interval trials. Previous research has linked instantaneous alpha frequency to alpha amplitude (Nelli et al., 2017), contrary to previous claims that alpha frequency and alpha power are independent measures (Cohen, 2014). This finding further hampers the interpretation of our results. In Chapter 4 we show that there was no significant alpha power difference in the time interval in which we observed the instantaneous frequency effect. However, it might be that a power effect is present, but not consistent enough to be picked up by cluster based permutation statistics.

The low sample size of the second experiment is a short-coming of the current experiment. Another important limitation of the current design is that we cannot rule out response biases. We counterbalanced response buttons over participants, but we did not counterbalance responses within participants. It could therefore be that participants prefer judging intervals as short or long and we cannot control for it in our current design, as evidenced by □, a measure of response bias, that was significantly different from 0 for Experiment 1. Moreover, the current design also makes it impossible to discern whether

participants keep a template of the short or long interval in their mind. Alternatively, we could have used a two-interval forced choice (2IFC) design. However, these designs make comparing EEG signals for the different conditions more challenging as participants are presented with two intervals on each trial.

Instantaneous frequency has been hypothesized to be related to a decrease in spiking thresholds and an increase in spike timing variability for lower frequencies (Cohen, 2014). In addition, instantaneous frequency has been hypothesized to be associated with integration and segregation of information in the visual system (Samaha & Postle, 2015). Nelli and colleagues (2017) suggested that a change in instantaneous frequency, specifically slowing of the peak frequency, allows the desynchronization in the alpha band that is necessary for communication. Taking these findings together, it might be argued that slower alpha leads to longer windows of information integration, and thus possibly more processing. From this it might follow that instantaneous frequency might be positively correlated with response times as we observed in our data. However, our data does not provide evidence for the idea that instantaneous alpha frequency represents the internal clock.

CHAPTER 3

Do theta oscillations from medial frontal cortex correlate with behavioral adjustments after errors?

ABSTRACT

Previous research suggests that the medial frontal cortex plays an important role in performance monitoring. This makes the medial frontal cortex an excellent candidate to exert cognitive control over downstream regions after an error was committed. In addition, previous research suggests there is functional connectivity between medial frontal cortex and occipital regions through theta-alpha amplitude coupling. This finding suggests that the medial frontal cortex might influence processing in downstream sensory regions including visual cortex. However, contradictory findings about the relationship between midfrontal theta activity and subsequent behavioral adjustments have been found. Some studies found that higher midfrontal theta power correlated with faster responses on subsequent trials, while others found that midfrontal theta correlated with slower responses. In this chapter I aim to examine this relationship in more detail. Moreover, I aim to understand how the functional connectivity between medial frontal cortex and parieto-occipital regions is related to behavioral adjustments after an error. How does the medial frontal cortex exert its influence over these downstream regions? And how does the functional connectivity relate to behavioral adjustments? In line with previous results we

found that participants show behavioral adjustments after errors as measured through post-error slowing. In addition we showed that theta power is higher and alpha power more suppressed after false alarms than hits. Contrary to previous findings we did not find functional connectivity between frontal theta and occipital alpha. Moreover, midfrontal theta power was not correlated with post-error slowing.

3.1 INTRODUCTION

Some of our daily acts have become quite habitual, which can lead to mistakes, for example when sending an email without the attachment. The ability to overcome distractions and/or competing (e.g. habitual) responses in favor of coordinated, goal-directed actions is called cognitive control (Alexander & Brown, 2010; Ridderinkhof et al., 2004; Shenhav et al., 2013). Cognitive control can be subdivided into: action selection, response inhibition, performance monitoring and reward-based learning (Ridderinkhof et al., 2004). When cognitive control fails, an error might be committed leading to post-error behavioral adjustments on subsequent trials in the form of higher accuracy scores (post-error accuracy; PEA) and longer response times (post-error slowing; PES; Laming 1979; Rabbitt, 1966; Rabbitt & Rodgers, 1977).

Behavioral adaptation on post-error trials might serve an adaptive purpose to prevent future errors. The conflict-monitoring theory is an influential adaptive theory in which Botvinick et al. (2001) proposed that coactivation of the correct and incorrect responses triggers activation of the anterior cingulate cortex (ACC), which subsequently increases the threshold to respond (Botvinick et al., 2001; Wessel, 2018). The increased respond

threshold makes participants more cautious in executing automated behavior, i.e. they respond slower and more accurately. In contrast, the orienting theory proposed that errors are rare events, which ─ similarly to oddball events ─ elicit an orienting response (i.e., a response that consists of physiological changes, such as pupil dilation and increased heart rate, that are elicited by events relevant to goal-directed behavior; Notebaert et al. 2009). The orienting response is followed by reorienting to the task at hand and this process costs time thereby leading to PES (Notebaert et al., 2009). The orienting theory is supported by findings of: i) lower PEA (e.g. Hajcak & Simons, 2008; Hajcak et al., 2003; Rabbitt & Rodgers, 1977), which suggests that an error is not always followed by more cautious and more accurate responses and ii) post-correct slowing, which is observed in paradigms where correct responses are rare (Notebaert et al., 2009). Post-correct slowing suggests that PES is not specific to behavioral adjustments after an error, but might be a general occurrence of behavioral adjustments after an unexpected event instead.

At the neural level the ACC, a region on the medial wall of the prefrontal cortex, is thought to play an important role in performance monitoring (Carter et al., 1998; Dehaene et al., 1994; Devinsky et al., 1995). Neurons in the cingulate are generators of theta band activity (e.g. Tsujimoto et al., 2016) and electroencephalography (EEG) records this activity at midfrontal electrodes on the scalp (Gevins et al., 1997). Increases in midfrontal theta (4-7 Hz; MFθ) activity on false alarm trials relative to hit trials have been commonly observed in response-locked data (e.g. van Driel et al., 2012; Mazaheri et al., 2009). A recent meta-analysis found evidence in support of the intuitive idea that higher MFθ correlates positively with PES on trials that follow the error (Cavanagh & Shackman, 2015). However, a recent study that looked at the correlation between MFθ and post-error slowing found the

opposite effect (Valadez & Simons, 2018, see also Narayanan et al., 2013): greater MFθ power was associated with less slowing on the post-error trial.

A possible explanation for these divergent findings may be the way PES is calculated (Schroder et al., 2019). Dutilh and colleagues (2012) showed that the traditional measure of PES, which takes the difference between response time (RT) on trials that follow false alarms and trials that follow hits ($PES_{TRADITIONAL} = MRT_{Post-error} - MRT_{Post-correct}$), is affected by time-on-task (e.g. fatigue or motivation). To counter time-on-task effects Dutilh et al. (2012) proposed to calculate PES as the difference between hits preceding the false alarm and hits following the false alarm ($PES_{ROBUST} = MRT_{Post-error} - MRT_{Pre-error}$). Valadez & Simons (2018) used PES_{ROBUST} but the meta-analysis of Cavanagh & Shackman (2014) correlated MFθ with RT on the post-error trial directly ($PES_{Error\ Trial}$ in Schroder et al., 2019). Moreover, the meta-analysis of Cavanagh & Shackman (2014) combined many different studies in their analyses, but Valadez & Simons (2018) performed their analyses on an Eriksen flanker task. Different processes may underlie errors on a flanker task (Maier et al., 2019), where target processing is influenced by congruent or incongruent distractors, compared to errors on a go/no-go task, where errors are likely due to prepotent response tendencies (Robertson et al., 1997).

Previous research used drift diffusion modeling (DDM) to understand what mechanism underlies PES (Dutilh et al., 2011). DDMs use response time distributions and accuracy scores to understand what latent psychological processes underlie behavior. DDMs assume that noisy sensory evidence is accumulated until enough evidence is accumulated in favor of one of the response thresholds. Dutilh and colleagues (2011) found that PES is

related to response caution, i.e. after an error participants become more cautious, which supports the conflict-monitoring theory of Botvinick et al. (2001). Cavanagh & Shackman (2014) also interpreted the correlation of MFθ and PES along these lines: Higher MFθ represents a shift in the starting point of the DDM. Valadez & Simons (2018) proposed that MFθ is related to the speed of evidence accumulation (i.e. drift rate) on post-error trials such that higher MFθ leads to a steeper drift rate on the following trial.

Turning next to the potential mechanisms by which MFθ might affect evidence accumulation, previous research showed that response-locked midfrontal theta increases are followed by alpha (~8-12 Hz) suppression on false alarm compared to hit trials (Carp & Compton, 2009; van Driel et al., 2012; Mazaheri et al., 2009). Moreover, Mazaheri and colleagues (2009) found that stronger increases in MFθ activity were correlated with larger parieto-occipital alpha suppression. Importantly, stronger alpha suppression has been linked to higher cortical excitability (Mazaheri & Jensen, 2010; van Dijk et al., 2008). Functional connectivity between MFθ and parieto-occipital alpha suggests that MFθ might influence sensory processing in lower-order regions by adapting cortical excitability of those downstream regions. Although the functional connectivity provides some insight into the network dynamics of cognitive control, it does not directly address the question how MFθ influences sensory processing or attention processes in down-stream regions during post-error behavioral adjustments.

The first aim of the current study therefore was to correlate single-trial measures of midfrontal theta activity collected with a go/no-go task with single-trial measures of PES_{ROBUST} (see also Navarro-Cebrian et al., 2013 or van den Brink et al., 2014 for an

application of PES$_{ROBUST}$). The second aim of the current study was to examine how midfrontal theta exerts its influence over motor and sensory regions on post-error trials. If MFθ implements the response caution in post-error trials directly, we would expect that single-trial MFθ is positively correlated with PES. Alternatively, MFθ might implement response caution by manipulating cortical excitability in primary sensory regions. In this case, we might not observe a direct relationship between MFθ and PES, but we would predict a positive correlation between the strength of functional connectivity as measured between MFθ and parieto-occipital alpha on the one hand and PES on the other.

3.2 MATERIALS & METHODS

3.2.1 Participants and EEG Procedure

A total of 19 participants participated in this study (13 female), with a mean age of 28 years ($SD \approx 11$ years). Participants had normal or corrected-to-normal vision and were right-handed according to their Annett Hand Preference Questionnaire (AHPQ; Annett, 1970) scores. Before commencing the experimental procedure, participants gave written informed consent in accordance with the local ethics committee guidelines of the University of Birmingham. The EEG cap (WaveGuard™ 10-20 system, ANT Neuro, 2016) with 64 Ag/AgCl electrodes was fitted to the participant and the impedance of the electrodes was adjusted to be below 20 kΩ. Scalp channels were referenced to electrode CPz during the recording and data was sampled at 500 Hz. Horizontal eye movements were measured with horizontal EOG channels, which were placed on the left and right outer canthi of the participant. Participants received a brief explanation of the task before they were moved to the testing room. In the testing room, participants performed a short practice block of 50 trials, to assure they understood the task before commencing the

actual experiment. Participants performed 10 blocks of 200 trials, leading to a total of 2000 trials.

3.2.2 Stimuli

In this experiment we used a modified version of the Go/No-Go task, implemented with Presentation software (Figure 3.1; Presentation, Version 0.70, Neurobehavioral Systems, Inc.). In a Go/No-Go task participants are required to press a button on most trials (Figure 3.1A; "Go") and to withhold a response on some trials (Figure 3.1B; "No-Go"). Typically, participants make false alarms (FA), by responding to a No-Go stimulus, because the frequent appearance of the Go stimulus is lulling participants into an automatic tendency to respond. In this task participants were presented with 1330 Go trials and 670 No-Go trials (i.e. 33.5% No-Go trials per block).

A go stimulus

1000 ms or until button press

700 ms

Time

B no-go stimulus

1000 ms or until button press

700 ms

Time

C

Trial types	button press	no button press
go (66.5%)	hit (99.7%)	miss (0.3%)
no-go (33.5%)	false alarm (9.9%)	correct rejection (90.1%)
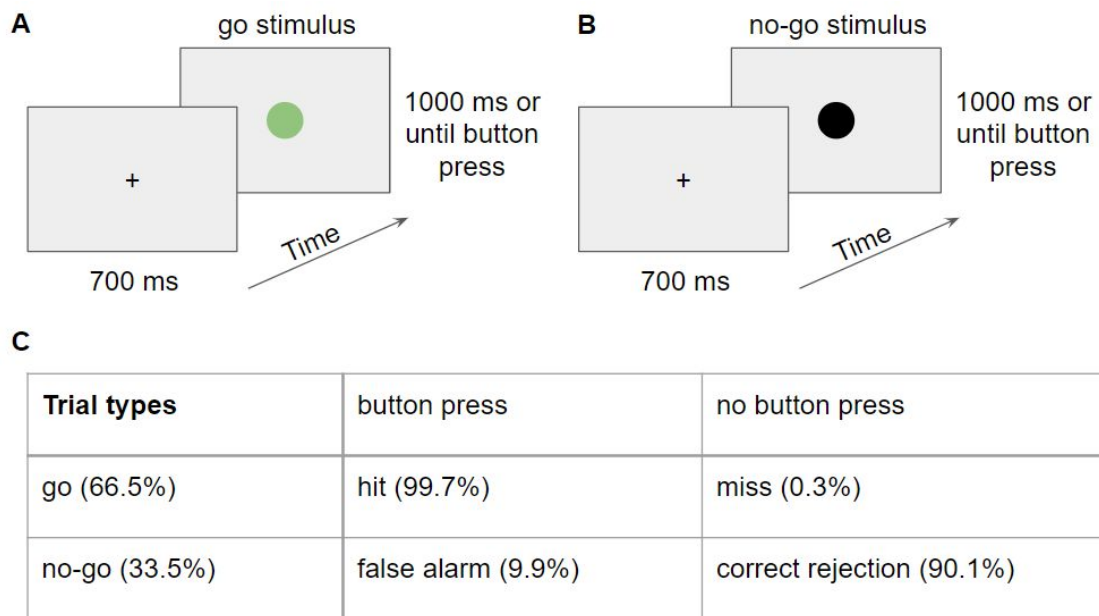
Figure 3.1 Go/No-Go paradigm. Participants were presented with Go stimuli (red, blue or green circle) on 66.5% of trials, which required participants to respond through a button press with their right index finger (A). Go trials could lead to hits (99.7% on average) and misses, but misses were very rare (0.3% on average; C). The no-go stimulus consisted of a black circle (B), which was presented on 33.5% of trials and led to correct rejections (90.1% on average) if participants withheld their response or false alarms (9.9% on average) if participants incorrectly pressed the button (C). We examined the EEG signal of the period directly following a button press (i.e. hits and false alarms). Stimuli were always ~1.4° (not to scale in this figure).

Participants were seated ~80 cm from the computer screen. In this experiment, the Go stimulus consisted or a red, green or blue circle with a visual angle of ~1.4°. The No-Go stimulus consisted of black circle of the same size. Participants responded by pressing the left mouse button (Razor Synapse) with their right index finger. Stimuli were presented for

1000 ms or until a response was made. After the button press or stimulus offset, an inter-trial interval of 700 ms followed before the start of the next trial.

3.2.3 EEG data preprocessing

The acquired EEG data was preprocessed offline and analysed in Matlab with custom scripts and functionality from the EEGLAB (Version 14.1.1; Delorme & Makeig, 2004) and Fieldtrip (Oostenveld et al., 2011; http://fieldtrip.fcdonders.nl) software packages. A high-pass filter of 0.1 Hz was applied to the data as implemented through the eegfiltnew functionality of EEGLAB. The data was then sliced in epochs locked to the button press from -1 to +2.5 s. A baseline correction in the temporal domain of -100 to 0 ms was applied to attenuate slow drifts. Manual inspection of the data was used to remove trials that: *i*) contained eye blinks upon stimulus presentation, *ii*) contained electrode jumps or *iii*) slow drifts. In total an average of ~18.5% of data was removed due to excessive noise. The average reference was calculated from the cleaned data through the reref functionality of EEGLAB. EOG, M1 and M2 were not included in the average reference. After manual trial rejection, independent component analysis (ICA; Bell & Sejnowski, 1995) was used to subtract blinks and muscle artefacts from the data. To this end, data was transferred to Fieldtrip and a principle component analysis (PCA) of 15 components was applied to reduce data dimensionality. The ICA was performed with the runica method as implemented in Fieldtrip.

After preprocessing the data, 1 participant was excluded because they missed more than 5% of trials, 2 participants were excluded because they made more than 10% false alarms and finally 1 participant was excluded because they made less than 20 false alarms.

Fifteen participants remained and all of the analyses presented below were performed on these 15 participants unless noted otherwise. For the EEG analyses trial counts and response times were matched by taking a subset of hits that corresponded to the trial counts and RT of false alarms, to make sure that any differences between hits and false alarms were not due to response time differences between these trial types.

3.2.4 Behavioral analyses

The table in Figure 3.1C shows that Go stimuli could be followed by a go-response (i.e. button press), which counted as a hit, or the stimulus could be followed by no response (i.e. no button press), which was counted as a miss. No-go stimuli could be followed by no response, which was counted as a correct rejection, or the stimulus could be followed by a go-response, which was counted as a false alarm. False alarms happened on 9.9% of the no-go stimuli. Double errors (a false alarm after a false alarm) were very rare and were not taken into account for any further analyses. Misses were also rare in this task (Figure 3.1), which makes the data unsuitable for modelling with drift diffusion models.

Signal detection theory analysis was used to calculate d' and bias (Green & Swets, 1966; Macmillan & Creelman, 2004), where d' is a measure of sensitivity or the ability to separate the go stimulus from the no-go stimulus:

$$d' = z(H) - z(FA) \qquad (1)$$

When stimuli are easy to discriminate, d' will be high and when task difficulty is high and stimuli are difficult to distinguish d' will be low. In line with previous research I expect to observe a high d', because the go/no-go stimuli are easy to discriminate (Kaiser et al.,

2003; Schulz et al., 2007; Wiemers & Redick, 2019). Bias (β) is a measure of a participant's inclination to prefer one response option over another:

$$\beta = -\frac{|z(H) + z(FA)|}{2} \qquad (2)$$

When β is close to 0, participants don't show a preference for one response over the other. A negative β indicates a bias towards the go response. In line with previous research I expect to find a negative bias, because participants were presented with more go than no-go stimuli (Young et al., 2018). Perfect hit (H = 1) and false alarm (FA = 0) rates were corrected with the $\frac{1}{2}N$ rule (Stanislaw & Todorov, 1999).

Response times were calculated as the difference between stimulus onset and button press for false alarms and hits. A dependent samples t-test was used to assess statistical differences. Previous research has consistently found that participants are faster on false alarms than hits for go/no-go tasks (van Driel et al., 2012; Manly et al., 1999; Mazaheri et al., 2009; Robertson et al., 1997), which I expected to replicate in the current study. Interestingly, some researchers have interpreted these results as a higher likelihood of errors for short RTs (e.g. Mazaheri et al., 2009 under the heading Behavioral Data). However, recent examination of response time distributions showed that this conclusion was made prematurely (Hawkins et al., 2019). Hawkins and colleagues (2019) indeed found that participants are on average faster on false alarms than hits, but due to the task-structure of the sustained attention to response task short RTs were in fact more likely to belong to hits than false alarms. To examine response time distributions for the go/no-go task in more detail I plotted defective cumulative distribution functions (CDFs) for hits and false alarms. For defective CDFs the final position on the y-axis of a response

distribution is determined by the total probability of that response (i.e. the CDF is scaled to the hit rate for hits and the false alarm rate for false alarms). This allows comparison of the cumulative distributions of two populations that have unequal sizes.

In addition, we examined whether participants adjusted their behavior upon making a false alarm. To this end, we calculated two measures of post-error slowing: $PES_{TRADITIONAL}$ = $MRT_{Post\text{-}error}$ - $MRT_{Pre\text{-}error}$ and PES_{ROBUST} = $MRT_{Post\text{-}error}$ - $MRT_{Pre\text{-}error}$, where MRT stands for median response time. Previous research has shown that PES_{ROBUST} might be more robust against time-on-task effects such as motivational and drowsiness fluctuations (Dutilh et al., 2011). Van den Brink and colleagues (2014) showed that both measures of PES are highly correlated. We expected to observe PES with both measures and we expected to replicate the previous correlation between these measures. We used dependent samples *t*-tests to assess statistical significance by comparing PES to 0.

3.2.5 EEG analyses

In order to eliminate volume conduction a spherical spline surface Laplacian was applied to obtain current source density data (Perrin et al., 1989). Then, power was estimated using the FieldTrip function 'ft_freqanalysis_mtmconv' for each trial by performing a fast Fourier transform (FFT) with a Hanning taper and a sliding time window. The time window was adapted to the frequency of interest (ΔT = 3/*f*). The frequency range of interest spanned from 2 to 30 Hz in steps of 1 Hz. I used non-parametric cluster based permutation statistics to compare false alarms and hits. False alarms and hits were matched on trial counts and response times.

To assess whether low-frequency differences were due to oscillatory activity and not due to phase-locked differences evoked by the response a control analysis was performed. To obtain the non-phase-locked power, the evoked response was subtracted from single trial data and then the time-frequency decomposition was applied as described above. There are different ways to get to the non-pase-locked (or induced) power and this method was chosen due to its ease of implementation and application in previous papers (Cohen & Donner, 2013; Cohen, 2014).

3.2.6 Correlation with behavior

The functional localizer of any power differences between false alarm and hit trials was used to examine whether post-error neural signatures would correlate with behavioral adjustments on trials following false alarms. This analysis was performed only for those frequency bands that showed a significant difference between false alarm and hit trials. We performed this analysis by calculating Spearman's ranked correlation value between power in the frequency band of interest on the false alarm trial and response time on the subsequent trial for every time point at every electrode. We normalized the correlation values by calculating Fisher's *z*-score following two steps:

$$z = .5 * ln(\tfrac{1+r}{1-r})$$

where ln is the natural logarithm and *r* is the Spearman correlation. Next, we divided *z* by the given standard error:

$$\sigma = \tfrac{1}{\sqrt{(N-3)}}$$

This yielded *z*-scored topographies at every time point and we used non-parametric cluster based time-locked statistics to assess whether there was a significant difference between

the average *z*-score (averaged over the time window of interest) by comparing this to 0 (and/or to the z-scored correlation values obtained for hit trials; Maris and Oostenveld, 2007, see below).

For the theta to alpha anti-correlation we first correlated theta power at the electrodes that showed the largest theta difference at 4 Hz from 0-200 ms between hits and false alarms, the theta seed, with all other electrodes at alpha power at 10 Hz for all time points (from -1 to + 2.5 s). We choose these frequencies of interest because they were in line with what we observed in our data and what was observed in previous research (Mazaheri et al., 2009). Moreover, we wanted to limit the chance of spurious correlations because the frequencies of interest were too close together. We therefore chose frequencies of interest that were as far away from each other as possible, but that still fell comfortably within the frequency bands identified by the functional localizer. Note though, that spurious correlations due to frequency smearing would come about as a positive correlation and we expect a negative correlation where higher theta power leads to lower alpha power. Power at 4 Hz was averaged from 0-200 ms post-response and was correlated with 10 Hz power at each electrode and time point separately across trials. Similar to the correlation analysis with response times, we calculated Spearman's ranked correlation values and applied Fisher's *z* transform. We averaged the *z*-scores across the different seed electrodes and assessed whether these *z*-scores were significantly different from 0 (or significantly different to the z-scored correlation values obtained for hit trials) with non-parametric cluster-based permutation statistics, 200-500 ms after the button press.

To increase the sensitivity of the power-power correlation analysis and to reduce the chance of missed effects due to volume conduction, the analysis was repeated on orthonormalized data. To this end, a Gram-Schmidt process was applied in the time domain, after calculating the current source density in the preprocessing pipeline (see Hipp et al., 2012 for an application on MEG data). For each of the three seed electrodes (FCz, FC2 and Cz) and for each trial separately, the single-trial activity at the seed electrode, e.g. FCz, was projected onto all other electrodes separately, e.g. Oz. Then, the projection was subtracted from the data at electrode FCz to obtain the orthogonal signal. The same procedure was applied in the opposite direction (i.e. from Oz to FCz) and the average of the orthogonal signal was stored and used to extract power as previously (see above).

3.2.7 Debiased weighted PLI as a measure of functional connectivity

In addition to the power-power connectivity analysis described in the previous section, a phase based measure of functional connectivity was used to assess the connectivity from midfrontal electrodes to other regions. Debiased weighted phase lag index (dwPLI; Stam et al., 2007; Vinck et al., 2011) was used to assess functional connectivity from midfrontal electrodes (FCz and Cz) and from parieto-occipital electrodes (PO3 and PO4) to all other electrodes for hits and false alarms (separately for the electrodes and conditions mentioned). The PLI measures how the phase angle differences are distributed on the imaginary axis of the complex plane. PLI is calculated as the absolute value of the sign of the imaginary part of the cross-spectral density. PLI can range from 0 to 1, where 0 indicates of random phase angle differences or zero phase-lag (i.e. volume conduction) and 1 indicates a perfect lag between electrodes. dwPLI is a variant of PLI, where the sign

of the phase angles are scaled with the magnitude of the imaginary component, such that phase angle differences close to the real axis (i.e. with phase angle differences close to 0° or 180° or 0 phase lag) are given less weight and a positive bias for low PLI values is controlled (Vinck et al., 2011). dwPLI was calculated with the ft_connectivity_wpli function of FieldTrip.

3.2.8 Non-parametric cluster-based statistics

We used non-parametric cluster-based statistics (Maris and Oostenveld, 2007) for significance testing, because this method corrects for the multiple comparison issue that arises when having many electrodes and time points. For time-frequency comparisons of false alarm and hit trials, the power was averaged over the frequencies and time points of interest at each electrode. Clusters were obtained when more than two neighbouring electrodes exceeded a threshold of $p < .025$ from a two-tailed dependent samples t-test. The Monte Carlo p-values of each cluster were obtained by randomly swapping condition labels within participants 2500 times. This randomization procedure is used to create a null distribution, which is subsequently used for comparison to the true effect. For correlation analyses, we compared false alarm and hit trials to each other or to 0. We specified in the text below whether we averaged over a time window of interest or whether we explored the time window of 0-0.5 s after the button press.

3.3 RESULTS

3.3.1 Participants slow down after commission errors

In line with previous research, participants were significantly faster on false alarm trials (see Figure 3.2A for RT distributions of an exemplar participant; M = 258.7 ms ± SD = 24.2, where M is the mean across participants of the median within participants and SD is the standard deviation across participants) than on hit trials (M = 305.3 ms ± SD = 23.8, $t(14)$ = 8.90, p < .001). Moreover, signal detection analyses showed that participants were well able to discriminate go- and no-go stimuli, as indicated by the high d' (M = 4.32 ± SD = 0.50). In addition, participants had a tendency towards the go response, as indicated by the negative β (M = -0.84 ± SD = 0.22).

Previous research showed that faster average responses on false alarms than hits does not necessarily mean that fast responses are more likely to be erroneous (Hawkins et al., 2019). Defective cumulative density functions of the current data showed that participants are not more likely to commit an error than to make a correct response on fast responses (Figure 3.2).

To make sure that behavioral and EEG measures of post-error trials were not affected by differences in response time on the error trials, we matched response times of hits to the response times of false alarms.
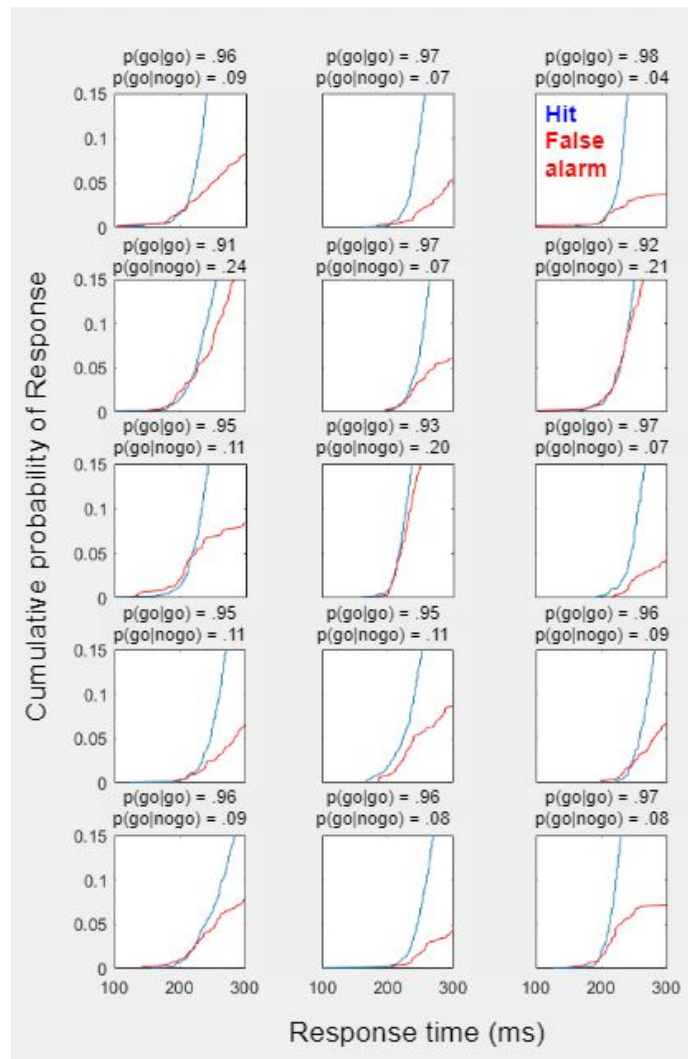
Figure 3.2 Defective cumulative density functions for hits and false alarms of single participants. On average participants respond faster on false alarms than hits (not shown here, but see Figure 3.3), but inspection of the cumulative density functions plotted until the hit (blue) and false alarm (red) rates indicates that a fast response is not more likely to be erroneous. Panels show individual participant data, where cumulative probability is plotted as a function of response time. Above the plot the probability of a hit (i.e. p(go|go)) and false alarm (i.e. p(go|nogo)) is shown for each participant.

Both measures of PES showed that participants slowed down after committing an error (Figure 3.3C). $PES_{TRADITIONAL}$ takes the difference between hits that followed false alarms and hits that followed hits. Participants were 19.9 ms (SD = 32.7 ms) slower on hits that followed false alarms than on hits that followed hits ($t(14)$ = 2.36, p = .035). PES_{ROBUST} is calculated as the difference between hits that followed and hits that preceded the false alarms. Participants were 29.5 ms (SD = 29.1 ms) slower on hits that followed false alarms than on hits that preceded the false alarm ($t(14)$ = 3.92, p = .0015). Moreover, Spearman ranked correlation showed that both measures of PES were significantly correlated (Figure 3.3D, r = 0.72, p = .0027).

Finally, we found that hits that preceded false alarms (M = 285.1 ms ± SD = 20.1) were significantly faster than hits that preceded hits (M = 308 ms ± SD = 25.5; $t(14)$ = -4.05, p = .0012; Figure 3.3C).
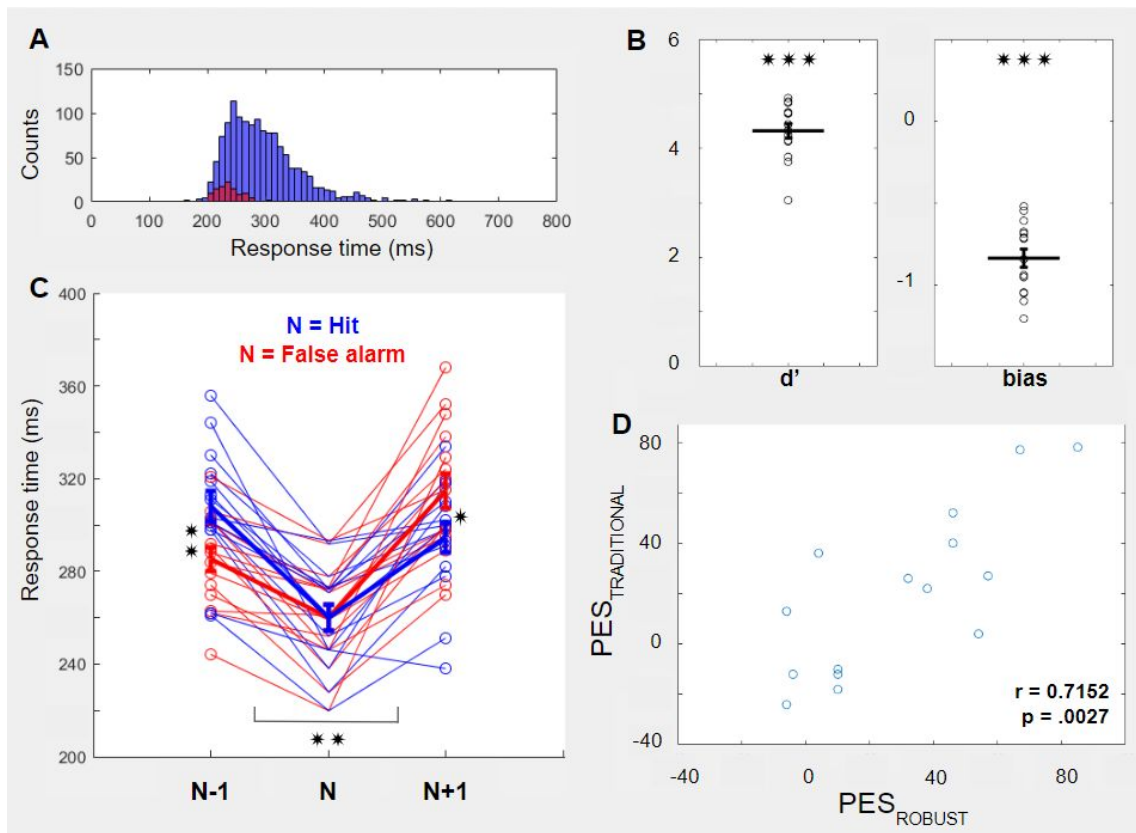
Figure 3.3 Behavioral results on Go/No-Go task. Full response time distributions showed that participants made little responses faster than 200 ms. Response time distribution of hits (in blue) and false alarms (in red) for an exemplar participant is shown in A. Signal detection analyses showed that participants are good at the task, as shown by d' scores (B, left). Participants also expressed a bias toward the go response (B, right). When response times (RT) were matched for hits and false alarms on the current trial (N), participants were significantly faster on hits that preceded (N-1) false alarms compared to hits (C). PES$_{TRADITIONAL}$ is measured as the difference between hits that followed false alarms and hits that followed hits. Participants were significantly slower on hits that followed false alarms compared to hits that followed hits (C). PES$_{ROBUST}$ is measured as the difference between hits that preceded and hits that followed the false alarm. Participants were significantly slower on hits that followed false alarms compared to hits that preceded false alarms (C). PES$_{TRADITIONAL}$ and PES$_{ROBUST}$ were significantly correlated with each other (D). * indicate significance such that * = p < .05, ** = p

< .01 and *** = p < .001. Error bars represent standard error of the mean, dots represent individual participants (which show the median for response times in C), thick lines represent the mean across participants.

3.3.2 Increased theta power and decreased alpha power after committing a false alarm compared to hits

I compared false alarms and hits locked to the response to examine whether there are post-response differences in neural signatures as measured with EEG after an erroneous vs. correct button press. Cluster-based permutation statistics identified a positive cluster ($p = 4×10^{-4}$) that spanned several frequencies from the delta to alpha frequencies (2-14 Hz; Figure 3.3B). The cluster extended from 0-500 ms after the response and spanned across most electrodes. In line with previous research I found that this difference was most pronounced in the theta range (3-7 Hz; Figure 3.3B), from 50-200 ms and over electrode FCz, FC2 and Cz (Figure 3.4C). Moreover, I found a negative cluster ($p = .029$; Figure 3.4A, cluster ii) that spanned the alpha/low beta range (8-20 Hz), where power is lower after false alarms compared to hits from 200-450 ms post-response. The negative cluster spanned parietal, parieto-occipital and occipital electrodes. The negative difference was most pronounced in the alpha band (9-13 Hz; Figure 3.4D) over occipital electrodes (Figure 3.4E).

In line with previous results, the difference between false alarms and hits in the theta range seems to be driven by higher power over midfrontal electrodes for false alarms compared to hits (Figure 3.5). The difference between false alarms and hits in the alpha range seems

to be driven by lower alpha power over occipital regions for false alarms than hits (Figure 3.6).

To make sure that the differences between false alarms and hits are oscillatory in nature, a control analysis was done, where the same cluster-based permutation analysis was performed on data where the time-frequency representation of the evoked related potential (ERP) was subtracted from the total power (Cohen, 2014; Cohen & Donner, 2013). By subtracting the ERP from single trial data and subsequently performing time-frequency decomposition, the phase-locked power (ERP) is subtracted from the total power and the non-phase-locked power remains. As in the total power, a positive cluster (i.e., cluster i from the total power analysis, $p = 4 \times 10^{-4}$) from 0-500 ms, spanning 2-14 Hz and all frontal and central electrodes was identified (Supplementary Figure 3.1; cluster i). A negative cluster (i.e., cluster ii from the total power analysis, $p = .055$) in the alpha range (9-13 Hz, 300-450 ms spanning right lateralized parieto-occipital electrodes) no longer reached statistical significance (Supplementary Figure 3.1; cluster ii). But when comparing total and non-phase-locked power it becomes clear that the ERP has only a small influence on the difference between false alarms and hits (Supplementary Figure 3.2 and 3.3).
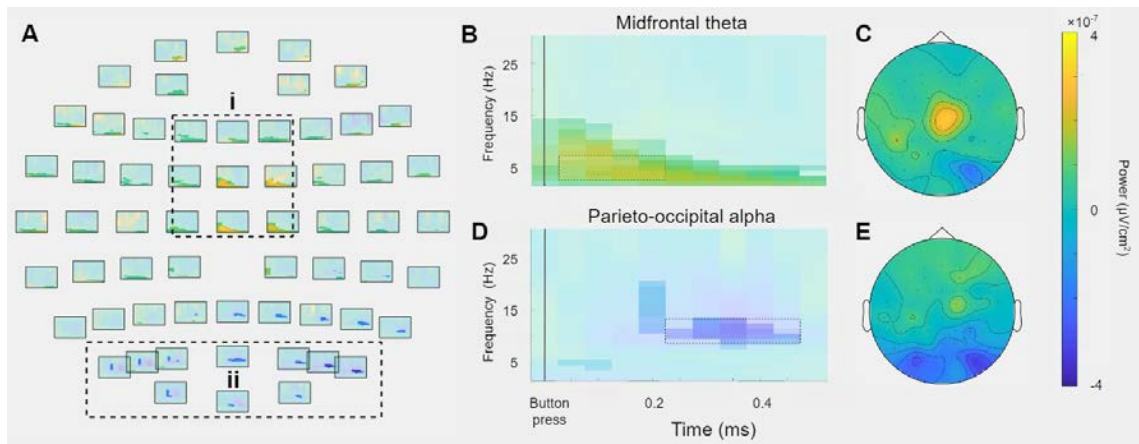
Figure 3.4 Post-response differences in midfrontal theta and parieto-occipital alpha between false alarms and hits. In line with previous results non-parametric cluster-based statistics identified a positive and negative post-response difference between hits and false alarms. The multiplot shows the time-frequency representations at each channel, where non-significant time-frequency points are masked (A, critical p-value at .05). For visualization purposes I honed in on the significant difference as indicated by the cluster-based permutation analysis. The positive difference (cluster i) was most pronounced over FCz, FC2 and Cz (C) and spanned the delta and theta band from 3-7 Hz from 50-200 ms after the button press (B). The negative difference (cluster ii) was most pronounced over parieto-occipital electrodes (E) and peaked later in time than the positive difference (200-450 ms; compare B and D). The negative difference was most pronounced in the higher alpha range 9-13 Hz (D).
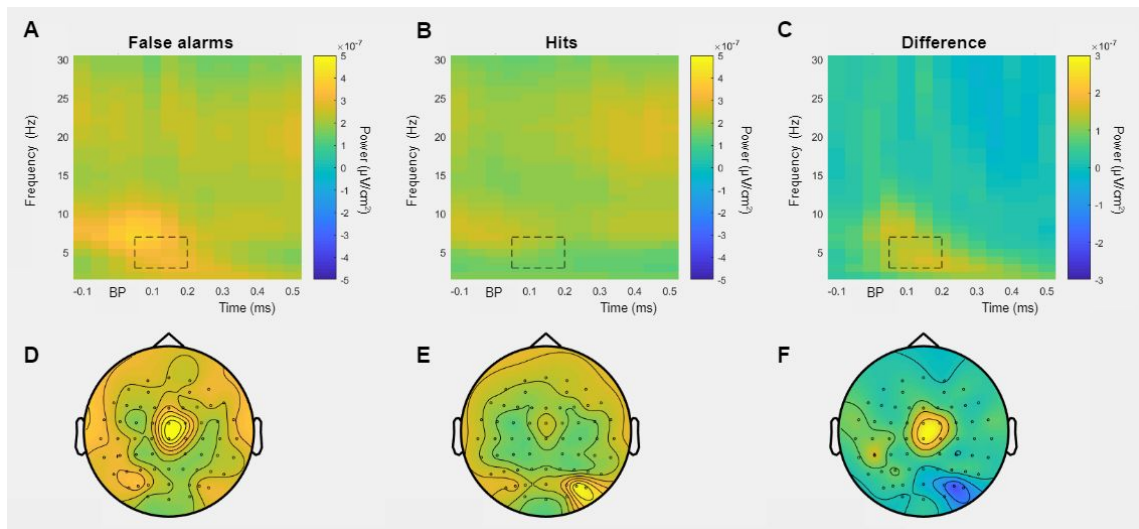
Figure 3.5 Early post-response differences between false alarms and hits in the theta range. The individual conditions are shown for the largest positive differences between false alarms and hits (cluster i from Figure 3.3). Average activity from electrodes FCz and Cz is shown for individual conditions (A, false alarms and B, hits) and the difference (C, false alarms-hits). Topographic plots (D,E,F) show the average activity of the black squares averaged from 50-200 ms after the button press and 3-7 Hz. Topographic plots have the same scales as the time-frequency representations (A,B,C).
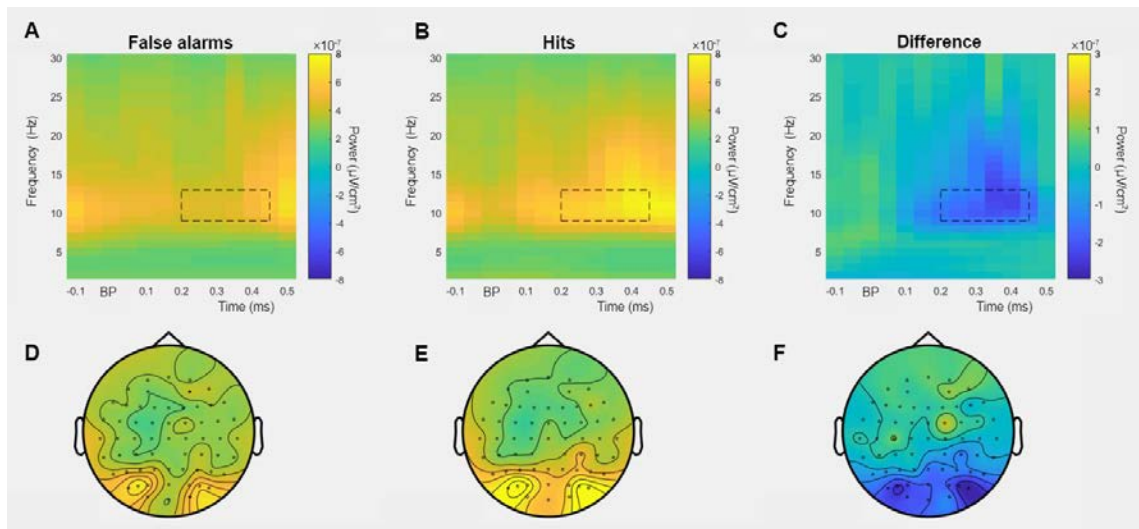
Figure 3.6 Later post-response differences between false alarms and hits in the alpha range. The individual conditions are shown for the largest negative differences between false alarms and hits (cluster ii

from Figure 3.3). Average activity from parietal, parieto-occipital and occipital electrodes is shown for individual conditions (A, false alarms and B, hits) and the difference (C, false alarms-hits). Topographic plots (D,E,F) show the average activity of the black squares averaged from 200-450 ms after the button press and 9-13 Hz. Topographic plots (D,E,F) have the same scales as the time-frequency representations (A,B,C).

3.3.3 Gauging the relationship between post-error neural signatures and post-error slowing

In line with previous results (Mazaheri et al., 2009; van Driel et al., 2012) I found that midfrontal theta power was higher and parieto-occipital alpha power lower after committing a false alarm compared to a hit. Next, I asked whether the post-response differences were correlated with PES. I used the difference between false alarms and hits as a functional localizer to assess whether the significant channel × time × frequency region correlated with PES. To this end, I calculated the Fisher's z-transformed correlation between single-trial values of PES and each channel × time × frequency point that survived multiple comparison corrections in the false alarms vs. hits contrast (Figure 3.4).

For the positive cluster, I calculated the Spearman correlation between power at each channel × time point that was part of the positive cluster and PES_{ROBUST} (channels: Fp1, Fpz, Fp2, F7, F3, Fz, F4, F8, FC5, FC1, FC2, FC6, T7, C3, Cz, C4, T8, CP5, CP1, CP2, CP6, P3, AF7, AF3, AF4, AF8, F5, F1, F2, F6, FC3, FCz, FC4, C5, C1, C2, C6, CP3, CP4, P1, PO5, PO3, FT7, FT8, TP7; time points: 0-500 ms; averaged over frequency: 2-14 Hz; Figure 3.4, cluster i). Next, I tested whether these correlation values were statistically different from 0 or from the correlation values obtained from power on hit trials and RT on post-hit hits. To test this, I either calculated the mean of all z-transformed Spearman correlations across all channel × time points and compared these to the correlation values obtained with hits or to 0 with dependent samples t-tests. Alternatively, I used

cluster-based permutation statistics to make the comparisons without collapsing over channel × time points. However, neither analysis indicated any significant results. For the negative cluster I used the same approach (channels: CP6, Pz, P4, P8, POz, O1, O2, CP4, P1, P2, P6, PO5, PO3, PO4, PO6, PO7, PO8, Oz; time points: 200-450 ms; averaged over frequency: 8-20 Hz; Figure 3.4, cluster ii). Again, I did not observe any significant results.

I repeated the analyses described for more traditional frequency bands, instead of the channel × time × frequency region of interest identified by the functional localizer of hits vs false alarms. Loosely based on previous research, I calculated the correlation values between power and PES for the delta (2-3 Hz), theta (4-7 Hz), alpha (8-14 Hz) and beta (15-30 Hz) frequency bands. For delta and theta frequency bands I used FCz and Cz electrodes. For the alpha band I used parieto-occipital electrodes. But no significant results were observed for either dependent sample t-tests that compared the means over time (averaged over 0-200 ms for the delta and theta bands and 200-400 ms for the alpha band) and channels. Or cluster-based permutation statistics without collapsing over time or channels. Finally, I repeated the analysis for all channel × time × frequency points by calculating the z-transformed correlation value between power at each channel × time × frequency point and PES. I used cluster-based permutation statistics to compare the correlation values of post-error and post-hit trials, but found no significant effects.

The z-transformed correlation values are plotted averaged over midfrontal (FCz and Cz) electrodes and over parieto-occipital (Oz, O1, O2, POz, PO3, PO4) electrodes in Figure 3.7.
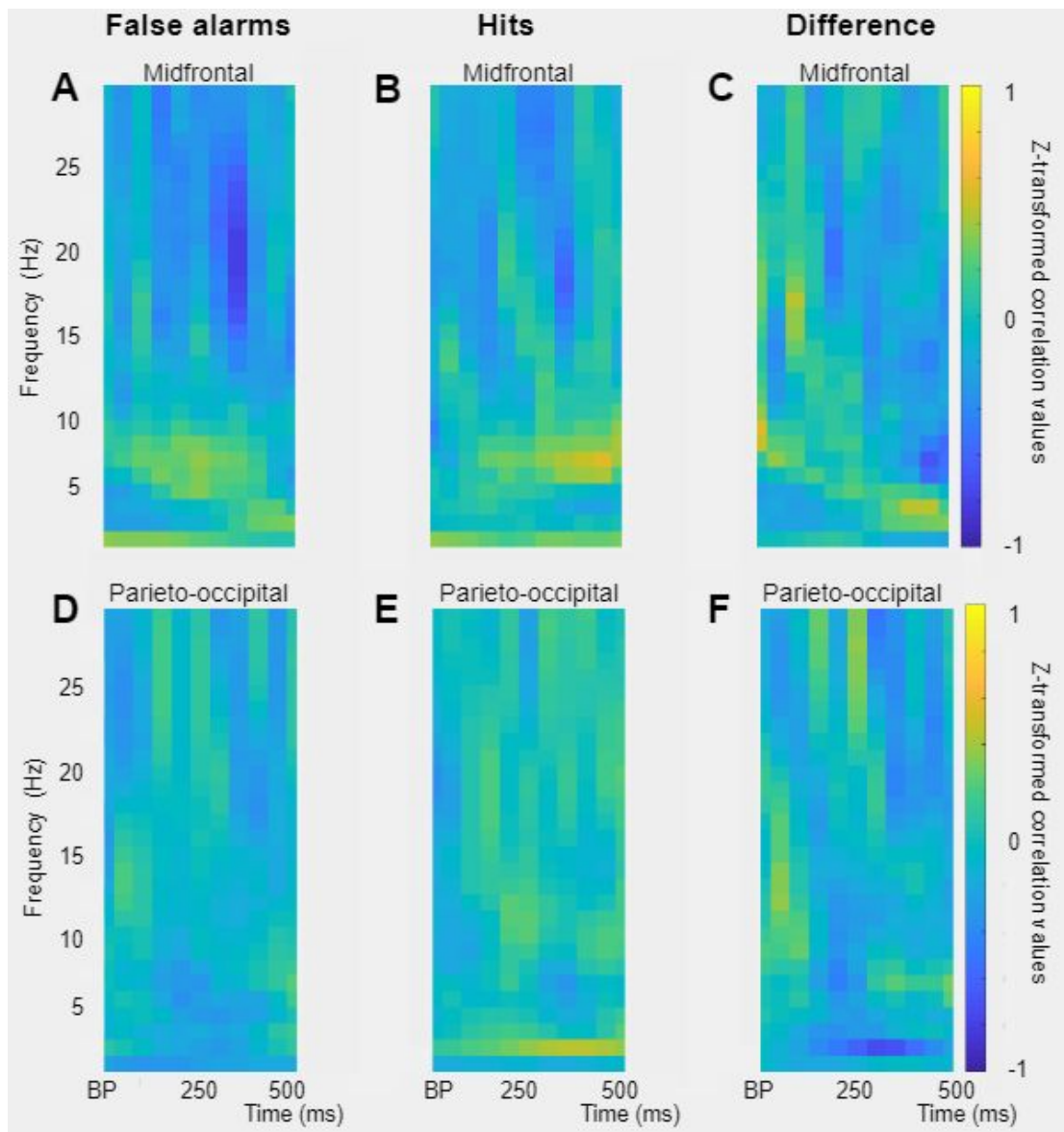
Figure 3.7 Post-error slowing is not significantly correlated with power at midfrontal or parieto-occipital electrodes. Power at each channel × time × frequency point after a false alarm was correlated with PES$_{ROBUST}$ across trials and the correlation values were z-transformed. For hits power at each channel × time × frequency point was correlated with RT of the post-hit hits. Cluster-based permutation statistics were used to compare the conditions, but no clusters survived corrections for multiple comparisons. Z-transformed correlation values over

midfrontal (FCz and Cz) electrodes are shown in the top row (A, B, C) and for parieto-occipital (Oz, O1, O2, POz, PO3, PO4) electrodes in the bottom row (D, E, F).

3.3.4 Functional connectivity from midfrontal to parieto-occipital regions

Previous research showed a negative correlation between theta power at frontal electrodes and alpha power at occipital electrodes with the sustained attention to response task (Mazaheri et al., 2009). I calculated the correlation between theta (4 Hz) power at a seed electrode and alpha (10 Hz) power at all other electrodes. I used FCz, FC2 and Cz as seed electrodes as these electrodes showed the largest power difference in the contrast between false alarms and hits. I compared the z-transformed correlation values from false alarms to 0 with cluster-based permutation testing and I compared the values from false alarms to hits. With this approach I was unable to replicate the pattern of functional connectivity in the visual go/no-go task (Figure 3.8). Because the negative cluster (cluster ii in Figure 3.4) observed in the contrast between false alarms and hits also included low beta power ranges, I repeated the analyses with beta (18 Hz) power at all other electrodes, but again no amplitude-amplitude coupling survived corrections for multiple comparisons (data not shown).
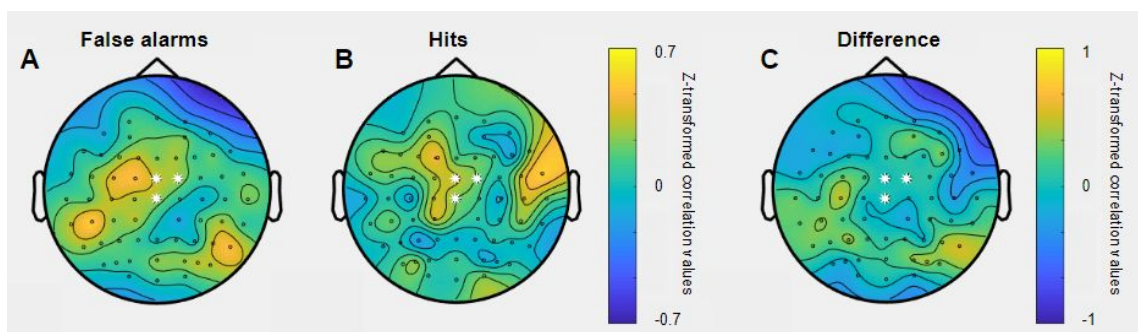
Figure 3.8 Midfrontal theta power at 4 Hz was not significantly anti-correlated with higher frequencies.
Power at 4 Hz was averaged from 0-200 ms and across electrodes that showed the largest power difference between false alarms and hits (white stars, FCz, FC2 and Cz). Across trials power was correlated to 10 Hz alpha power at all other electrodes. The correlation values were z-transformed and non-parametric cluster-based statistics were used to examine whether there was a negative correlation between midfrontal theta and occipital alpha with correlation values averaged from 200-500 ms post-response. False alarm trials showed an anticorrelation between midfrontal theta and occipital power (A), but the effect was too weak to reach the cluster threshold.

To exclude the possibility that any anti-correlations were missed due to volume conduction, a Gram-Schmidt process was applied to single-trial data (see methods; Hipp et al., 2012). This analysis did not change the absence of the anti-correlation observed above (Supplementary Figure 3.4). It is possible that the Laplacian transform of the data already accounted for any shared variance between the different channels.

3.3.5 Phase based functional connectivity

In addition to the power-power connectivity analysis presented in 2.3.4 phase-based functional connectivity was also examined by computing debiased weighted phase lag index (dwPLI; Stam et al., 2007; Vinck et al., 2011). To assess whether there were differences in functional connectivity after an error was committed dwPLI was averaged across the midfrontal electrodes (FCz, FC2, Cz) that showed the largest power difference between hits and false alarms. Cluster-based permutation statistics showed that functional connectivity was significantly higher in false alarms than in hits. Three different clusters were identified by cluster-based permutation statistics: The first cluster was right lateralized, in the frequency range of 2-4 Hz and from 50-500 ms after the response (p =

.0004; Figure 3.9), the second cluster was a left lateralized cluster from 2-4 Hz, from 0-450

ms (p = .0004; Figure 3.10) and the third cluster was a midfrontal cluster from 5-10 Hz,

from 100-200 ms post-response (p = .001; Figure 3.11).

Next, I used a similar analysis with the seed electrodes over left and right occipital areas

(PO7 and PO8). This analysis again identified larger functional connectivity after a false

alarm than after a hit. The difference was most pronounced across a small centro-partietal

cluster at 4 Hz, from 350-450 ms post-response (p = .05; Figure 3.12).
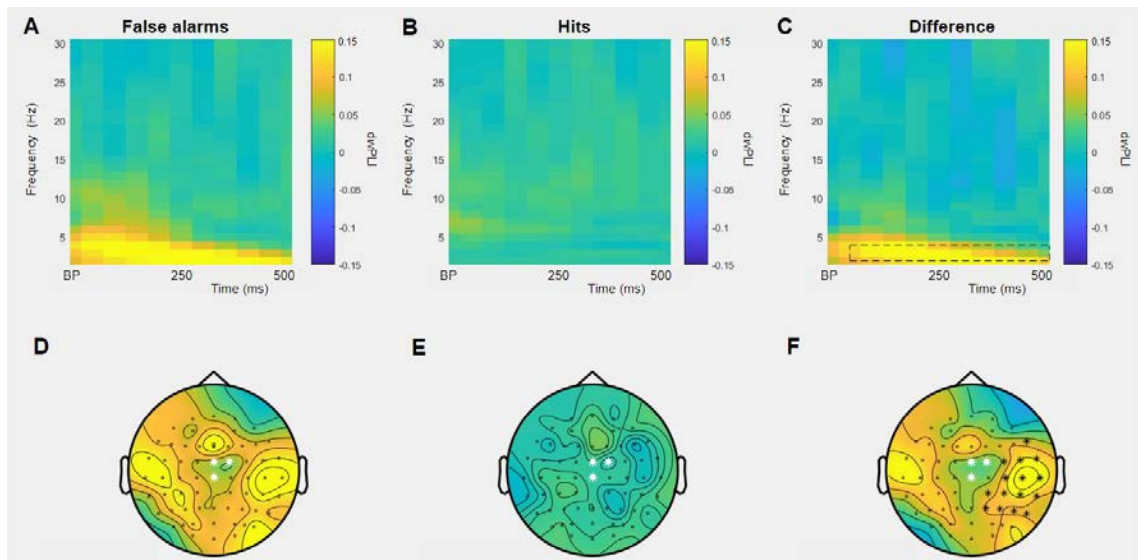
**Figure 3.9 Functional connectivity from midfrontal electrodes to right lateralized cluster of electrodes
for false alarms but not hits.** dwPLI was averaged across the midfrontal electrodes that showed the largest

difference between hits and false alarms to assess phase-based connectivity differences between false alarms

and hits. dwPLI was averaged across the electrodes that were identified in the cluster-based permutation

approach (F) and dwPLI values are shown for false alarms (A), hits (B) and the difference (false alarms - hits,

C). The topographies in D-F were obtained by averaging over the time window indicated by the cluster-based

permutation approach from 50-500 ms post-response and frequencies from 2-4 Hz. White stars indicate the

seed electrodes FCz, FC2 and Cz. Black stars indicate electrodes that survived corrections for multiple comparisons.
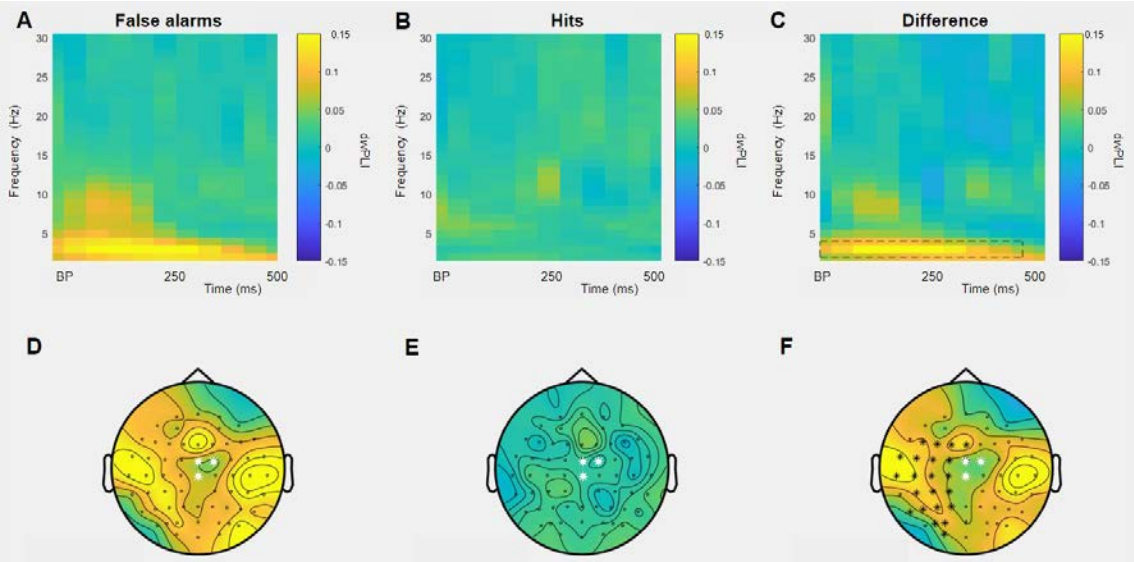
Figure 3.10 Functional connectivity from midfrontal electrodes to left lateralized cluster of electrodes for false alarms but not hits. Same conventions as 2.9, 2-4 Hz, 0-450 ms post-response.
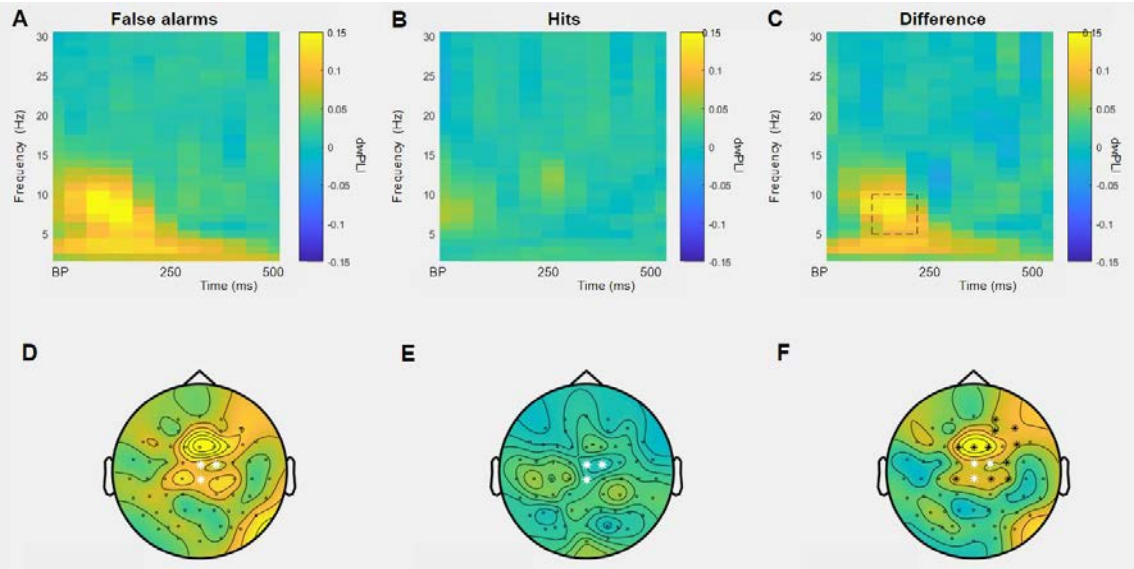
Figure 3.11 Functional connectivity from midfrontal electrodes to midfrontal cluster of electrodes for false alarms but not hits. Same conventions as 2.9., 5-10 Hz, 100-200 ms post-response.
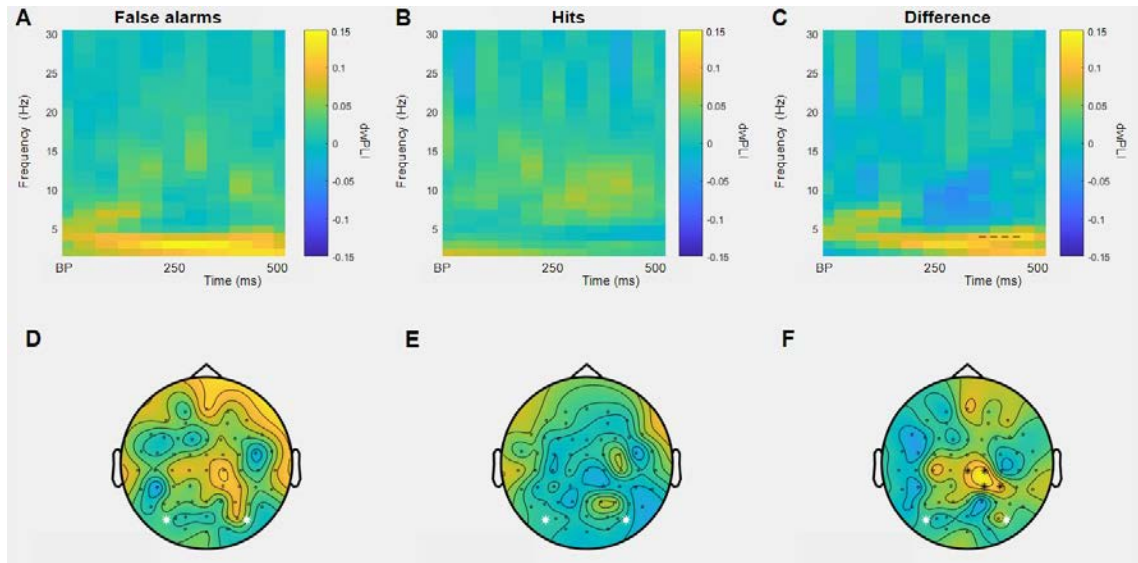
Figure 3.12 Functional connectivity from occipital electrodes to centro-parietal cluster of electrodes for false alarms but not hits. Same conventions as 2.9., 4 Hz, 350-450 ms post-response.

3.4 DISCUSSION

The current chapter aimed to understand how cognitive control implements behavioral adjustments to prevent future errors. Midfrontal theta oscillations are hypothesized to fulfil an important role in performance monitoring and as such offer a likely candidate to implement behavioral adjustments after an error is committed. Previous research has presented evidence that larger midfrontal theta signals can lead to either post-error slowing or speeding. Moreover, several different measures of post-error adjustments have been used in the literature. Here, I focused on post-error slowing (PES) measured as the difference in response time (RT) between the hit that followed and the hit that preceded false alarms.

Behaviorally, the data showed that participants are faster on average when they commit a false alarm than a hit. The likelihood that a fast response is a hit however, does not automatically follow from that, as evidenced by the defective cumulative density functions (CDFs). The data showed that for most participants fast responses are equally likely to belong to hits or false alarms, as the defective CDFs were mostly overlapping. If one takes into account the likelihood of go and no-go stimuli, fast responses were actually three times more likely to belong to hits than false alarms. This finding is in line with a recent report from Hawkins and colleagues (2019) and highlights the importance of studying response time distributions in full.

When calculating PES as the difference in RT on hits that preceded vs. followed false alarm trials (known as PES_{ROBUST}), participants showed significant PES. There was also a significant difference between hits that followed hits vs. hits that followed false alarms (known as $PES_{TRADITIONAL}$). In line with previous research (van den Brink et al., 2014), both measures of PES were highly correlated. Moreover, false alarms were preceded by faster hits than hits. Signal detection measures of performance showed that participants could easily discriminate go and no-go stimuli and participants had a tendency to execute the go response.

Taken together, these behavioral data suggest that errors on a visual go/no-go task are heralded by speeding of responses on preceding hits. In addition, when examining post-error neural dynamics it is important, whenever possible, to match RTs and trial counts of hits to false alarms.

In line with previous research we found higher power shortly after the response for false alarms compared to hits. The largest difference was observed over midfrontal electrodes in

the theta range from 50-200 ms after the response. This difference was followed by lower power for false alarms than hits. And this negative difference was largest over occipital electrodes in the alpha range from 200-450 ms. Previous research has suggested that the medial frontal cortex exerts cognitive control over downstream regions through long-range theta mediated connections (Mazaheri et al., 2009). If theta activity reflects more cognitive control, one would predict that more theta activity is (directly or indirectly through interactions with occipital regions) related to behavioral adjustments on subsequent trials. A meta-analysis provided some evidence of a positive relationship between midfrontal theta (MFθ) and response times on the subsequent trial (Cavanagh & Shackman, 2014). However, most studies included in the meta-analyses did not use the PES$_{ROBUST}$ measure. Moreover, recent studies have found a negative relationship between MFθ and post-error RT (Narayanan et al., 2013; Valadez & Simons, 2018). However, in the current chapter I did not find significant relationships between MFθ and post-error RT.

A possible explanation of the lack of effects in the current chapter is that I used a go/no-go task whereas Valadez & Simons (2018) used an Eriksen flanker task. It is important to note that Valadez & Simons also RT matched the errors and hits, as I did, but the main difference in methodological approaches is that Valadez & Simons used a quantile split and compared the fastest and slowest quantile to each other, whereas I used false alarms without any data splits. However, it might be that behavioral adjustments after errors on flanker tasks are different from adjustments after errors on go/no-go tasks. A flanker error comes from incongruent information from the flankers, whereas a go response to a no-go stimulus likely comes from unsuccessful inhibition of the go response. Future research should elucidate whether post-error behavioral adjustments are different in different tasks.

Based on previous research (Mazaheri et al., 2009), I also expected to observe a negative correlation between MFθ and parieto-occipital alpha power after false alarms. However, I did not observe any negative correlations between MFθ and parieto-occipital alpha power that survived corrections for multiple comparisons. It is known that MEG and EEG are differentially sensitive to underlying sources, such that radial sources are not picked up on by MEG. It is possible that the MFθ from EEG and MEG stem from different sources, such that the EEG is more likely to reflect activity from the ACC whereas the MEG source is more likely to be pre-SMA (M.X. Cohen, personal communication).

In addition to the power-power correlation analysis a phase-based functional connectivity analysis was performed to examine whether midfrontal electrodes would be functionally coupled to occipital regions. Debiased weighted phase lag index (dwPLI) was larger for false alarms than hits when FCz, FC2 and Cz were used as seed electrodes. There was functional coupling to the left and right fronto-temporal hemispheres in the delta band and there was functional coupling at midfrontal electrodes at 5-10 Hz. in line with previous findings (Cavanagh et al., 2009; Hanslmayr et al., 2008; Oehrn et al., 2014), I hypothesize that medial frontal cortex connectivity with dorsolateral prefrontal cortex in the (high) theta range might reflect frontal control updating, whereas the delta connectivity with SMA and motor cortex might reflect response adjustments. When PO7 and PO8 were used as occipital seed electrodes theta connectivity emerged between occipital regions and a centroparietal region for false alarms, but not hits. I hypothesize this reflects parietal influences on sensory regions that might be related to attentional updating (Behrmann et al., 2004). However, an important shortcoming of the dwPLI is that this is not a directed measures. As such, it is unclear which regions is leading and which region is following.

An important limitation of the current chapter is its small sample size in both participant numbers and false alarm trials. Future studies should aim to collect a larger dataset with more false alarms and more double-errors to apply computational modeling by fitting drift-diffusion models and measuring EEG data in the same experiment. It will be interesting to see how EEG measures and computational modelling parameters relate to one another in paradigms that examine behavioral adjustments after errors. In addition, a limitation is the uncertainty about the sources underlying the effects described here. Intracranial studies that directly record from anterior cingulate cortex, dorsolateral prefrontal cortex, parietal cortex and primary occipital cortex might provide better insight into the functional connectivity between these regions after errors.

Supplementary Figures
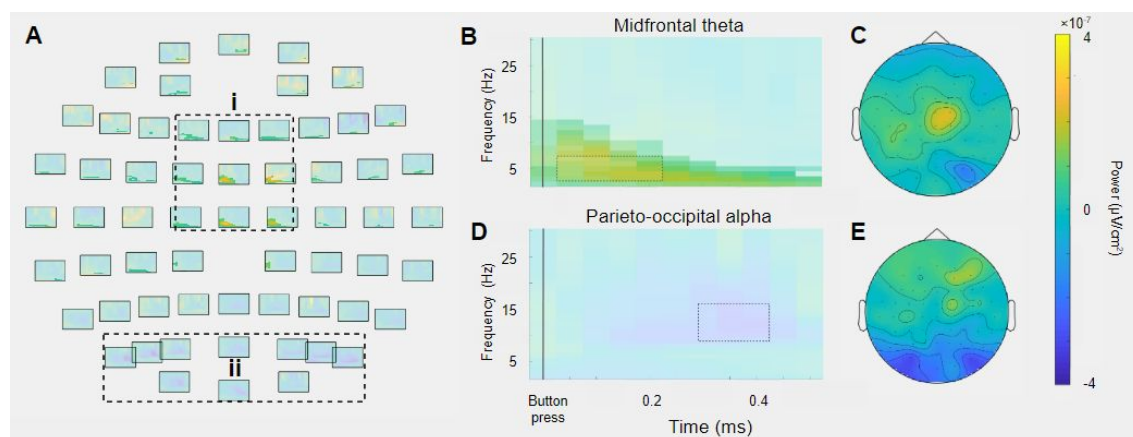
Supplementary Figure 3.1 Phase-locked power was subtracted from the total power to obtain non-phase-locked power. Convetions in this plot are the same as in Figure 3.4. Note that the second cluster had a p-value of .055 and as such, all power values are masked. The positive cluster, cluster i in A, spanned almost all frontal and central electrodes and ranged from 2-14 Hz from 0-500 ms post-response. The biggest difference was observed between 4-9 Hz from 50-200 ms post-response (B), over FCz, FC2 and Cz (C). The

negative cluster, cluster ii in A no longer reaches statistical significance. Over parieto-occipital regions (E), the difference between false alarms and hits was most pronounced in the alpha band from 9-13 Hz from 300-450 ms (D).
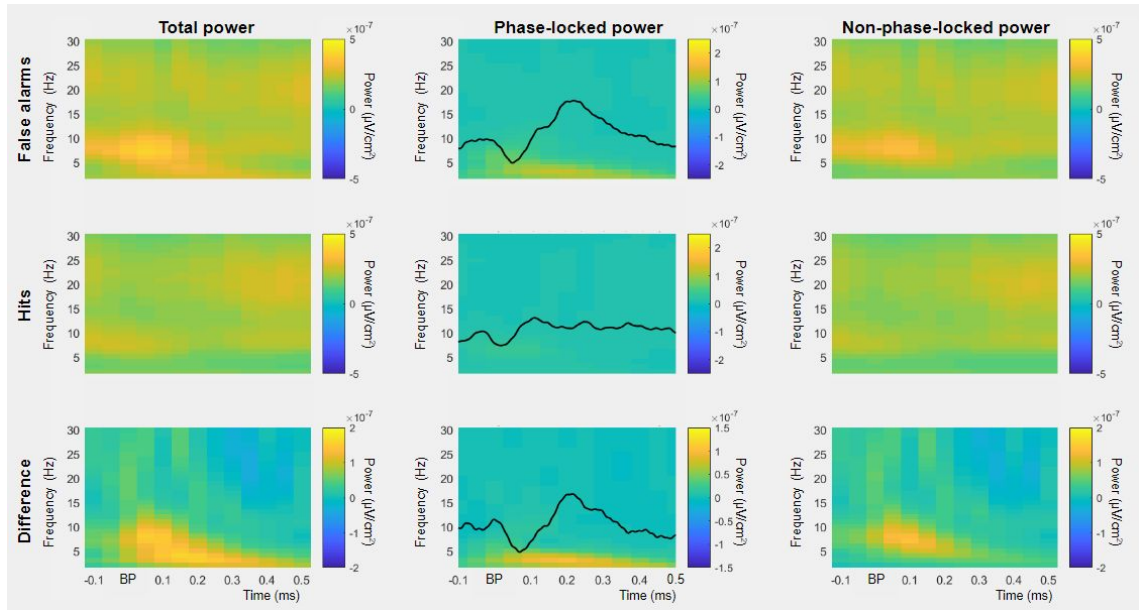
Supplementary Figure 3.2 Phase-locked power was subtracted from the total power to obtain non-phase-locked power, shown here for midfrontal electrodes. Time-frequency representation of the total power, the phase-locked and non-phase-locked power at midfrontal electrodes (Fz, F1, F2, FCz, FC1, FC3, Cz, C1, C2) are visualized side-by-side. The ERP in the middle row was scaled arbitrarily to show the shape of the ERP on top of the phase-locked activity. Note that the ERP mostly affects lower frequencies in the delta range.
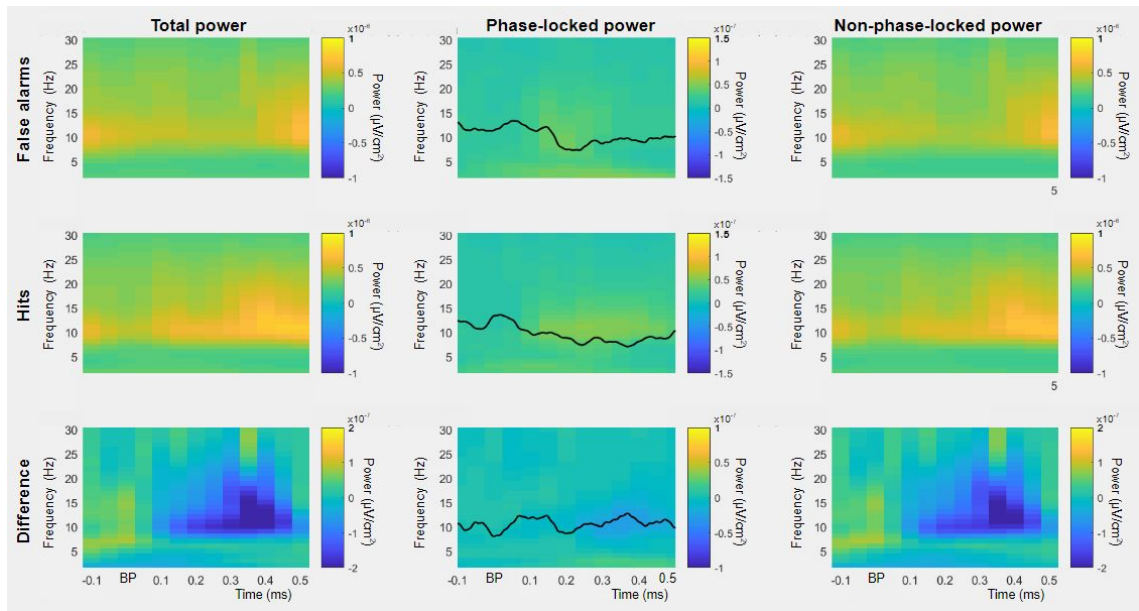
Supplementary Figure 3.3 Phase-locked power was subtracted from the total power to obtain non-phase-locked power, shown here for occipital, parieto-occipital and parietal electrodes. Same as in Supplementary Figure 3.2 but now for occipital, parieto-occipital and parietal electrodes (Oz, O1, O2, POz, PO3, PO4, PO5, PO6, PO7, PO8, Pz, P1, P2, P3, P4, P5, P6, P7, P8). Note that some alpha power stems from phase-locked activity (middle row), but also note that the difference between total power and non-phase-locked power is small.
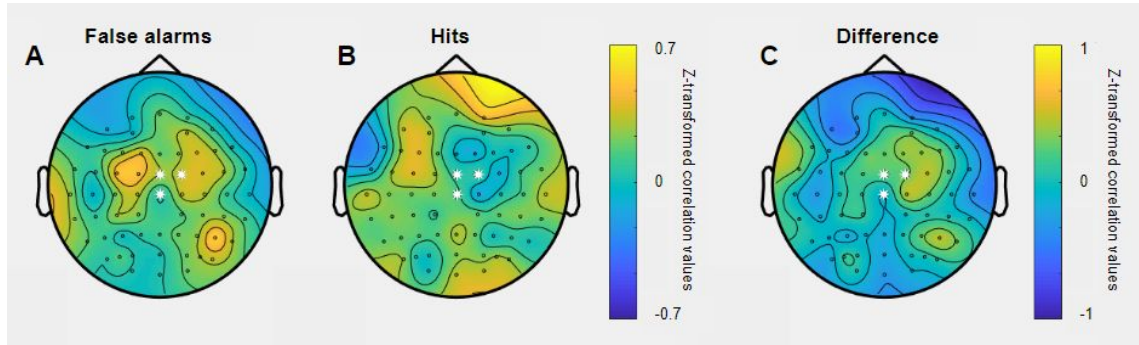
Supplementary Figure 3.4 Functional connectivity between midfrontal electrodes at 4 Hz and all other electrodes at 10 Hz after Gram-Schmidt orthonormalization in the time-domain. Conventions are the same as in Figure 3.8. As negative correlations might be more difficult to detect due to volume conduction, an

orthonormalization procedure was applied to the time domain data. However, this normalization did not aid the detection of an anti-correlation between midfrontal theta and occipital alpha after errors.

CHAPTER 4

Oscillatory power and temporal judgements

ABSTRACT

Previous research showed that theta (~4-7 Hz) oscillations play an important role in interval timing in both rats and humans. These oscillations were recorded from medial frontal cortex and dopamine depletion abolished the involvement of theta oscillations and interval timing abilities. In addition, beta oscillations have been hypothesized to play an important role in indexing interval timing. Taken together, previous work suggests that phasic dopaminergic activity can be measured with scalp EEG as theta or beta power increases. This chapter examined the relationship between oscillatory power and temporal decision making by contrasting correct and incorrect responses during two very similar timing experiments, which were different from the interval timing tasks used in previous work. Interestingly, we find theta power increases in correct judgements of long interval trials after the short interval has elapsed. Importantly, this data was consistent between the different experiments. In addition, we found alpha and beta suppression that was related to temporal judgement, irrespective of interval length, where alpha/beta power was higher for trials that were subjectively experienced as short. These findings were consistent for short and long interval trials in Experiment 1. However, this effect did not replicate in Experiment 2. Finally, we show that in correct long interval judgements higher theta power correlated with shorter response times. This suggests that when more temporal evidence was accumulated, as reflected in theta power over midfrontal electrodes, participants more readily responded.

4.1 INTRODUCTION

Time perception and human experience are tightly bound and play an important role in our everyday life (e.g. when playing whack-a-mole at a fun fair). Understanding how we perceive the passage of time has been an endeavour in psychology and neuroscience for over half a century (Matthews & Meck, 2016; James, 1890). And although it is well known that the human brain has a dedicated brain region for circadian rhythms (Turek, 1985), the neural underpinnings of time perception on shorter time scales (~1 s) remain to be elucidated (Muller & Nobre, 2014). Recently, Parker and colleagues (2014) reported an important role for the power of delta and theta oscillations in medial frontal cortex. They showed that low-frequency power increased in both humans and rats upon the presentation of a cue that indicated that subjects needed to perform an interval timing task. Moreover, this effect was absent in patients with Parkinson's Disease and in rats after dopamine depletion (Parker et al., 2014). Taken together, these results suggest that low-frequency power from the medial frontal cortex might reflect dopaminergic activity from deeper brain structures and might serve as a start-gun to interval timing (Kononowicz, 2015).

Other research has extended the relevance of the power of oscillatory activity beyond the delta and theta band. In a self-paced key-press task trial-to-trial beta power, over a central-motor electrode site, positively correlated with the length of produced durations, while theta band oscillations were found to be negatively correlated to produced durations (Kononowicz & van Rijn, 2015). Crucially, the correlation between beta power and interval duration was already present during the pre-interval period (before the first button press).

However, given changes of the beta rhythm locked to the onset of motor responses (Pfurtscheller & Lopes da Silva, 1999), it remained to be elucidated if beta oscillations are involved in temporal judgements.

The role of beta band oscillations was further substantiated by a recent working-memory study. Kulashekhar et al. (2016) extended the findings of Kononowicz & van Rijn (2015) when they found that beta band power increased while storing and retrieving temporal but not colour information. This important finding suggests that beta oscillations are indeed involved in temporal judgements, specifically in the memory encoding and retrieval of temporal information. However, Schlichting and colleagues (2018) recently asked whether beta oscillations are specifically related to time perception or to magnitude perception in general. Interestingly, they found no difference in beta power when participants made judgments about time or numerosity, contesting the straightforward relationship between beta power and time perception (Schlichting et al., 2018).

Previous research in monkeys also found a relationship between increased beta power and longer durations between consecutive taps (Bartolo et al., 2014; Bartolo & Merchant, 2015). A possible interpretation of the relationship between beta power and interval timing was provided in the framework of dopamine levels (Kononowicz & van Rijn, 2015). Higher beta power might reflect low dopamine levels (Jenkinson & Brown, 2011) and low dopamine levels are related to a slowing of subjective timing (Meck, 1996; Lewis & Miall, 2006). In a production task, high beta power and low dopamine levels would lead to longer interval productions, because subjective time is passing more slowly. Alternatively, beta power might index temporal evidence accumulation (Balci and Simen, 2014; Luzardo et al., 2011; Simen et al., 2013; Kononowicz & van Rijn, 2015).

Interestingly, evidence accumulation of noisy sensory information over time in non-temporal decision making has been related to both alpha (~8-12 Hz) and beta band oscillations (Kelly & O'Connell, 2013; Rohenkohl & Nobre, 2011; Donner et al., 2009). Kelly and O'Connell (2013) showed that alpha oscillations had an inverse relationship with the slope of the centro-parietal positivity (CPP), which is thought to reflect the accumulation rate at which noisy sensory evidence is accumulated. Rohenkohl & Nobre (2011) showed that alpha power was higher for temporally unexpected compared to expected events. Taken together, these findings suggest that higher alpha power negatively affects sensory processing in temporal and non-temporal decision making, but it remains unclear what role the power of alpha oscillations play in time perception. Previous research showed that alpha (8-14 Hz) power correlated with produced time intervals, such that higher power was correlated with shorter temporal intervals (Makhin & Pavlenko, 2003). However, this finding was not replicated in a reproduction task by Kononowicz & van Rijn (2015), where alpha power was not related to reproduced intervals.

All in all, these studies indicate that the power of theta, alpha and beta band oscillations might play a role in temporal and non-temporal decision making. In the current EEG study power in these frequency bands and its relationship to correct and incorrect temporal judgements were examined. Participants were required to judge the time between a tone and a visual stimulus as 1 or 1.5 s in Experiment 1 and 1.5 or 2 s in Experiment 2. The 2 × 2 design of interval length (short and long) and response (correct and incorrect) allows the comparison of over- and underestimation to correctly accumulated temporal information. If oscillatory (theta/alpha/beta) power is related to interval length or evidence accumulation of temporal information, a pattern should emerge where intervals judged as long,

irrespective of the physical interval length, should have higher (theta/alpha/beta) power than intervals judged as short. If (theta/alpha/beta) power from medial frontal cortex (possibly pre-SMA) reflects the activity of the internal clock, we would expect higher power in correctly judged temporal intervals than in incorrectly judged intervals.

4.2 MATERIALS & METHODS

The paradigm has been described in detail in Chapter 2. The exclusion criteria were the same as before and the same data is analyzed for Experiment 1 and 2 as in Chapter 2, albeit in a different way. Please refer to Chapter 2 for the behavioral results and analyses. Here, we compared power differences between correct and incorrect responses for theta (3-6 Hz), alpha (7-14 Hz) and beta (15-25 Hz) power. These frequency bands were loosely based on previous literature (Palva & Palva, 2007; Weisz et al., 2011; Zumer et al., 2014) and we used a cluster-based randomization approach to correct for multiple comparisons (Maris and Oostenveld, 2007).

4.2.1 Preprocessing: TFR analyses

Using EEGLAB, the data was divided in epochs from -1000 to 3500 ms from tone onset. Subsequently, the data was baselined from -100 to 0 ms to remove any slow drifts. Missed trials were discarded. Based on visual inspection trials were removed for the following reasons: muscle artefacts, noise (i.e. electrode jumps or other electrode related noise), horizontal eye movements and blinks at visual stimulus presentation. The cleaned data was then average referenced (excluding bipolar electrodes), from which electrode CPz was reconstructed. Ocular artefacts were removed in FieldTrip using independent component analysis (ICA, infomax algorithm) incorporated as the default "runica" function.

Prior to the ICA, a PCA (15 components) was performed on the data to reduce dimensionality of the data.

4.2.2 Time Frequency Representation

Using the FieldTrip function 'ft_freqanalysis_mtmconv' time frequency representation (TFR) of power was obtained for each trial by performing a fast fourier transform using a Hanning taper in combination with a sliding time window. The time window was adapted to the frequency of interest ($\Delta T = 3/f$). The frequency range of interest was from 2 to 40 Hz in steps of 1 Hz. TFRs were calculated for the long and short interval and for correct and incorrect responses separately, leading to 4 different subsets of trials. After we assessed that there were no differences in baseline (i.e. pre-cue) oscillatory power for our frequency bands of interest between correct and incorrect responses, data in each condition was normalized to be the relative change in power according to the following formula,

$$\Delta p \;=\; \frac{(P_t - P_r)}{P_r}$$

where P_r was the mean power during the pre-cue period (700 – 200 ms before tone onset) and P_t was the power at each specific time point.

4.2.3 Statistics: TFR analyses

The differences in oscillatory power between conditions were statistically assessed by means of the cluster level (channels and time-points) randomization approach (Maris and Oostenveld, 2007). Here, the power of the frequencies of interest in each channel and

time point within the time intervals of interest, were clustered according to exceeding a threshold of p < .05 obtained from a two tailed dependent samples t-test. The time interval of interest was from tone onset until visual stimulus onset for all frequency bands. Next, the Monte Carlo p-values of each cluster were obtained by randomly swapping the condition labels within participants 2500 times. A difference between conditions was deemed significant if the cluster p-value was smaller than .025 (two-sided test).

4.2.4 Single-trial analyses

In addition to the trial-average analyses described above, we asked whether the differences between correct and incorrect responses were behaviorally meaningful beyond the distinction between correct and incorrect responses. We examined whether single trial power values correlated with response time. To this end, we used Spearman's ranked correlation to correlate response times and power. Ranked correlation was used, because power data is not normally distributed (Cohen, 2014; Cohen & Donner, 2013). We transformed the obtained correlation values to z-scores with Fisher's z-transform. To avoid double-dipping we looked within responses and compared obtained correlation estimates to 0 through cluster based permutation tests, rather than comparing the z-scored correlation values of correct and incorrect responses to each other. We used 10000 iterations for the permutation test and we set the critical alpha value to .05 because we had directional hypotheses (one-sided test). We expected higher theta power to correlate with faster response times. Theta power was averaged over 3-6 Hz and the z-scored correlation values were averaged over the time windows of interest we obtained from the comparison of correct and incorrect trials.

4.3 RESULTS

For the behavioral results please refer to Chapter 2. In short, in Experiment 1 participants responded fastest to correctly judged long (1.5 s) interval trials. In Experiment 2 participants responded faster when they judged a trial as long irrespective of the true trial length.

In Experiment 1 participants judged a 1 s interval correctly as short or incorrectly as long (Figure 4.1A). First we examined the baseline period of 700-200 ms before tone onset for differences for the different frequency bands of interest. We observed no clusters for any of the frequency bands. We baseline corrected our data and compared correct and incorrect responses for the different frequency bands from tone onset until visual stimulus onset.

For the short (1 s) interval of Experiment 1 we found that beta power averaged over 15-25 Hz was significantly (p = .011) higher for correct (μ = -0.223 ± .020, with mean over significant electrodes and time points and standard error of the mean across participants) than incorrect (μ = -0.286 ± .028) responses from 750-1000 ms (Figure 4.1B and C). For the alpha band averaged over 7-14 Hz we observed a similar effect such that alpha power was higher (p = .023) for correct (μ = -0.208 ± .024) than incorrect (μ= -0.289 ± .035) responses from 750-950 ms. The 95% confidence interval of the p-value of the alpha band effect did include the .025 critical value. However, running 10000 iterations instead of 2500 did not change this.
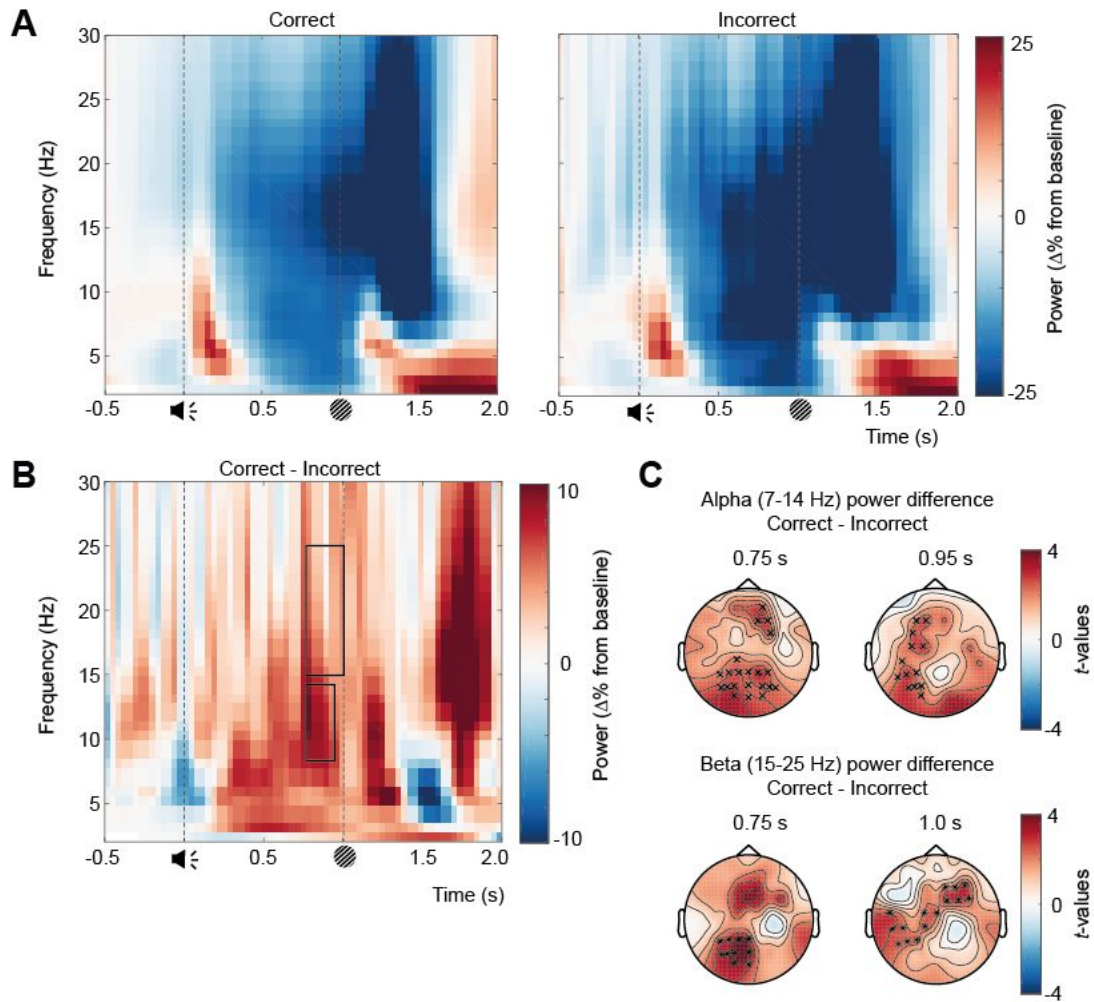
Figure 4.1 Time-frequency representation averaged across all electrodes for correct and incorrect responses when participants judge 1 s time intervals. The tone evoked a response in the low frequency ranges followed by sustained power decreases in the higher frequency ranges (A). The difference plot shows that power values are higher for correct compared to incorrect responses (B) and this difference was significant (p = .011) in the beta range from 750-1000 ms and marginally significant (p = .023) in the alpha range from 750-950 ms after tone onset (C). Block box in B shows the extent of the clusters in time and stars/crosses in C show electrodes that were part of the cluster at the time points depicted.

To make sure that these differences in alpha and beta bands were not caused by differences in trial count (participants had on average 400 correct trials versus 50 incorrect

trials), we matched the trial counts for correct and incorrect responses and reran the analysis (note that we only performed this analysis for matching trial counts on the short interval with Experiment 1, because all other conditions had less severe trial count differences such that on average there was >1 incorrect trial collected for each 3 correct trials). Trial counts were matched by randomly drawing a sub-selection of correct responses such that the trial count matched the number of incorrect responses. We performed this control analysis once and the effect remained for both frequency bands (cluster extent was topographically similar and lasted from 750-900 ms for the beta band, p = .01, μ = -0.227 ± .026 for correct and μ = -0.303 ± .031 for incorrect responses; and 750-1000 ms for the alpha band, p = .012, μ = -0.167 ± .028 for correct and μ = -0.279 ± .034 for incorrect responses).

In addition to 1 s intervals, participants also judged a 1.5 s interval correctly as long or incorrectly as short in Experiment 1 (Figure 4.2A). We used a similar approach to the 1 s interval and first examined if there were any baseline differences, by testing the baseline window of 700-200 ms before tone onset for differences for the frequency bands of interest. No differences were observed, therefore we baseline corrected the data and used cluster based permutation statistics.

We found significantly (p = .01) more theta power averaged from 3-6 Hz from 1050-1500 ms after tone onset for correct (μ = -0.13 ± .030) compared to incorrect (μ = -0.20 ± .026) responses (Figure 4.2B and C top). For alpha power averaged from 7-14 Hz we found significantly (p < .01) lower power for correct (μ = -0.248 ± .034) compared to incorrect (μ = -0.184 ± .031) responses from 600-1250 ms after tone onset (Figure 4.2B and C middle).

For beta power averaged from 15-25 Hz we found significantly (p < .001) lower power for correct (μ = -0.252 ± .022) compared to incorrect (μ = -0.195 ± .019) responses from 550-1500 ms after tone onset (Figure 4.2B and C bottom).
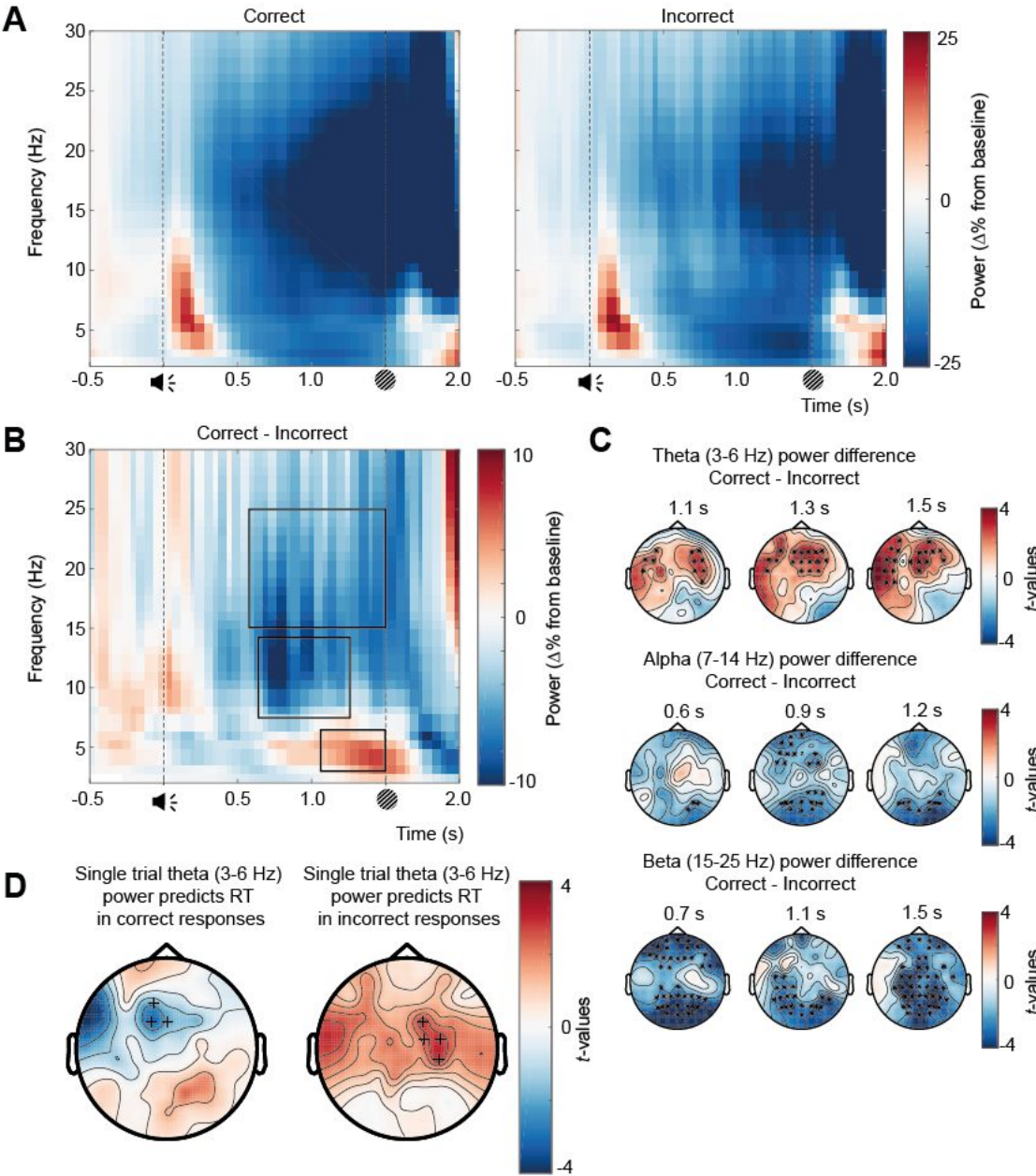
Figure 4.2 Time-frequency representation averaged across all electrodes for correct and incorrect responses when participants judge 1.5 s time intervals. The tone evoked a response in the low frequency ranges followed by sustained power decreases in the higher frequency ranges (A). The difference plot shows that power values are lower for correct compared to incorrect responses for higher frequencies, but power values were higher for correct compared to incorrect responses for lower frequencies (B). Topographies of the significant differences are shown in C. Block boxes in B shows the extent of the cluster in time and stars in C show electrodes that were part of the cluster at the time points depicted. D shows the topographies of electrode clusters that showed a (trending) correlation with response times.

For Experiment 2 we ran the same analyses. Here, participants judged a 1.5 s interval correctly as short or incorrectly as long (Figure 4.3A). No significant differences were observed between correct and incorrect responses in the baseline or in the time window of interest (from tone onset to visual stimulus onset; Figure 4.3B).

In Experiment 2 participants also judged a 2 s interval correctly as long or incorrectly as short (Figure 4.4A). Again, we did not find any differences in the baseline period, so we baseline corrected our data. We found that theta power averaged over 3-6 Hz was significantly ($p < .001$) higher for correct ($\mu = -0.091 \pm .049$) than incorrect ($\mu = -0.185 \pm .047$) responses from 1400-2000 ms.

Taken together, we found for both Experiment 1 and Experiment 2 that theta power was higher for correct than incorrect responses in the long time interval. This difference became significant around the end time of the short interval. We therefore asked whether theta power might be associated with response times. To this end we used Spearman correlation and correlated averaged theta power over 3-6 Hz with response times over trials for each participant at each time point and each electrode. The correlation values

were z-scored and subsequently compared to 0 with cluster based permutation statistics. We expected that if theta power represented accumulated evidence in line with previous research, response times would be shorter for higher theta power.
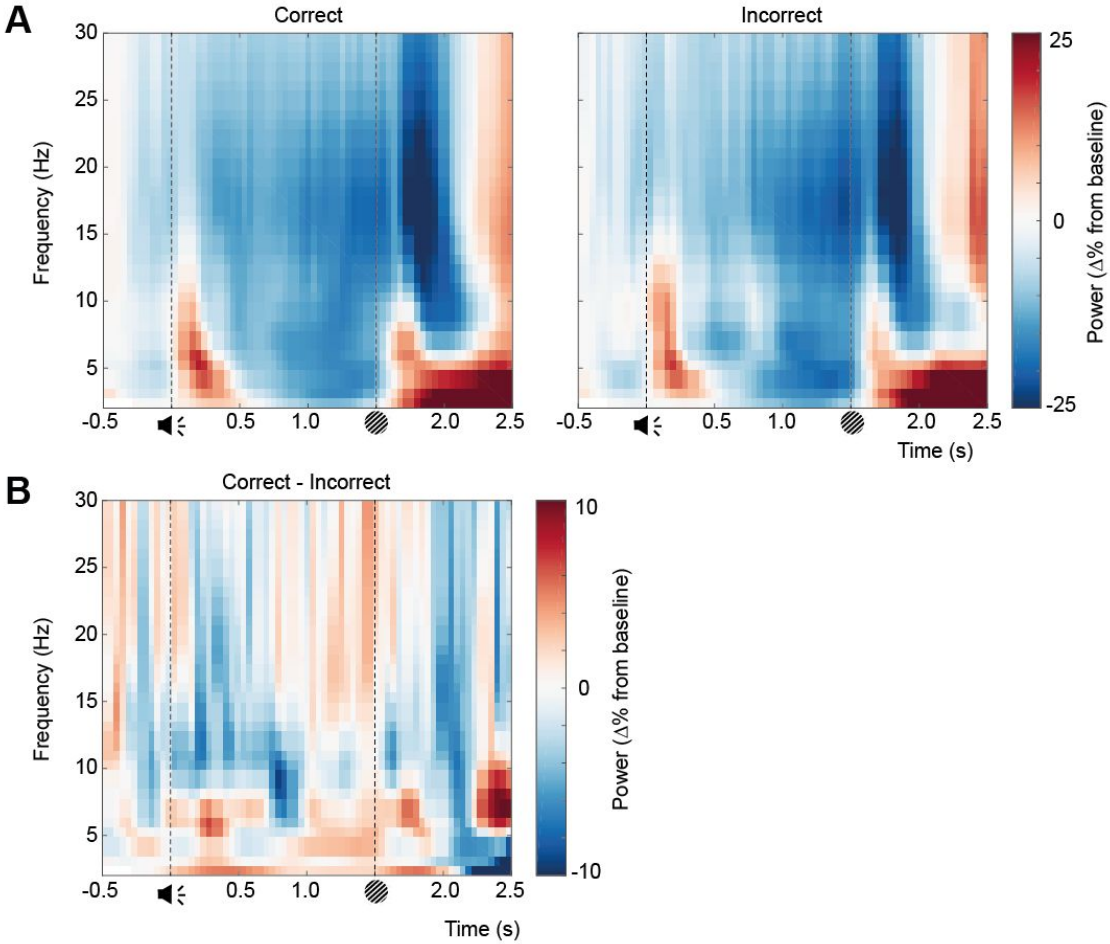
Figure 4.3 Time-frequency representation averaged across all electrodes for correct and incorrect responses when participants judge 1.5 s time intervals. The tone evoked a response in the low frequency ranges followed by sustained power decreases in the higher frequency ranges (A). The difference is plotted in B.

For Experiment 2 we found that theta power significantly (Figure 4.4D; p = .0014) correlated with response times, such that higher theta power was associated with faster response times (μ_z = -0.665 ± .150 for the significant cluster with standard error of the mean over participants). We did not observe this relationship for incorrect responses. For Experiment 1 we found that theta power showed a trend (Figure 4.2D; p = .085) in the correlation with response times for correct responses (μ_z = -0.482 ± .17). In Experiment 1 we found that theta power in incorrect responses positively correlated, albeit marginally significant, with response times (p = .051; μ_z = 0.463 ± 0.136; Figure 4.2D) such that higher theta power predicted longer response times. Taken together, these findings suggest that higher theta power after the short time window has elapsed leads to faster responses when participants correctly judge a long interval. And we found partial support for the reverse: higher theta power after the short time window has elapsed leads to slower responses when participants incorrectly judge a long interval.
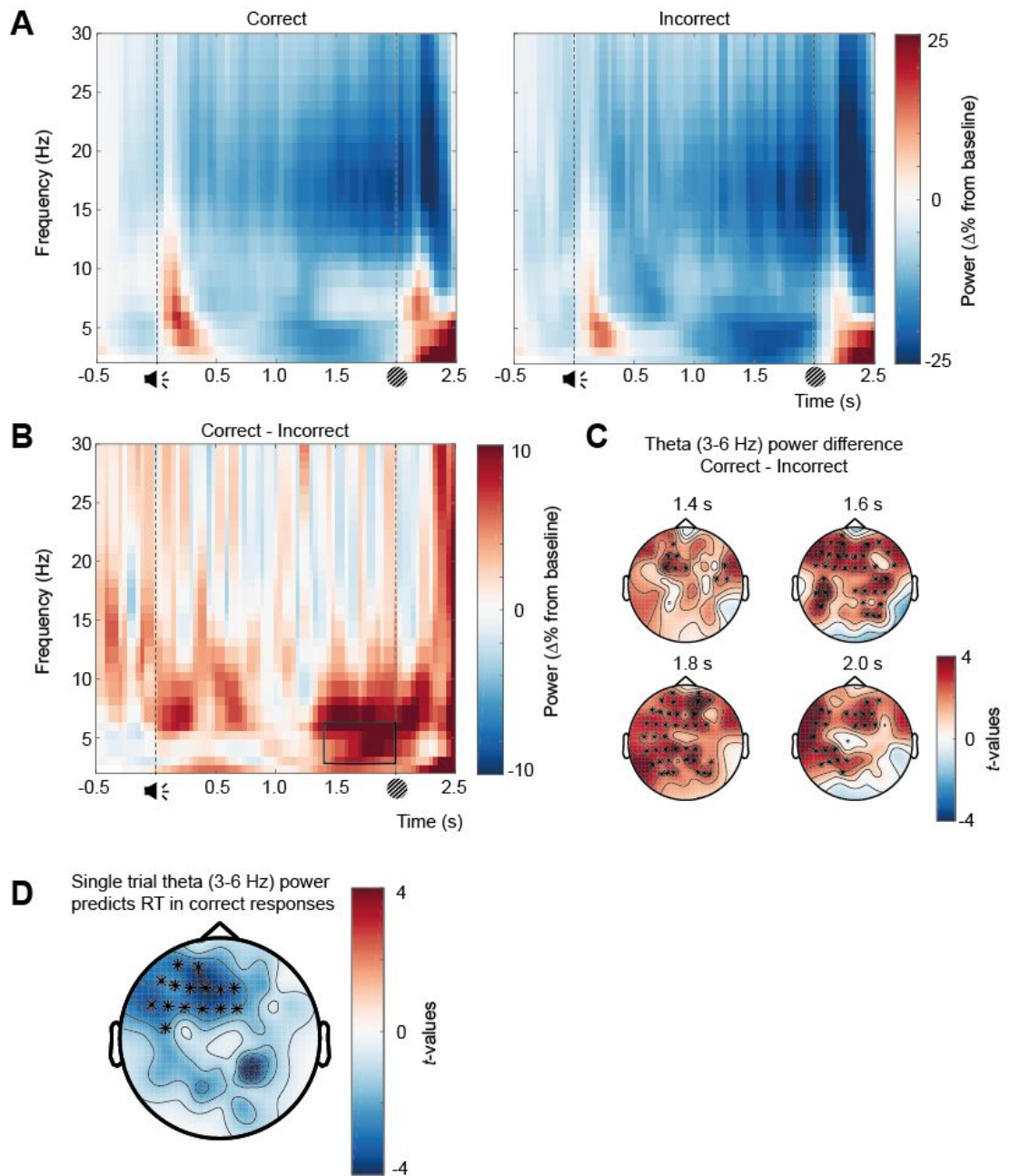
Figure 4.4 Time-frequency representation averaged across all electrodes for correct and incorrect responses when participants judge 2 s time intervals. The tone evoked a response in the low frequency ranges followed by sustained power decreases in the higher frequency ranges (A). In the lower frequency range power was higher for correct compared to incorrect responses (B). Topographies of the significant difference in the theta range are shown in C. Block box in B shows the extent of the cluster in time and stars in

C show electrodes that were part of the cluster at the time points depicted. D shows the topography of the electrodes that had correlation values that were significantly (p = .0014) different from 0.

4.4 DISCUSSION

With the analyses discussed in this chapter we compared power differences between correct and incorrect responses on an interval discrimination paradigm. We consistently found higher theta power in long interval trials after the short time interval had elapsed for correct compared to incorrect responses. In Experiment 2 this theta signature was also associated with response times such that higher theta power was indicative of shorter response times for correct responses. This finding was partially supported by the data of Experiment 1 where short response times on correct responses were marginally significantly associated with higher theta power. In Experiment 1 we also found that higher theta power was associated with slower responses on incorrect judgements, albeit marginally significant, but we did not observe this pattern in Experiment 2. In addition to the theta power effects, we also found that alpha and beta power were significantly lower for correct than incorrect responses on the long interval trials of Experiment 1. Moreover, the beta power effect reversed on short interval trials of Experiment 1 such that beta power was higher for correct than incorrect responses. However, the effect of alpha and beta power did not replicate in Experiment 2.

4.4.1 Theta power difference between correct and incorrect long intervals

In the long time intervals of both experiments we found that theta power was higher for correct than incorrect responses after the short time interval had elapsed. Scalp-recorded EEG is sensitive to volume conduction, which makes it hard to read the topographies of

the theta activity difference (van den Broek et al., 1998). However, the topographies suggest a lateralized frontal activity pattern for the data in Experiment 1 and a more widespread topographic difference in the data from Experiment 2 (compare Figures 4.4C and 4.2C, top). For future work looking at interval discrimination and EEG, it might be advisable to apply a spatial filter such as the surface Laplacian to reduce volume conduction (e.g. Wong et al., 2018 and Chapter 3 of the current thesis).

Theta power has been linked to working memory and cognitive control (Jensen & Tesche, 2002; Fell & Axmacher, 2011; Sauseng et al., 2009; Cohen & Donner, 2009) and theta power is also hypothesized to play a role in interval timing (Gu et al., 2015). In addition, theta power was found to differ for different temporal expectations, such that theta power was highest during critical moments, when temporal expectation was also highest (Cravo et al., 2011). Recent research in rats showed that hippocampal theta was related to duration discrimination (Nakazono et al., 2015) and an EEG study in humans showed that midfrontal theta power negatively correlated with produced intervals (Kononowicz & van Rijn, 2015). We found that theta power was higher for correct compared to incorrect responses on long interval trials, which supports the notion that theta oscillations play a role in interval timing.

Alternatively, the theta effect might come about through differences in attention. Previous research has linked theta power to attentional demand (Sauseng et al., 2007), where higher theta power was associated with more demanding conditions. It might be that longer intervals are more attention demanding, but this would not necessarily explain the difference in theta power between correct and incorrect responses on long interval trials.

Theta oscillations in human neocortex have also been related to cortical excitability (Jensen & Colgin, 2007; Canolty et al., 2006). It might be that participants are accumulating more temporal evidence when cortical excitability is high, which leads to the observed pattern of higher theta power for correct responses on long interval trials. However, this finding does not explain why we don't observe a reversed pattern of this effect on short interval trials.

4.4.2 Theta power and response time correlations

Interestingly, we did observe associations between theta power and response times. Higher theta power after the short interval had elapsed was correlated to shorter response times on correct trials in Experiment 2. In Experiment 1 we observed a similar pattern, albeit only trending significant. In Experiment 1 we also observed the, marginally significant, opposite pattern for incorrect responses, such that higher theta power led to longer response times. Previous research has also linked higher theta power and faster response times (Delorme et al., 2007). However, cortical excitability does not fully account for our findings. If theta power reflected cortical excitability, we would expect a negative correlation between theta power and response times irrespective of the response. But our finding of the positive correlation between incorrect responses and response times suggest that theta power reflects actual temporal evidence accumulation. When theta power is high, evidence in favour of long time intervals is accumulated, which makes participants respond slower on incorrect trials with high theta power.

4.4.3 More alpha/beta suppression for trials judged as long in Experiment 1

For experiment 1 we also found alpha and beta power to be more suppressed on correct than incorrect trials in the long interval. In addition, alpha and beta power showed the opposite effect in short interval trials. However, none of these effects replicated in Experiment 2. Recent evidence suggests that beta oscillations play an important role in time estimation (Kononowicz & van Rijn, 2015), where beta power was found to correlate with produced interval lengths. The most convincing evidence for beta involvement in a temporal discrimination task stems from Kulashekhar and colleagues (2016) that found that beta power was higher when temporal information was kept in working memory compared to colour information. Moreover, a recent reanalysis suggested that beta oscillations may be linked to keeping a standard interval in working memory rather than to perceived duration as such (Wiener et al., 2018). Wiener and colleagues (2018) extended this reanalysis by applying transcranial alternating current stimulation at alpha and beta bands, where they showed that participants were more likely to judge a stimulus as long during beta stimulation. These findings are in line with the results we observed in Experiment 1. When beta power is higher, participants are more likely to overestimate the short interval and when beta power is lower, participants are more likely to underestimate the long interval. However, it is unclear why we did not observe this pattern in Experiment 2.

Our data in Experiment 1 was suggestive of a general mechanism for beta power, where higher beta power led participants to judge the elapsed time as long. For alpha oscillations we observed a similar effect. Alpha power was higher for short trials that were incorrectly

judged as long and alpha power was higher for long trials that were correctly judged as long.

CHAPTER 5

The CNV (and other slow evoked potentials) and temporal judgements

---

ABSTRACT

This chapter aims to examine event-related potentials in a temporal decision-making task. Previous research has suggested that the accumulation of temporal evidence is reflected in slow evoked potentials, which might reflect climbing neural activity. In this chapter two almost identical experiments were used, where participants judged a time interval, which was demarcated by a tone and a visual stimulus, as short or long (Experiment 1: 1 vs. 1.5 s, Experiment 2: 1.5 vs. 2 s). This so-called single stimulus discrimination task allows the comparison of correct and incorrect temporal judgements. Behaviorally, participants had higher error rates for the second experiment, which is in line with Weber's law where higher error rates are predicted for longer time intervals. In the EEG, a significantly larger slow-evoked potential was observed over parietal electrodes for correct compared to incorrect judgements of a 2 s interval. However, no effects were observed in other conditions. Response-locked data identified several differences across conditions, but these differences mostly coincided with the offset of the to-be-timed interval, i.e. the visual stimulus. When the data was locked to the visual stimulus the post-stimulus N2 amplitude was larger for incorrect compared to correct responses for the 1.5 s interval in Experiment 1. Post-error related signals showed larger a error-related negativity (ERN) over frontal electrodes for incorrect compared to correct responses for long, but not short, intervals. The error-related positivity (Pe), interestingly, was larger for incorrect compared to correct responses for short intervals, and this pattern was reversed for long intervals.

5.1 INTRODUCTION

Time perception and evidence accumulation can be studied through event related potentials (ERPs). These signals are obtained by averaging cortical activity recorded with electroencephalography (EEG) across many trials. Non-phase locked oscillatory activity is averaged out and the activity that remains is thought to be evoked (i.e. phase locked and time-locked) by the stimulus or task demands (Coles & Rugg, 1995). In the literature of time perception, climbing neural activity is often seen as a potential neural substrate of the accumulator as hypothesized by scalar timing theories (STT; Gibbon et al., 1984). In STT a pacemaker generates pulses, which are subsequently stored in an accumulator and the accumulator is read out in order to judge how much time has passed. Climbing neural activity, as indexed through slowly evolving ERPs, might reflect the accumulation process of temporal information (Macar et al., 1999; Macar & Vidal, 2009; Macar & Vitton, 1972; Pfeuty et al., 2005).

The Contingent Negative Variation (CNV) is a slow (i.e. in the range of several hundreds of milliseconds) negative-going potential that has been related to time estimation since its discovery (Walter, 1964). The relation between time perception and the CNV was further developed by Macar and colleagues (1999), who found that the CNV at electrode FCz positively correlated with produced intervals on a trial-by-trial basis. This finding led to the appealing hypothesis that the CNV reflects the accumulation of temporal information (Macar et al., 1999; Pfeuty et al., 2003). However, a direct relationship between the CNV and time estimation was called into question after more recent research was unable to replicate the original correlation and instead found that the CNV diminished with time-on-task (i.e. the CNV showed habituation; Kononowicz & van Rijn, 2014; Kononowicz

& Penney, 2016). If the CNV is related to time estimation, one would not expect the amplitude of the CNV to decrease with time-on-task as this would negatively affect temporal estimation ability. These recent findings led to the suggestion that the CNV is instead related to time-based response preparation (Kononowicz & van Rijn, 2014; van Rijn et al., 2011). But this interpretation of the CNV was also recently called into question when Mento and colleagues (2013) used a passive task (i.e. no motor responses were required), where participants were over-exposed to a time interval of 1500 ms and less often exposed to a time interval of 2500 or 3000 ms. In this experiment the CNV became more pronounced (i.e. the opposite of habituation) with time-on-task, even in the absence of a motor component (Mento et al., 2013). Taken together, these results show that the role of the CNV in time estimation is not fully understood, although it seems unlikely that there is a straightforward relationship between the accumulator, as proposed by STT, and the CNV.

A theoretical framework that has gained substantial attention in the last 2 decades in decision making neuroscience is sequential sampling. Sequential sampling models suggest that noisy sensory evidence is accumulated until the balance is tipped in favour of one decision outcome over the other (Kelly & O'Connell, 2013). Interestingly, these models show strong similarities to the STT because both models depend on evidence accumulation over time. A recent decision-making study (O'Connell et al., 2012), where participants detected a gradually developing change in the stimulus, identified a possible accumulation signal: the centro-parietal positive potential (CPP). This signal was found to correlate both with cumulative evidence and response times (O'Connell et al., 2012). O'Connell and colleagues showed that the CPP underlies the accumulation of noisy

sensory information in non-temporal decision making, but it is currently unknown whether this ERP also reflects evidence accumulation of temporal information. Moreover, previous research has described a late component of the earlier described CNV with a more centro-parietal topography (Trillenberg et al., 2000; Verleger et al., 1999), compared to the frontal topography described in other studies (e.g. Kononowicz & van Rijn, 2014; Macar et al., 1999; Pfeuty et al., 2003). Taken together, these studies suggest that temporal evidence for the accumulation process should not be limited only to fronto-central electrodes, but should test central and parietal topographical locations.

In addition to ERPs locked to the onset of the to-be-timed interval (i.e. the CNV), previous research has also investigated offset-locked ERPs. The offset-locked ERPs most studied in temporal decision making are the N1-P2 complex and the late positive component of timing (LPCt). Kononowicz and van Rijn (2014) used temporal comparison intervals that were more or less similar to the standard interval by varying the length of the comparison interval at 3 shorter and 3 longer levels. They showed that the sensory-evoked N1-P2 complex reflected the similarity of the standard and comparison interval, because the N1P2-complex was larger for comparison intervals that were less similar (i.e. the more extreme levels) to the standard interval. Importantly, this also held for comparison intervals that were longer than the standard interval, which suggested that timing processes continued after the elapsing of the standard interval and the resolution of the CNV (Kononowicz & van Rijn, 2014). The offset-locked LPCt appeared as a large positive deflection over prefrontal electrodes (Paul et al., 2003) or central/centro-parietal electrodes (Lindbergh & Kieffaber, 2013). Lindbergh & Kieffaber (2013) showed that the LPCt scaled with the subjective experience of elapsed time. In addition, Paul et al. (2003) showed that

the LPCt increased as a function of stimulus duration but only if the short comparison interval was presented before the long comparison interval and not vice versa. Paul et al. (2003) suggested that the LPCt might reflect the comparator as proposed by STT. All in all, offset-locked ERPs present a relatively understudied field of temporal discrimination research and it remains an open question whether N1-P2 differences also arise when the same physical stimulations leads participants to different responses.

Several MR-neuroimaging studies have focused on the brain regions involved in time perception. An influential meta-analysis showed that automated time perception (i.e. time intervals <1 s) mostly relies on the cerebellum, whereas cognitively controlled time perception of supra-second time intervals rely mostly on cerebral regions (Lewis & Miall, 2003). Pouthas and colleagues (2003) contrasted functional MRI of short and long time interval estimation and found that a caudate-preSMA circuit may reflect a clock mechanism, the anterior cingulate may reflect decision making and premotor-inferior frontal regions may reflect response related processes. In addition, rodent studies have shown that the medial prefrontal cortex plays an important role in interval timing (Kim et al., 2009; Kim et al., 2013; Narayanan et al., 2012; Xu et al., 2014). This same region plays an important role in action monitoring (Luu et al., 2000) and is thought to be the source of the error-related negativity (ERN). Luu and colleagues (2000) showed that the ERN was more pronounced when temporal response criteria were not met. However, how errors in temporal decision making influence the error signals like the ERN remains poorly understood.

Hence, the aim of this chapter was to examine whether temporal decision making might give rise to a slow evoked potential over centro-parietal regions like the late CNV or the

CPP, specifically by comparing correct and incorrect temporal judgements. In these experiments I used a time estimation paradigm where participants were exposed to intervals of two different lengths and participants had to classify each interval as short or long. If the CNV tracks subjective timing, one would expect that the CNV would be more pronounced when participants judge an interval as long compared to short, irrespective of the physical stimulus duration. Likewise, if the CPP tracks temporal evidence accumulation, one would expect similar results for the CPP. In addition, since previous research suggested that offset-locked ERPs might reflect temporal decision-making, I also looked at offset-locked ERPs, when each interval should be compared to a reference interval implicitly kept in working memory. Finally, I looked at whether error signals can be recorded reliably, as has been done for many instances of non-temporal decision making (Gehring et al., 1993; Ridderinkhof et al., 2004).

5.2 MATERIALS & METHODS

5.2.1 Participants, paradigm & behavior

The data from Chapter 2 was reanalyzed here. Please refer to Chapter 2 for more information about the participants, paradigm & behavior.

5.2.2 EEG Data Acquisition

EEG was acquired using the EEGO Sports system (ANT Neuro, Enschede, Netherlands) and Waveguard caps housing 64 Ag/AgCl electrodes arranged in a 10/10 system layout (including left and right mastoids, CPz as reference and AFz as ground). Impedances were kept below 20 kΩ, and the data was acquired using a sampling rate of 500 Hz. EOG was

collected for horizontal eye movements, by placing bipolar electrodes on the outer canthi of the left and right eye. ECG was collected for heart rate data, by placing one bipolar electrode on the right chest, one bipolar electrode on the left abdomen and an electrode on the left collar bone served as the ground. This latter electrode acted as a ground electrode for the ECG signal. Offline data analysis took place in Matlab with eeglab functions (version 13.1.1b; Delorme & Makeig, 2004) and the FieldTrip software package (Oostenveld et al., 2011).

5.2.3 Preprocessing

Using EEGLAB, the data were epoched around -1000 to 3500 ms from tone onset. Subsequently, the epochs were baselined from -100 to 0 ms to remove any slow drifts. Missed trials were discarded. Based on visual inspection trials were removed for the following reasons: muscle artefacts, noise (i.e. electrode jumps or other electrode related noise), horizontal eye movements and blinks at visual stimulus presentation. The cleaned epochs were then average referenced (excluding bipolar electrodes), from which electrode CPz was reconstructed. Ocular artefacts were removed in FieldTrip using independent component analysis (ICA, infomax algorithm) incorporated as the default "runica" function. Prior to the ICA, a PCA (15 components) was performed on the data to reduce the dimensionality of the data.

5.2.4 ERP analysis and statistics

To assess whether there were differences in early evoked responses to correctly and incorrectly estimated time intervals I compared the N1 and P2 ERPs and the N1-P2 complex, which were evoked by the visual stimulus that marked the offset of the time

interval. Visual inspection of ERPs averaged over correct and incorrect responses were used to define a region of interest. For both short and long intervals and for Experiment 1 and 2 electrodes O1, O2, PO5, PO6, PO7 and PO8 over occipital regions showed the largest responses to visual stimulation. Visual inspection of averaged correct and incorrect responses at these electrodes were used to select a time window of interest for the N1 and P2. Dependent samples t-tests were used to compare mean amplitude over the time interval and electrodes of interest for correct and incorrect responses. Statistical tests were performed separately for short and long intervals and Experiment 1 and 2.

For the tone-locked CNV/CPP I examined a predefined region of interest. For the CNV I focused on midfrontal electrodes: FCz, FC1, FC2, Cz, C1 and C2 and for the CPP I focused on centroparietal electrodes: CPz, CP1, CP2, CP3, CP4, Pz, P1, P2, P3 and P4. I examined the time interval from 500 ms after tone onset until the visual stimulus onset, in part to lower the number of time points to compare, but also to rule out potential spill-over into the CNV/CPP from differences in the processing of the tone. Next, I examined the same time windows without a predefined region of interest. In addition, I applied a more powerful analysis by combining the data of both experiments in a mixed ANOVA. Data at midfrontal electrode FCz was averaged from 500 ms after tone onset until visual stimulus onset. A 2 × 2 mixed ANOVA with interval length and experiment was applied to difference values of correct - incorrect responses. For response-locked examinations of the CNV/CPP I performed similar cluster-based analyses described earlier without pre-specifying a spatial region of interest and focused on data from 1 s and 1.5 s before the response for the first and second experiment, respectively.

For examination of the visually evoked N1 and P2 visual inspection of averaged ERPs of correct and incorrect responses were used to select a time window and electrodes of interest. Mean amplitudes were averaged over time, 170-206 ms post-stimulus for the N1 and 232-262 ms post-stimulus for the P2 for experiment 1 and 180-210 ms and 240-270 ms for experiment, respectively, and occipital electrodes: O1, O2, PO5, PO6, PO7 and PO8. Baseline corrections of 50 ms pre-stimulus until stimulus onset were applied in a condition specific way to assure that potential CNV differences did not contribute to differences in N1 and P2 amplitude (Kononowicz & van Rijn, 2014). In addition, and in line with previous research (Kononowicz & van Rijn, 2014), the N1-P2 complex was calculated as the sum of the absolute values of the N1 and P2. Dependent samples t-tests were applied to assess differences between correct and incorrect responses of mean amplitudes. In addition, a mixed ANOVA was applied to allow for a more powerful analysis. A 2 × 2 mixed ANOVA was applied with interval length and experiment as factors with the difference between correct and incorrect N1-P2 complexes averaged over occipital electrodes.

To exclude the possibility that effects at the level of the N1, P2 and N1-P2 amplitude were not affected by response times, I regressed out response times. To this end, I applied a linear regression of single-trial ERP amplitudes at each time and channel point for correct and incorrect responses with response times, which were log transformed and centered around 0 by subtracting the average response times over correct and incorrect responses. After applying the linear regression the residuals were divided back into correct and incorrect responses. Importantly, trials counts were matched for all analyses that used linear regression to regress out response times as this approach is much more sensitive to

trial count differences than normal ERP analyses. For the N1-P2 complex, regressing out response times was done by taking the difference between the residuals of correct and incorrect responses and subtracting the residuals of the P2 difference from the N1 difference.

To assess differences in error-related processing, a similar approach to inspection of N1 and P2 differences was applied: Visual inspection of response-locked ERPs averaged over correct and incorrect responses identified time windows of interest. Cluster based permutation statistics were used to control for multiple comparisons across electrodes. For the error-related negativity (ERN) data was averaged from 0-64 ms and 0-70 ms post-response for experiment 1 and 2, respectively. And from 94-140 ms and 104-154 ms for the error related positivity (Pe).

The differences in event-related potentials between responses were statistically assessed by means of the cluster level (channels and time-points) randomization approach (Maris and Oostenveld, 2007). Here, the activity in each channel and time point within the time intervals of interest (i.e. from tone onset to visual stimulus onset), were clustered according to exceeding a threshold of $p < .05$ obtained from a two tailed dependent samples t-test. Next, the Monte Carlo p-values of each cluster were obtained by randomly swapping the condition labels within participants 2500 times. A difference between conditions was deemed significant if the cluster p-value was smaller than .025 (two-sided test).

5.2.5 Correlating ERPs and response times

We expected that any differences between correct and incorrect responses might reflect variation in the internal clock. If the internal clock also reflects the speed of the whole

system, we would expect a relationship between the slow evoked response and response times. To examine this relationship, we performed a median split analysis. We compared the ERPs of fast and slow responses on correct trials with cluster based permutation statistics and did the same for incorrect trials. We examined the time window of interest from tone onset to visual stimulus onset and we averaged over the significant time window from the cluster based permutation test from 3.2.6. Next, we examined this association by correlating response times with trial-to-trial amplitude fluctuations. Median-split analyses are less sensitive to true effect and trial-by-trial analyses do not need the data to be split arbitrarily (Cohen, 1983). To this end, we took the average amplitude of the time window that showed a significant difference in the cluster based permutation approach. We performed this analysis both within our topographically significant region and for each electrode.

For the topographically significant region we took the average amplitude both over the time points and electrodes that reached significance in the cluster based permutation test. For each participant we calculated the ranked correlation of response time and average activity and used Fisher's z-transform to normalize the data (see 2.2.5). At the group level we compared the z-transformed correlation values to 0 with a t-test.

We also calculated Spearman's ranked correlation value at each electrode and each time point by correlating response times over trials with the amplitude value at each time point and electrode. Fisher's z-transform was applied and then we used cluster based permutation statistics to compare these correlation values to 0.

Finally, we performed a fixed effects analysis by calculating the Spearman correlation for the average amplitude of the significant cluster and response times, irrespective of individual participants.

5.3 RESULTS

5.3.1 Event-related potentials

<u>i) Offset-locked potentials</u>

First, I examined whether there were differences in visually evoked responses to the offset of correct- and incorrectly timed intervals. Previous research showed that comparison intervals that were physically more different from the standard interval evoked larger N1-P2 complexes than comparison intervals that were more similar to the standard interval (Kononowicz & van Rijn, 2014). Here, I examined whether there are also differences in the N1, P2 and N1-P2 complex for physically identical stimulation, but with different subjective experiences. I compared correct and incorrect responses to short and long intervals separately for the intervals and experiments. I compared mean amplitude values over occipital electrodes (O1, O2, PO5, PO6, PO7, PO8) for time windows based on the averaged activity across correct and incorrect responses (N1 time window: 170-206 and 180-210 ms; P2: 232-262ms and 240-270 ms, for Experiment 1 and Experiment 2, respectively; Figure 5.1 and 5.2).

For the short interval of Experiment 1 I did not observe differences between correct and incorrect responses for the N1 or P2 over occipital regions (Figure 5.1A, B and C). The long interval of Experiment 1 did not show any significant difference for correct compared

to incorrect judgements in the N1, but I did find a smaller P2 for correct compared to incorrect responses (Figure 5.1D, E and F).
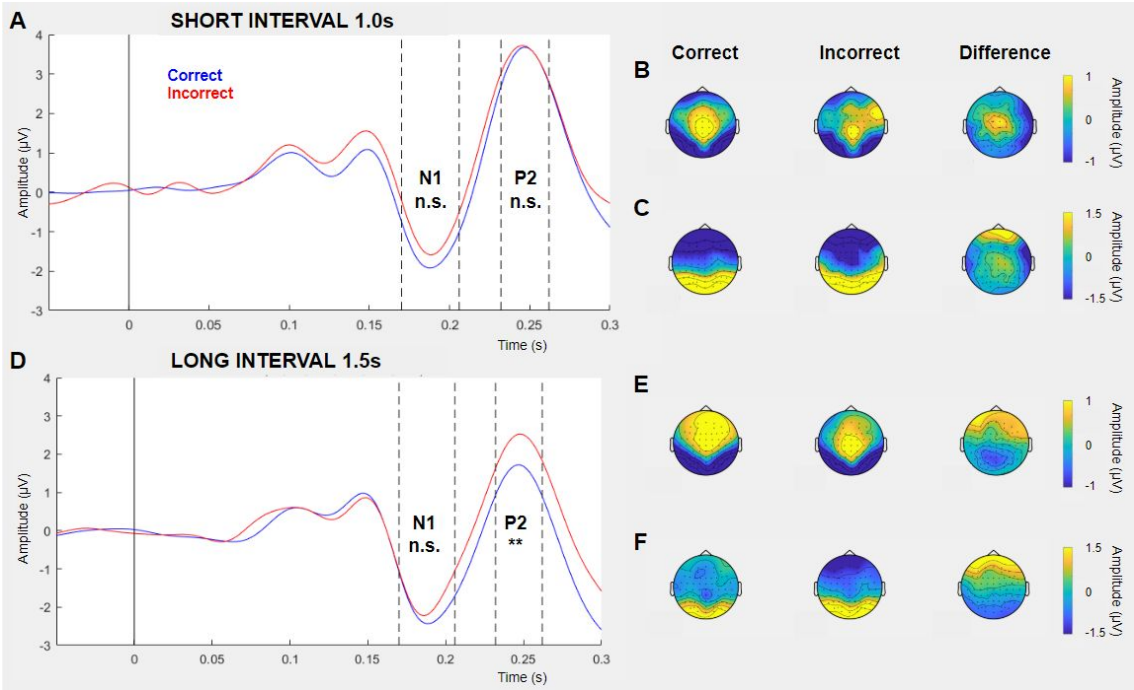
Figure 5.1 Larger P2 visually evoked responses to the offset of the time interval for incorrect compared to correct responses. There were no significant differences in visually evoked N1 and P2 for the short interval (A). The visually evoked ERP to correct responses is shown in blue and incorrect responses in red. Over occipital regions, the topography also looked similar (B shows the topography of the N1 and C shows the topography of the P2). For the long interval there was no difference in the N1, but the P2 was more pronounced for incorrect than correct responses (D).

For Experiment 2 there were no differences between correct and incorrect responses for the short or the long interval in either the N1 or P2 (Figure 5.2).
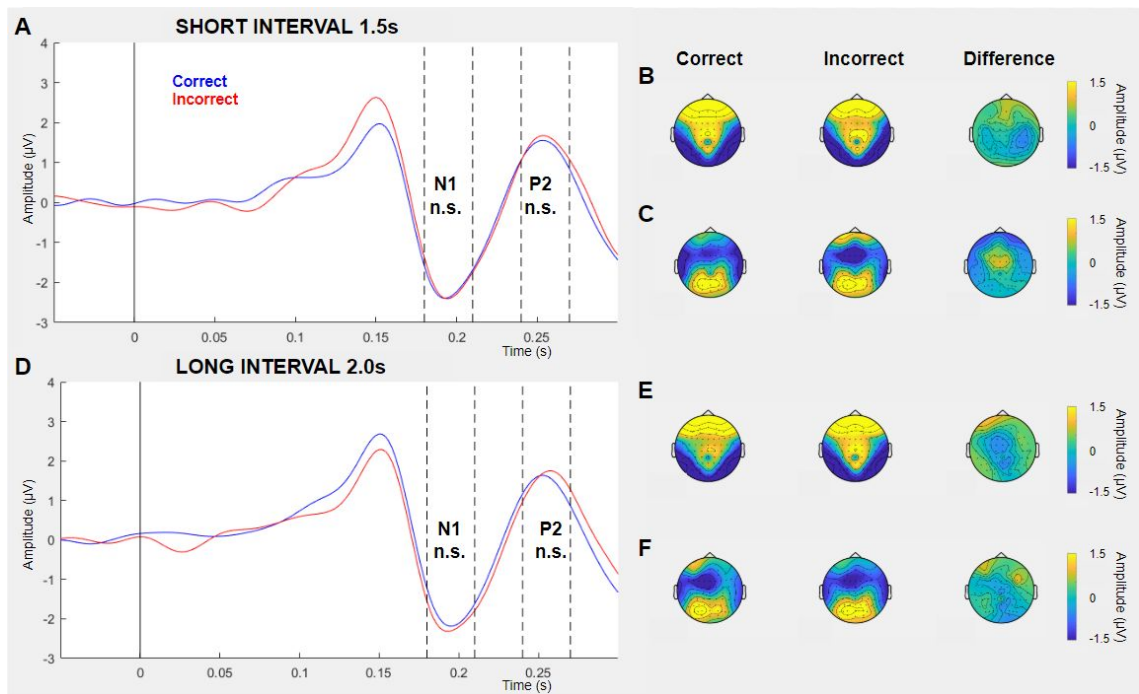
Figure 5.2 No differences in visually evoked responses to the offset of the time interval in Experiment 2. Same conventions as Figure 5.1.

I also examined the N1-P2 complex, but I observed no difference in correct and incorrect responses for the short or long interval of either experiment (Table 5.2). Moreover, a mixed ANOVA indicated that there was no effect of experiment on the N1-P2 complex ($p = 0.7$), nor was there an interaction between interval and experiment ($p = 0.6$).

To assess whether differences between correct and incorrect temporal judgement as indicated by differences in N1 and P2 mean amplitude was contaminated by response time differences between the conditions, I regressed out the response times (Table 5.1 and 5.2). Even after regressing out response times there was a significant difference in P2 amplitude between correct and incorrect judgements of the long interval in Experiment 1.

Table 5.1 N1 and P2 amplitudes and statistics. This table shows the amplitude averaged over occipital electrodes (see main text) in a time window based on visual inspection of the average visually evoked ERP of correct and incorrect responses. I = interval length in s; R = response, C = correct, I = incorrect; Reg is ERP after regressing out response times

	I	R	N1	Stats	N1 Reg*	Stats	P2	Stats	P2 Reg*	Stats
Exp 1	1.0	C	-1.5 ± 2.3	t(17) = -1.6	-0.4 ± 0.8	t(17) = -2.0	3.3 ± 2.1	t(17) = -0.3	-0.1 ± 0.8	t(17) = -0.8
		I	-1.1 ± 2.5	p = 0.13	0.4 ± 0.8	p = 0.07	3.4 ± 2.6	p = 0.76	0.1 ± 1.0	p = 0.45
	1.5	C	-2.0 ± 1.9	t(17) = -1.5	-0.2 ± 0.5	t(17) = -1.8	1.4 ± 1.8	t(17) = -3.9	-0.4 ± 0.4	t(17) = -3.8
		I	-1.7 ± 1.7	p = 0.15	0.2 ± 0.5	p = 0.09	2.2 ± 2.2	**p < .001**	0.4 ± 0.4	**p = .002**
Exp 2	1.5	C	-2.1 ± 2.4	t(12) = -0.16	-0.1 ± 0.2	t(12) = -1.5	1.3 ± 2.7	t(12) = -0.47	0 ± 0.6	t(12) = -0.1
		I	-2.1 ± 2.4	p = 0.87	-0.1 ± 0.2	p = 0.15	1.4 ± 2.3	p = 0.64	0 ± 0.6	p = 0.92
	2.0	C	-1.9 ± 2.3	t(12) = -0.64	-0.1 ± 0.3	t(12) = -0.83	1.4 ± 2.4	t(12) = -0.51	-0.1 ± 0.3	t(12) = -1.13
		I	-2.1 ± 2.3	p = 0.53	0.1 ± 0.3	p = 0.42	1.5 ± 2.7	p = 0.62	0.1 ± 0.3	p = 0.28

* Residuals are symmetrical along the x-axis for the correct and incorrect responses.

Table 5.2 N1-P2 complex. The N1-P2 complex was determined for the ERP data as the sum of the absolute values of the N1 and P2, which were the minimum and maximum amplitude values respectively in time windows based on the average ERP to correct and incorrect responses. Same conventions as table 5.1.

	Interval	Response	N1-P2	Stats	N1-P2 Reg**	Stats
Exp 1	1.0	C	7.2 ± 3.7	t(17) = -0.36 p = .72	-0.5 ± 1.8	t(17) = -1.1 p = .27
		I	7.3 ± 3.1			
	1.5	C	5.6 ± 3.3	t(17) = -1.95 p = .068	0.3 ± 1.2	t(17) = -1.2 p = .26
		I	6.1 ± 3.8			
Exp 2	1.5	C	5.9 ± 3.4	t(12) = -0.03 p = .98	-0.2 ± 1.2	t(12) = -0.5 p = .65
		I	5.9 ± 3.6			
	2.0	C	5.4 ± 3.0	t(12) = -0.46 p = .66	0.05 ± 1.0	t(12) = 0.2 p = .85
		I	5.6 ± 3.1			

** To extract residual values for the N1-P2 complex, I took the difference between residuals at time points where the average ERP was at its minimum (N1) or maximum (P2) in the time windows of interest (see main text). The N1-P2 complex was calculated as the difference between the value indicated at the N1 and P2.

Taken together, these findings suggest that the offset of the time intervals, which was marked with a visual stimulus in our paradigm, was processed differently for correct and incorrect responses to the long interval in the first experiment. However, this finding was only reflected in the P2, not in the N1-P2 complex or in any of the other experimental conditions.

ii) CNV and CPP

Next, I asked what role the CPP and the CNV play in temporal decision-making in this single stimulus task design. To this end, I first examined a frontrocentral (FCz, FC1, FC2, Cz, C1 and C2) and a centroparietal (CPz, CP1, CP2, CP3, CP4, Pz, P1, P2, P3 and P4) cluster of interest by averaging over electrodes. I used cluster-based permutation statistics

to assess whether there were differences between correctly and incorrectly judged time intervals, while simultaneously correcting for multiple comparisons over time. To exclude any influences of potential differences in evoked responses to the tone I examined the time windows from 500 ms after the tone onset until the visual stimulus onset, i.e. the time interval offset.

For Experiment 1 I did not observe any significant differences between correct and incorrect responses for the short and long interval at frontocentral or centroparietal electrodes (Figure 5.3). Both intervals showed an increase in amplitude over centroparietal and frontopolar electrodes and a decrease in amplitude over occipital electrodes (Figure 5.3E and F), but there was no difference between correct and incorrect temporal judgements.
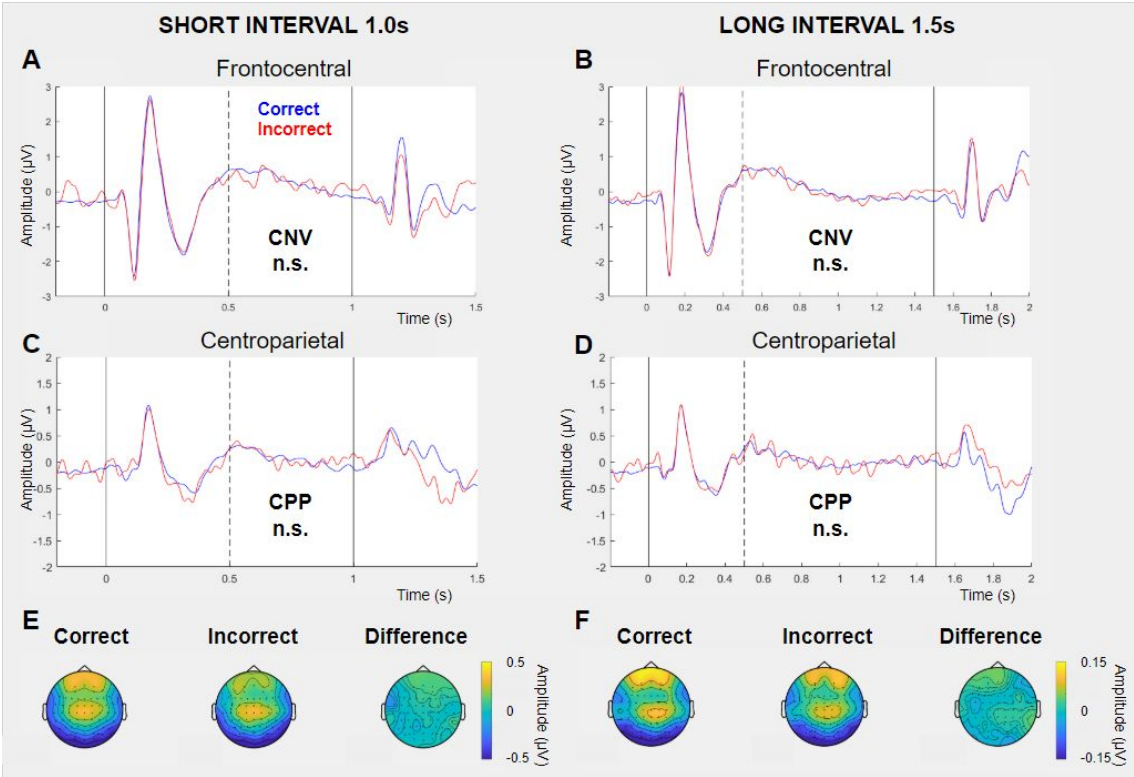
Figure 5.3 No difference in CNV and CPP for correct and incorrect responses at frontocentral and centroparietal electrodes for Experiment 1. Cluster-based permutation statistics did not identify any significant differences between correct and incorrect temporal judgements for short and long intervals in Experiment 1 at either frontocentral or centroparietal electrodes. ERPs locked to the onset of the tone are shown over frontocentral (A and B) and centroparietal (C and D) electrodes for the short (A and C) and long (B and D) interval. Correct responses are shown in blue and incorrect responses are shown in red. The topographies (E and F) show the averaged activity across time for the correct (left) and incorrect (middle) responses and the difference (correct - incorrect, right).

I applied the same approach to the data of Experiment 2 and again found no significant differences between correct and incorrect responses (Figure 5.4). The topographies showed a similar pattern for the short interval of Experiment 2 as compared to the topographies of Experiment 1, but the frontopolar increase was not visible for the long interval of Experiment 2.
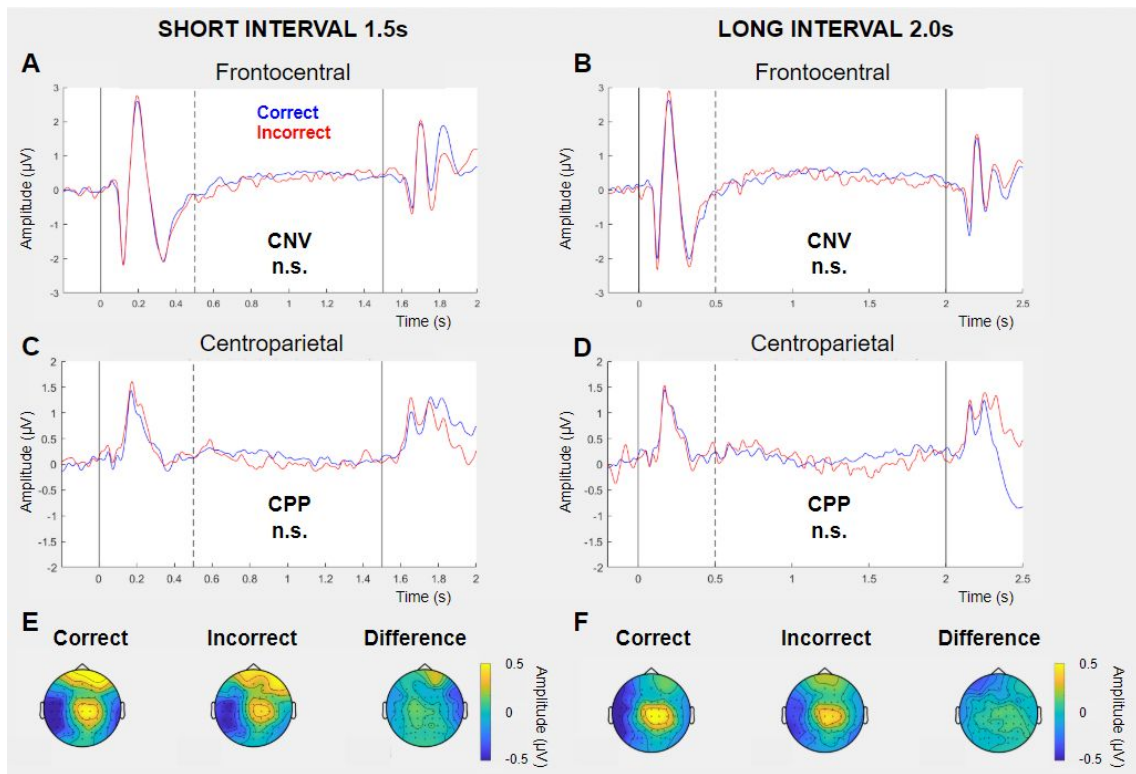
Figure 5.4 No difference in CNV and CPP for correct and incorrect responses at frontocentral and centroparietal electrodes for Experiment 2. Conventions for this figure are the same as in Figure 5.3.

Next, I explored the difference between correct and incorrect responses without a predefined region of interest. In this analysis the cluster-based permutation approach corrected for multiple comparisons across time and space (i.e. electrodes). For Experiment 1 we compared time-locked activity from 500 ms after the tone onset until the visual stimulus (at 1 or 1.5 s) was presented. The clusters we observed did not reach significance for the short or the long interval (Figure 5.5A and B).

For Experiment 2 we used the same approach (with the visual stimulus coming on at 1.5 or 2 s) and found a positive cluster (Figure 5.5D and E; $p = .01$) for long (2 s) interval trials

when we compared correct to incorrect responses that survived multiple comparisons corrections. The difference between correct (μ = 0.142 ± .05 μV) and incorrect (μ = -0.153 ± .06 μV) responses was most pronounced over a right lateralized parieto-occipital cluster (Figure 5.5E, right). Interestingly, the difference was largest around the end of the short (1.5 s) interval from 1458-1532 ms (Figure 5.5D). We did not find any significant differences for the short (1.5 s) interval. This finding suggests that for interval discrimination of 2 s intervals the CPP might play a role.
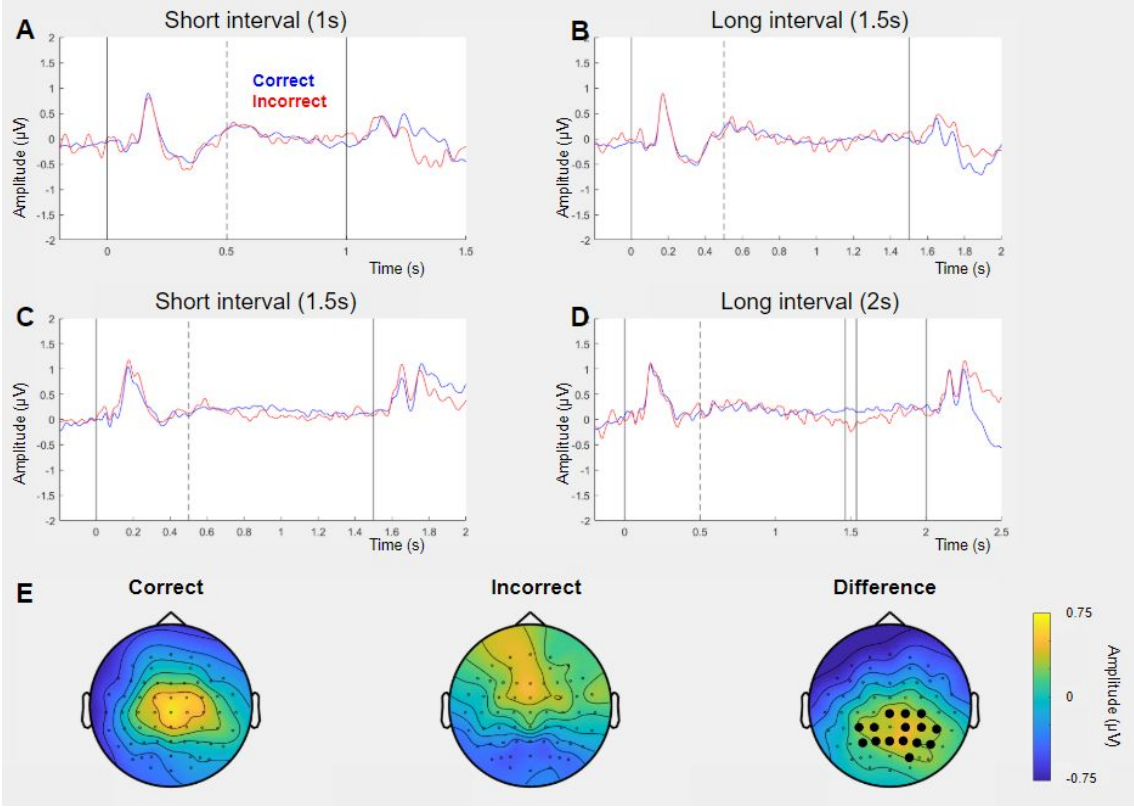
Figure 5.5 A larger tone locked CNV for correct compared to incorrect responses for the long interval of Experiment 2. The cluster-based permutation approach was performed from 500 ms after tone onset until visual stimulus onset. For the long (2 s) interval trials of Experiment 2 we found a significant positive difference. We plotted the amplitude averaged over the electrodes that showed the largest difference (E, most rightward

plot, black dots) as a function of time for correct (blue) and incorrect (red) responses for each interval and experiment (A-D).

To combine the data of both experiments a mixed-effects ANOVA was applied to data from FCz averaged from 500 ms past tone-onset until visual stimulus onset. The mixed ANOVA indicated that there was no effect of experiment on the CNV amplitude (p = 0.11), nor was there an interaction between interval length and experiment (p = 0.5).

iii) Response locked ERPs

I examined response locked ERPs for correct and incorrect responses in a temporal decision-making task. I examined the CNV/CPP locked to the response and used cluster-based permutation statistics to examine the time window from 1s before the response until the response. Similarly, to the tone locked analyses of the CNV/CPP I examined a frontocentral and a centroparietal region of interest. When averaging over these spatial regions of interest I observed no clusters. Next, I examined the differences between correct and incorrect responses without averaging over electrodes. For Experiment 1 I observed no difference in the CNV/CPP locked to the response for the short interval between correct and incorrect responses (Figure 5.6A and C). For the long interval there were 3 clusters that survived corrections for multiple comparisons. A positive and negative cluster were most pronounced for overlapping time windows from 804 to 756 ms before the response (Figure 5.6B and D, cluster i, p = .025 for the positive and p = .015 for the negative cluster, Fp1, Fpz, F3, Fz, FC1, FC2, C3, Cz, C4, AF3, F5, F1, FC3, FCz, FC4, C1, C2 black dots in Di, P7, P4, P8, POz, O1, O2, P5, P6, PO5, PO3, PO4, PO6, PO7, PO8, Oz white dots in Di). Closer to the response, from 202 to 128 ms pre-response,

there was a negative cluster where the CNV was more pronounced for incorrect compared to correct responses across central electrodes (Figure 5.6B and D, cluster ii, *p* = .021, Fz, FC1, FC2, C3, Cz, C4, CP2, F1, FC3, FCz, FC4, C1, C2 white dots in Dii).
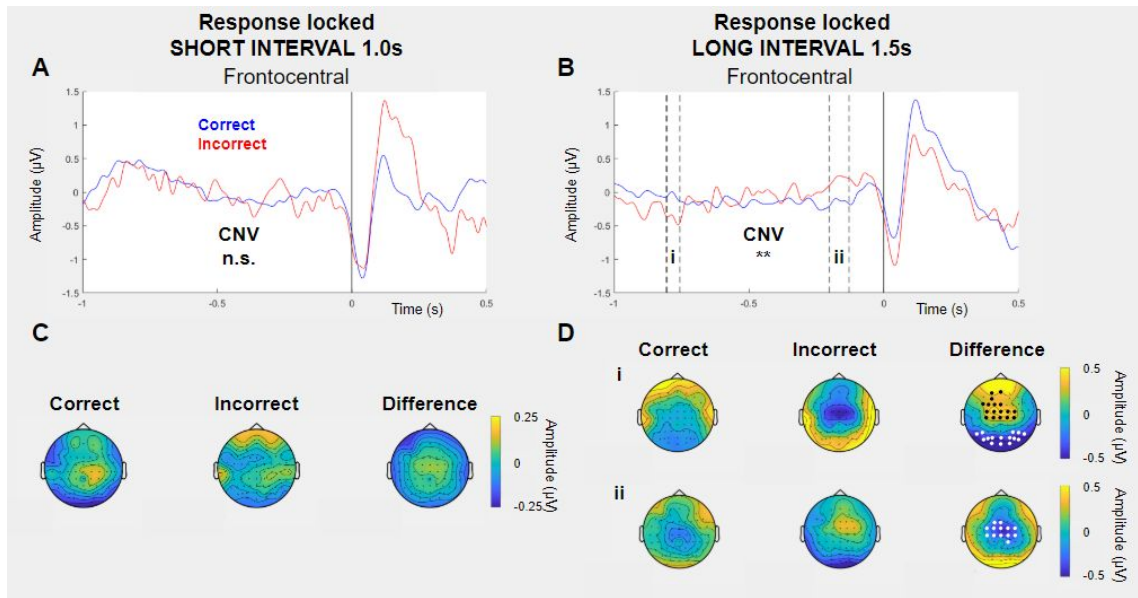
Figure 5.6 Response locked CNV/CPP for Experiment 1 showed several differences for correct and incorrect judgements of the long interval. The CNV of the short interval showed no differences between correct (in blue) and incorrect (in red) responses (A). Topographies show the averaged activity from 1s before until the response (C). For the long interval 3 clusters indicated a significant difference between correct and incorrect responses. A positive and negative cluster overlapped in time (cluster i) and a negative cluster closer to the response (cluster ii). Topographies show the activity for the time points that were indicated to show the largest differences by the cluster based permutation statistics.

The same analysis was performed on the data of Experiment 2. I found a larger response locked CNV/CPP for correctly judged short intervals compared to incorrectly judged short intervals from 354 to 190 ms pre-response (Figure 5.7C, *p* = .009, CP1, CP2, P3, Pz, POz,

O1, C1, CP3, P5, P1, P2, PO5, PO3, PO4, PO7, Oz, black dots). The opposite effect was observed for the long interval, where the response locked CNV/CPP was larger for incorrect compared to correct judgements of the long interval from 204 to 138 ms pre-response (Figure 5.7D, p = .026, C3, Cz, C4, CP1, CP2, P3, Pz, P4, POz, C2, CP3, CP4, P1, P2, PO3, PO4, white dots).
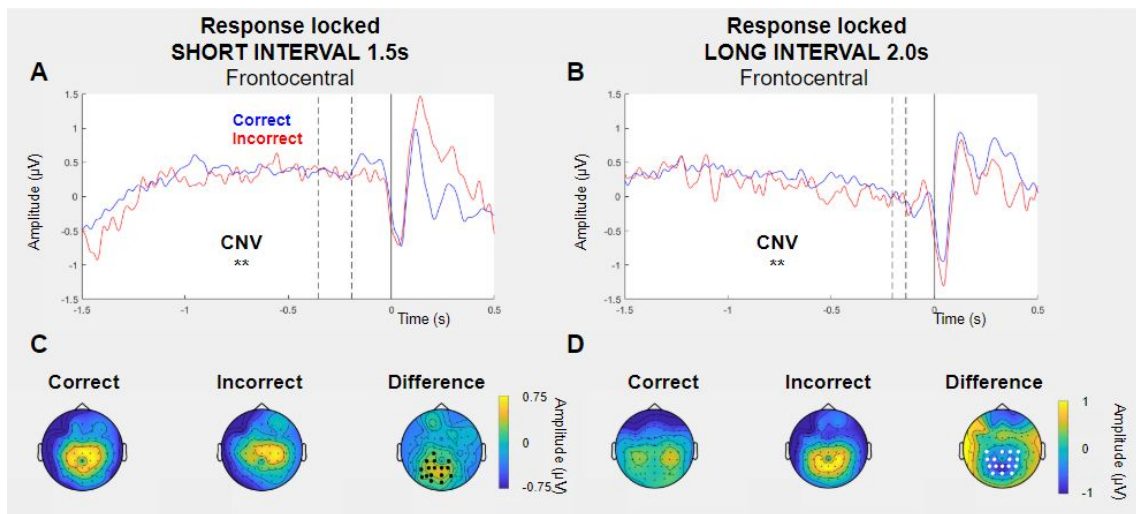
Figure 5.7 Response locked CNV/CPP for Experiment 2 showed differences for correct and incorrect judgements of both the short and long interval. The CNV of the short interval showed a positive difference between correct (in blue) and incorrect (in red) responses over parieto-occipital electrodes (C). Topographies show the averaged activity from over the time window indicated by the cluster based permutation statistics (C and D). There was no difference over frontocentral electrodes (A). For the long interval a negative cluster indicated a significant difference between correct and incorrect responses.

It is important to note that the significant differences in Experiment 2 and cluster ii of Experiment 1 fall between presentation of the visual stimulus and the response. Rather than reflecting true differences in CNV/CPP the differences might reflect processing differences of the visual stimulus that demarcated the end of the time interval.

Finally, I examined error-related activity as reflected by the error-related negativity (ERN) and the error-related positivity (Pe). To this end, I examined the ERN and Pe by selecting two time windows based on the average of correct and incorrect responses. For Experiment 1 there was a difference between correct and incorrect responses for the Pe, 94 to 140 ms post-response, over left-temporal electrodes (p = .018, T7, CP5, P7, C5, FT7, TP7, black dots in Figure 5.8C) and over midfrontal electrodes (p = .0056, FC1, FC2, Cz, C4, CP2, FCz, FC4, C1, C2, white dots in Figure 5.8C) for the short interval. I did not find a difference between correct and incorrect responses in the time window of the ERN, 0 to 64 ms post-response, for the short interval. For the long interval of Experiment 1 I found a significant positive difference between correct and incorrect responses in the time window of the ERN over frontal electrodes (p = .0008, Fpz, Fp2, F7, F3, Fz, F4, F8, FC5, FC6, AF3, AF4, AF8, F5, F1, F2, F6, FC4, FT8, black dots Figure 5.8D, top row) and a significant negative difference over parietal electrodes (p = .006, CP5, CP1, CP2, P3, Pz, POz, CP3, CP4, P5, P1, P2, PO5, PO3, PO7, white dots Figure 5.8D, top row). In addition to these differences in the ERN time window I also observed differences in the Pe time window. Cluster based permutation statistics identified a positive difference which was most pronounced over midfrontal electrodes (p = .009, Fz, F4, FC1, FC2, AF4, F1, F2, FCz, FC4, black dots Figure 5.8D, bottom row) and a negative difference which was most pronounced over occipital electrodes (p = .05, POz, O1, Oz, O2).
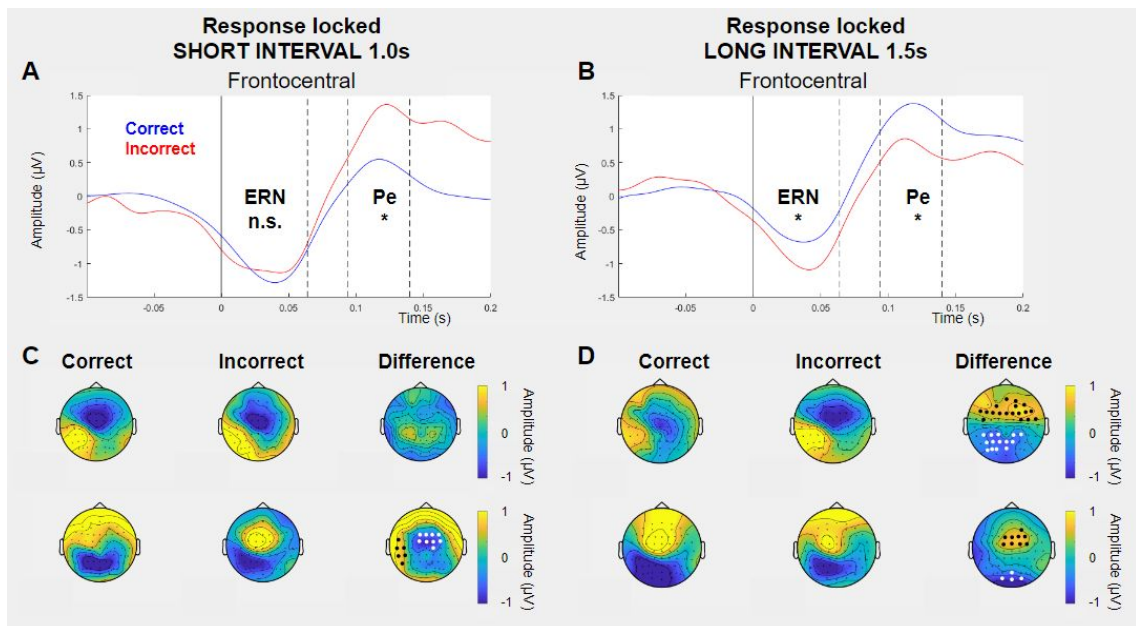
Figure 5.8 Error-related activity for Experiment 1 shows significant differences between correct and incorrect responses. The Pe was more pronounced for incorrect (red line) compared to correct (blue line) responses to the short interval (A) over midfrontal electrodes (C) and vice versa over left-temporal electrodes. There was no significant difference between correct and incorrect responses in the time window of the ERN for the short interval. For the long interval there were significant differences in the time window of the ERN and the Pe (B), where the ERN was more pronounced for incorrect compared to correct responses over frontal electrodes (D). However, the Pe was more pronounced for correct compared to incorrect responses over midfrontal electrodes (D).

The same analyses for Experiment 2 did not identify differences in the time window of the ERN, from 0 to 70 ms post-response, nor for the Pe, from 104 to 154 ms, for the short interval. Although the cluster-based statistics did identify a cluster for the Pe, it did not survive correction for multiple corrections ($p = .06$, Figure 5.9C bottom row). For the long interval there was a significant difference in the ERN time window over right-lateral

fronto-temporal electrodes (*p* = .04, FC6, F6, FC4, C6, FT8, black dots Figure 5.9D). There was also a significant difference in the Pe time window over parietal electrodes (*p* = .04, C4, CP2, Pz, C2, CP4, P2, white dots Figure 5.9D).
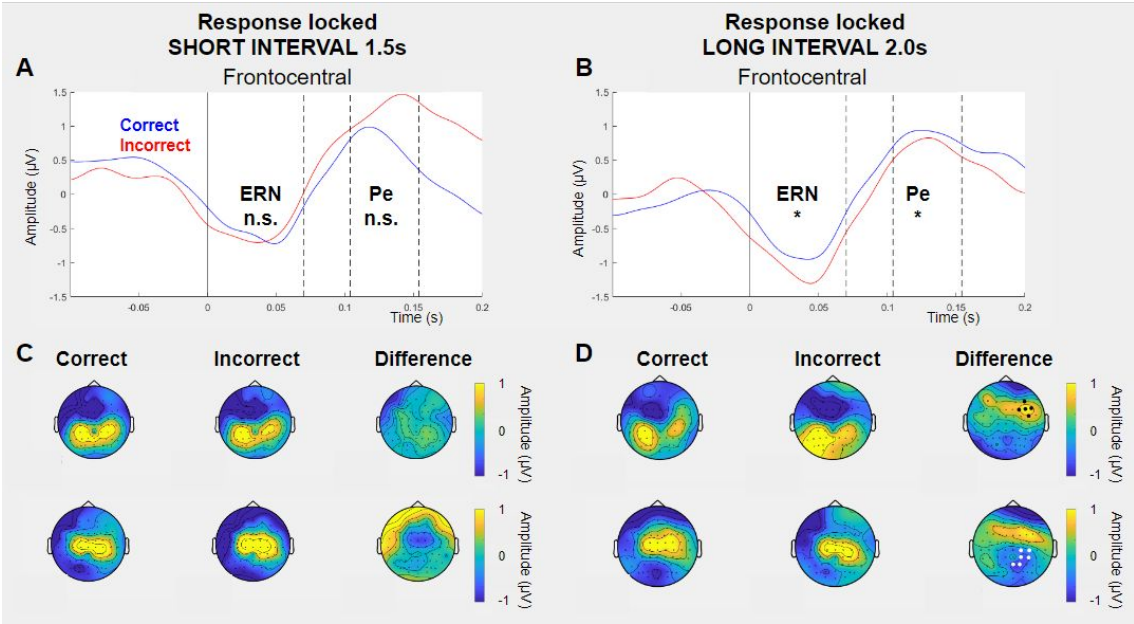
Figure 5.9 Error-related activity for Experiment 2 shows significant differences between correct and incorrect responses. The Pe was more pronounced for incorrect (red line) compared to correct (blue line) responses to the short interval (A, but this effect did not survive corrections for multiple comparisons across electrodes, *p* = .06). There was no significant difference between correct and incorrect responses in the time window of the ERN for the short interval. For the long interval there were significant differences in the time window of the ERN and the Pe (B), where the ERN was more pronounced for incorrect compared to correct responses over right frontal electrodes (D, black dots). The Pe was more pronounced for correct responses than incorrect responses over parietal electrodes (D, white dots).

5.3.2 Correlations of ERPs and behavior

Finally, I asked whether differences in CPP/CNV amplitude was predictive of response times (Figure 5.9). To this end, we performed a simple median split analysis, where we compared fast and slow responses separately for correct and incorrect responses. However, we did not find any significant differences for either correct or incorrect responses when comparing fast and slow responses. A median split can lower our ability to detect true effects (Cohen, 1983; MacCallum et al., 2002). To overcome this issue, we correlated single trial activity averaged over the electrodes and time points from the cluster that was indicated by the permutation test (see Figure 5.5) with response times of each trial through a ranked correlation. We used Fisher's z-transformation to normalize the correlation values. At the second level we compared the correlation values to 0 and we compared the correlation values of correct and incorrect responses to each other. None of these analyses showed significant differences. In addition, we used the same approach of calculating ranked correlations between response time and EEG activity for each time point and channel. We then used a cluster based permutation approach to assess whether the Fisher's z-transformed correlation values were different between correct and incorrect responses and we compared them to 0. Again, we found no significant differences. In a final step, we performed a fixed effect analysis (Figure 5.10), where we correlated response times with EEG activity collapsed over participants. Ranked correlation values did not reach significance for the correct or incorrect trials.
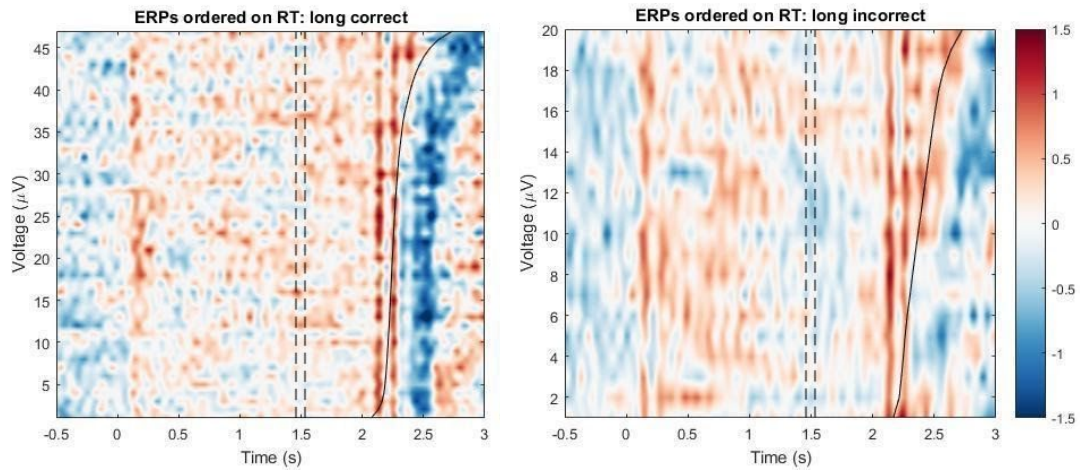
Figure 5.10 Event related potentials collapsed across participants ordered in response time bins. Data of all participants were divided in 75 trial bins (yielding 48 bins for correct and 21 bins for incorrect responses, respectively) based on response times and the event-related potential, averaged over significant electrodes from the cluster based permutation test, was calculated for each bin. Dotted lines indicate significant time window from the previous cluster based analysis. Time 0 s is tone onset and time 2 s is visual stimulus onset. The difference between correct and incorrect responses does not seem to correlate with response times.

5.4 DISCUSSION

This chapter shows that the data of our time estimation experiments is accompanied by a difference in slow-evoked ERP activity. For long (2 s) interval trials in Experiment 2 we found that activity over right-lateralized (Üstün et al., 2017; Pouthas et al., 2005) parieto-occipital cortex was higher for correct than incorrect responses. Strikingly, the two response types differed in amplitude around the offset of the short (1.5 s) interval. We propose that the centro-parietal positive potential tracks the elapsed time similar to the evidence accumulation as discovered by O'Connell et al. (2012). However, we did not find

any differences in slow potentials for the other conditions in either experiment. Moreover, the difference between correct and incorrect responses on the 2 s interval shows a right lateralized topography, but the topography of correct responses looks more fronto-central. This might suggest that for our paradigm we are examining a positive CNV, rather than a CPP.

In addition to analyses of the CNV locked to the tone onset, which demarcated the start of the time interval, I examined the CNV/CPP locked to the response. For the long intervals of both Experiments I found higher amplitudes on incorrect compared to correct responses over centro-parietal electrodes. A similar region showed higher amplitudes for correct compared to incorrect responses for the short intervals, but this effect was only significant for short interval trials of the second experiment. Moreover, all these effects appeared at times of the visual stimulus onset, making these effects more difficult to interpret. It might be that these are not necessarily CNV/CPP effects, but differences in the processing of the visual stimulus. Importantly, this analysis also identified an effect much earlier in the long interval of the first experiment, which was probably not affected by the visual stimulus as this effect appeared earlier than the presentation of the visual stimulus.

Taken together, the data showed a CNV/CPP-like difference in both experiments for the long interval. However, the effect in the first experiment was response locked, whereas the effect in the second experiment was locked to the tone. Moreover, in the first experiment the amplitude of the CNV was more pronounced for incorrect compared to correct responses over midfrontal electrodes and vice versa at occipital electrodes. The tone locked data of the second experiment revealed a more pronounced CNV for correct

compared to incorrect judgements over parietal electrodes. These differences between correct and incorrect responses make a straightforward interpretation of CNV/CPP-like patterns difficult. A possible explanation might be that a CNV and a CPP are affecting the averaged ERPs differently, and where the CNV is going down, the CPP might be going up. However, this is not in line with previous research from interval-timing paradigms where a clear CNV was observable over centrofrontal electrodes (e.g. Gontier et al., 2013; Kononowicz & van Rijn, 2014). It is currently unclear why the ERPs of the current experiment did not show more deviations but stayed close to values around 0 µV (but see the limitations below for a possible explanation).

In addition to slow-evoked ERP activity, I looked at differences in visually evoked N1 and P2 amplitudes. Previous research showed that comparison intervals that are physically more different from the standard interval have larger N1-P2 complexes (Kononowicz & van Rijn, 2014). Here, I examined whether this is also true for intervals that evoke subjectively different experiences, but are physically identical. To this end, I compared correct and incorrect judgements of different time intervals. I did not find any significant differences between correct and incorrect judgements. The N1-P2 amplitude for correct compared to incorrect responses to the long interval of Experiment 1 approached significance. Moreover, the P2 amplitude was larger for incorrect compared to correct responses for the long (1.5 s) interval of Experiment 1. A straightforward interpretation of this effect is complicated, because I did not observe any significant differences for other conditions. In addition, off-set locked ERPs might be contaminated by response time differences between conditions. However, I used a linear regression to regress out any differences in response times and the P2 difference seemed independent of response time difference

between correct and incorrect responses. Alternatively, it might be that this P2 effect is indicative of a true effect, where a larger N1-P2 is evoked for visual stimuli that demarcate the interval offset, when time is under-estimated, but that I did not have enough participants in the second experiment to pick up on this effect.

Finally, we looked at error-related activity in temporal decision making. Interestingly, the error-related negativity (ERN) and the error-related positivity (Pe) showed the most consistent results of all ERP signals discussed so far for Experiment 1 and 2. The long intervals of both experiments showed smaller ERNs but larger Pes for correct compared to incorrect responses. For the short interval there was no difference in the ERN time window, but the Pe was larger for incorrect responses in both experiments, although it only reached significance in Experiment 1. Previous research suggests a dissociation for the ERN and Pe based on conscious awareness of errors. Overbeek et al. (2005) suggested that the ERN arises when an error is committed, but that the Pe is only present for errors that reach awareness. However, more recent findings showed that the distinction between the ERN and Pe is not that straightforwardly related to conscious awareness of the error (Hewig et al., 2011). The experiments in the current chapter did not examine to what extent participants were aware of errors.

One potential explanation for differences between short and long intervals in error-related signals is that processing of errors is quicker in long than in short intervals. And as such, error-related signals only become evident in short interval estimations further away from the response (i.e. later in time, at the P2 time window). If a participant has a short interval in mind as a template of the to-be-timed interval, an overestimation of a short interval

(hence reported as long) can be less readily identified as an underestimation of a long interval (which was reported as short). This might explain why there were no apparent differences for the ERN for short intervals, which were only observed for long intervals.

The differences at the level of the Pe are more complicated to explain. The Pe was larger for incorrect responses to the short interval, but the Pe was actually smaller for incorrect compared to correct responses to long intervals. Especially, this last part is puzzling as previous research has shown that errors typically elicit an ERN followed by a Pe, but long interval trials here showed differences for the ERN, and not the Pe. It would be very interesting to see how these differences in the Pe relate to subjective reports of participants on their perceived correctness. Unfortunately, I did not collect information on this in the current experiments.

5.4.1 Limitations

The most important limitation of the current experiments were the timing issues that were identified in the paradigm after data collection of the first experiment. Participants' behavior suggests that they were still able to perform well on the task. However, interpretation of ERPs that are short-lived, i.e. the N1, P2, ERN and Pe, will be quite severely affected by temporal jitter in the current design.

Another limitation in our data which might be related to the temporal jitter is that we did not observe any clear slow-evoked potentials. An outstanding question is whether these effects were caused by the temporal jitter or whether in a temporal decision-making task such as the current design, the CNV and CPP are accumulating evidence which is reflected in slow-evoked potentials that are not separable at the scalp-level at which EEG

is collected. As such, the negative going potential of temporal expectation and movement preparation normally captured by the CNV is countered by a positive going potential of (temporal) evidence accumulation as captured by the CPP. Future research should try to combine computational modelling and neural modelling of the CNV and the CPP to explore the feasibility of this explanation.

Taken together, our data show that time estimation does not seem to be linked to the slow-evoked potentials in the EEG in a straightforward manner. Although the analyses performed here did identify a difference in slow-evoked potentials for the 2 s interval when comparing correct and incorrect responses. This effect was not present in any of the other conditions. Moreover, this effect was not related to response times of correct and incorrect judgements of the 2 s interval. In addition, a difference was observed for correct and incorrect responses to the 1.5 s interval when the data was locked to the response. Similar electrodes seemed to be involved in bost experiment, but the effect was in opposite directions, i.e. the CPP was larger for correct responses in the 2 s intervals, whereas the effect was flipped in the 1.5 s intervals. The timing issues of the current task design do not allow strong conclusions to be drawn from the data presented here, as it is currently unknown how human behavior is affected by temporal jitter in the range of tens of milliseconds on 1-2 s time intervals.

CHAPTER 6

GENERAL DISCUSSION

The overarching goal of the current thesis was to examine the role of oscillations and slow-evoked potentials as measured with electroencephalography (EEG) in temporal evidence accumulation and the termination of automated behavior. Specifically, theta band oscillations from the medial frontal cortex were hypothesized to play a role in behavioral adjustments after commission errors and in temporal decision making. In Chapter 2 we examined a long-standing hypothesis that suggests that alpha frequency reflects the pacemaker of the internal clock, by comparing correct and incorrect judgements in a temporal decision making task. In Chapter 3 we examined how theta oscillations from medial frontal cortex were related to behavioral adjustments after errors as measured with post-error slowing. In Chapter 4 we examined if oscillatory power in the theta (and alpha/beta) bands reflect the pacemaker of the internal clock by re-analyzing the data of Chapter 2. In Chapter 5 we examined whether slow-evoked potentials reflected temporal evidence accumulation in the same data.

Before placing the findings of the Chapters into the literature at large I will briefly summarize the findings for each of the Chapters.

Chapter 2: Alpha frequency and temporal judgments

It is well-known that animals have a dedicated brain region to keep track of circadian rhythms. However, it remains to be elucidated how humans are capable of keeping track of time on short (~1-2 s) time scales. In 1961 Surwillo described a relationship between alpha

frequency and response times, which led to the suggestion that alpha frequency might reflect the speed of information processing in the brain (Treisman, 1963). Moreover, recent findings have linked alpha frequency to the resolution of the visual system when Samaha & Postle (2015) showed that instantaneous alpha frequency was correlated with the segregation of visual information when alpha frequency was high and integration of visual information when alpha frequency was low. Here, we used a temporal discrimination task where participants judged 1 vs. 1.5 s intervals in Experiment 1 and 1.5 vs 2 s intervals in Experiment 2, which were delimited by a tone and a visual stimulus. If alpha peak frequency reflects the pacemaker of the internal clock higher alpha frequency should correspond to overestimation of physical time, whereas lower alpha frequency should correspond to underestimation of physical time. We found limited support for this prediction in our data when we showed that instantaneous alpha frequency was higher in correct than incorrect judgements of the long (2 s) interval of Experiment 2. However, this effect flipped in the opposite direction after the short time interval had elapsed. Moreover, higher alpha frequency was positively correlated with response times, such that shorter cycles of the alpha oscillation correlated with slower responses. This is opposite the prediction that alpha frequency reflects the speed of information processing.

Chapter 3: Do theta oscillations from medial frontal cortex correlate with behavioral adjustments after errors?

The medial frontal cortex is thought to play an important role in performance monitoring, which makes this region an excellent candidate to influence sensory processing in primary sensory regions after commissions errors. Theta (~4-7 Hz) power oscillations are thought

to be generated in the medial frontal cortex (e.g. Cohen, 2011), but as of yet no clear relationship between this neural signature and behavioral adjustments as measured with post-error slowing (PES) have been described. In Chapter 3 we examined the relationship between midfrontal theta and PES, but found no evidence for a clear relationship. Moreover, contrary to previous results from Mazaheri and colleagues (2009), we did not observe any amplitude-amplitude coupling between midfrontal theta and occipital alpha (~8-12 Hz) power.

Chapter 4: Oscillatory power and temporal judgements

Previous research implicated oscillatory power in different frequency ranges to temporal decision making. The data from Chapter 2 was re-analyzed with a focus on differences in power between correct and incorrect temporal judgments. Previous research identified a role for theta power oscillations in interval timing when theta power was shown to increase upon the presentation of a cue that signified that participants should time an interval (Parker et al., 2014). In addition, alpha power oscillations were lower at expected compared to unexpected moments in time (Rohenkohl & Nobre, 2011). Finally, beta power was higher when participants reproduced longer time intervals (Kononowicz & van Rijn, 2015). In Chapter 2 we examined power in these frequency bands when comparing correct and incorrect temporal judgements. We found higher theta power in correct compared to incorrect responses in long interval trials of Experiment 1 (1 vs. 1.5 s) and 2 (1.5 vs 2 s intervals). In addition, we found suppressed alpha and beta power for long compared to short judgements irrespective of physical interval length in Experiment 1, but this effect did not replicate in Experiment 2.

Chapter 5: The CNV (and other slow evoked potentials) and temporal judgements

In the last empirical chapter we examined whether the contingent negative variation (CNV) or the centro-parietal positivity (CPP) played a role in temporal decision making. Previous research suggested that the CNV might play a role in time estimation (a.o. Macar et al., 1999), where it was thought that climbing neural activity underlying the CNV might reflect temporal evidence accumulation. However, this relationship was scrutinized when earlier findings did not replicate and the CNV showed habituation over the course of the experiment (Kononowicz & van Rijn, 2014). If the CNV would reflect the pacemaker of the internal clock, habituation would be detrimental to timing abilities. Around the same time studies appeared that identified the CPP as the neural correlate of evidence accumulation in perceptual decision making (O'Connell et al., 2012). In Chapter 5 we examined whether temporal decision making might be explained by the CNV or CPP by re-analyzing data from Chapter 2. We found a higher amplitude over parietal electrodes for correct compared to incorrect temporal judgments in the long interval trials of Experiment 2. However, this finding did not replicate for short interval trials or in Experiment 1.

Alpha peak frequency and the internal clock

The current thesis aimed to identify an internal clock by examining EEG collected in two experiments, where participants were engaged in a temporal decision making task. A long-standing hypothesis has been put forward by Treisman (1963; 2013) in the sixties, where it was proposed that the frequency of alpha oscillations might reflect the pacemaker of the internal clock. This hypothesis was partially fuelled by the relationship alpha

frequency had with response times (a.o. Surwillo, 1961), where faster alpha frequencies were related to faster responses. Recent findings have related alpha frequency to the temporal resolution of the visual system (Cecere et al., 2015; Samaha & Postle, 2015; vanRullen, 2016). Moreover, recent advances in the estimation of alpha frequency might allow more sensitivity to subtle effects (Cohen, 2014; Mierau et al., 2017).

In Chapter 2 we did not find conclusive evidence to support the claim that alpha frequency reflects the internal clock or the speed of information processing. Alpha peak frequency (APF) was measured with an automated procedure as proposed by Corcoran and colleagues (2018). It should be noted that this procedure yielded good fits for most participants at frontocentral and posterior-occipital electrodes. Corcoran et al. (2018) showed that compared to previous approaches such as Gaussian fits on the power spectrum (Haegens et al., 2014), the automated peak-fitting procedure found more peaks across participants. Irrespectively, we did not observe any significant differences in APF between correct and incorrect temporal judgements for each of the experiments or of the interval lengths. Nor did we find any effects when we combined the data across both experiments in a mixed effects ANOVA.

In addition to the automated approach to calculate APF we calculated instantaneous alpha frequency (Cohen, 2014). In line with our hypothesis, we found that participants had higher instantaneous alpha frequency over a left lateralized parieto-occipital region in correct compared to incorrect judgments of a 2 s interval (long interval in Experiment 2). However, this effect flipped direction after the short interval had elapsed, such that instantaneous alpha frequency was higher for incorrect compared to correct responses. This finding is difficult to reconcile with the idea that alpha frequency reflects the internal clock. It might

be that instantaneous alpha frequency in this case is reflecting surprise as the participant might have expected the visual stimulus to be presented as the short interval unfolded. Previous work has related alpha oscillations to temporal expectations and it would be interesting to see how alpha relates to the hazard rate (Rohenkohl & Nobre, 2011).

Moreover, instantaneous alpha frequency was positively correlated with response times such that higher instantaneous alpha frequency resulted in slower responses for correct and incorrect responses. If alpha frequency represents the internal clock, higher alpha frequency would lead to more accumulated pulses, which does not fit with the positive relationship between response time and instantaneous alpha frequency in correct responses to the long interval trials (higher alpha frequency — more accumulated evidence — should lead to faster responses). If alpha frequency would represent the speed of information processing, responses should be faster when instantaneous alpha frequency is high. However, Klimesch and colleagues (1996) already showed that a direct relationship between alpha peak frequency and response times could be explained by differences in alpha power. Interestingly, we did not observe power differences in this condition (as we uncovered in Chapter 4).

In order to substantiate any null findings in the relationship between alpha frequency and the temporal decision making task the analyses were repeated on aggregate data, where the data of one experiment were treated as belonging to one participant. Through this analysis higher instantaneous alpha frequency was observed for correct compared to incorrect responses to the long interval of Experiment 1. The difference was significant after the short interval had elapsed. It should be noted that the effects of the analysis on the aggregate data were found in the data of Experiment 1 (1 and 1.5s intervals), whereas

the effects described earlier were found in the data of Experiment 2 (1.5 and 2 s intervals). Moreover, the effect in Experiment 2 after the short time window had elapsed showed a higher instantaneous frequency for incorrect compared to correct judgements, which was in the opposite direction of the effect in the aggregate data of Experiment 1. In the current analyses it is tempting to directly compare data from both experiments, but a different group of participants participated in both experiments. Taken together, the current data makes it difficult to reach any satisfactory conclusion on the relationship between instantaneous alpha frequency and temporal decision making.

The interpretation of the current data is hampered by the temporal jitter in the paradigm. However, it remains to be elucidated to what extent a jitter of 20-40 ms will affect temporal judgements in the seconds range. Another limitation of the current data is that several different cortical sources of alpha might exist, which are lumped together in the EEG recording. A laplacian transform could have helped to attenuate volume conduction (Perrin et al., 1989). Alternatively, magnetoencephalography (MEG) or intracranial EEG would be less sensitive to distortion of several alpha sources by the skull.

To further examine the relationship between alpha frequency and the internal clock, future research might examine a combination of trait and state APF with a temporal bisection paradigm, where several interval lengths are tested. Participants with higher trait alpha peak frequency would be expected to better discriminate different time intervals. State alpha frequency differences should lead to over- and underestimation of different time intervals. Alpha frequency should be measured with source localized M/EEG, but preferably with intracranial recordings over parietal and/or medial frontal regions.

Medial frontal cortex involvement

The second aim of the current thesis was to examine how the medial frontal cortex (MFC) is involved in performance monitoring and temporal decision making. Previous research showed that theta (~4-7 Hz) power is increased after the presentation of a cue that signifies participants need to time a temporal interval (Parker et al., 2014). This power increase was observed in the MFC of humans and rats. Moreover, dopamine depletion in rats and human patients with Parkinson's Disease did not show theta increases (Parker et al., 2014; Parker et al., 2015), which suggests that this signal might reflect dopamine levels. This is important, because dopamine has been linked to interval timing extensively through pharmacological studies that have shown that the internal clock can be sped up or slowed down through the administration of dopamine agonists and antagonists, respectively (Balci, 2014; Matell & Meck, 2004; Meck, 2006).

MFC is also thought to play an important role in performance monitoring (Ridderinkhof et al., 2004) and this region has been identified as the generator of the error related negativity (ERN) (Gehring et al., 1999). Theta power as measured at midfrontal electrodes is likely stemming from MFC and is higher shortly after an erroneous button press compared to a correct one (Cohen, 2011; Mazaheri et al., 2009). In Chapter 3 we asked how medial frontal cortex influences down-stream, sensory regions after an error is committed. In this work behavioral adaptation after an error is measured through post-error slowing (PES). Mazaheri and colleagues (2009) showed that midfrontal theta was correlated with occipital alpha in a sustained attention to response task (SART; Robertson et al., 1997), such that higher theta power after an error was correlated with stronger alpha suppression. This work inspired the hypothesis that medial frontal cortex might be sending

a wake-up call to primary sensory regions and when this functional coupling (theta-alpha power anti-correlation) is more pronounced, participants might show more response caution on the next trial.

Fast responses and errors

The behavioral data of Chapter 3 showed, in line with previous research (a.o. Mazaheri et al., 2009), that participants respond faster on average on false alarms than on hits. Importantly, the defective CDFs showed that fast responses were not necessarily more likely to belong to a false alarm than to a hit. Previous research has reached the same conclusion when analysing behavioral data of the SART (Hawkins et al., 2019). An influential hypothesis with regards to the SART is that participants make errors because they are lulled into an automated response bias (Robertson et al., 1997; Manly et al., 1999; Mazaheri et al., 2009). Mazaheri and colleagues stated that their finding of faster mean response times for false alarms than hits: "replicates previous studies showing that errors are more likely for short RTs" (Mazaheri et al., 2009, under results, behavioral data). The defective CDFs in Hawkins et al. (2019) showed that this might not be the case.

The go/no-go data of Chapter 3 also showed an important difference with the SART data from Hawkins and colleagues (2019), who reported a high amount of trials with response times <200 ms (reflected by the leading edges in their Figure 2). This pattern in the response time distributions was not evident in our data where participants had very few responses faster than 200 ms (there was also no leading edge in the response time distributions across all trials). Interestingly, the leading edge in the data of Hawkins et al. (2019) resulted in poor fits by conventional drift diffusion modelling. Instead the data was

better explained by a rhythmic race model. Previous fits of drift diffusion models on go/no-go data used lexical decision making data (Gomez et al., 2007; Ratcliff et al., 2018), where responses <300 ms were excluded. Systematic exploration of different experimental set-ups is necessary to examine when participants show automated response biases and a direct comparison of the SART to non-numerical go/no-go experiments seem promising. Previous attempts to systematically vary trial lengths and no-go probability showed that automated response tendencies are most pronounced in fast-paced trial structures with a low no-go probability (Wessel, 2018).

Detection of an error leads to subsequent behavioral adjustments in post-error trials, but if response times are not matched between hits and false alarms, post-error neural signals might reflect regression toward the mean (Valadez & Simons, 2018), instead of differences between false alarms and hits. In addition to the defective CDFs, signal detection measures of behavior showed that participants had a clear bias to the go response as indicated by the low β value. Taken together, our behavioral findings highlight the importance of taking into account full response time distributions. Future research should attempt computational modelling to explain post-error behavior. It should be noted that our current design yielded very few misses in general and very few double errors in specific, which should be taken into account by future research when attempting computational modelling approaches (see Dutilh et al., 2012 for an application to a large lexical decision making dataset).

Previous research indicated the relevance in calculating PES by taking into account the speed on the preceding trial (Dutilh et al., 2012). Traditionally, PES is measured as the difference in response times between post-error and post-correct trials. The proposed

measure of PES measures PES as the difference on the pre-error and post-error trials (Dutilh et al., 2012). Our data showed, in line with previous results (van den Brink et al., 2014), that both measures of PES are highly correlated, which suggests that the exemplar participants in Dutilh et al. (2012) might represent extreme cases where both measures of PES were not in accordance. Nonetheless, the robust PES measure might account for attentional fluctuations across the course of the experiment and is therefore the recommended measures when examining behavioral adjustments after errors.

Behavioral outcomes in temporal decision making

In the time estimation experiments the behavioral data showed that participants were faster on correct trials to the long interval of Experiment 1, whereas the data of Experiment 2 indicated that participants were faster when they judged an interval as long irrespective of the physical duration. In addition, participants in Experiment 1 had a clear bias to responding short, as indicated by a positive criterion, which was not replicated in Experiment 2. Finally, we showed that participants had response time distributions that showed more overlap in Experiment 2 than in Experiment 1. This final finding relates to scalar expectancy theory (SET), which predicts that longer (re)produced intervals will have wider distributions than short intervals (Gibbon, 1977). Here, we showed that this scalar property might apply to response times in temporal decision making. It would be interesting to further explore this relationship by collecting data in the same participants on interval timing, temporal and non-temporal decision making tasks.

Midfrontal theta

In Chapter 3 we replicated previous findings by showing that theta power over frontal regions is higher and alpha power is lower over occipital regions for false alarms than hits (Mazaheri et al., 2009; van Driel et al,. 2012). It remains to be elucidated how medial frontal cortex regulates down-stream regions after an error is committed to prevent future errors to occur. Mazaheri and colleagues (2009) suggested that midfrontal theta power might be functionally coupled to occipital alpha power, which could mediate the regulation of cortical excitability in primary sensory regions. However, contrary to Mazaheri and colleagues (2009), we did not observe any amplitude-amplitude coupling between midfrontal theta and occipital alpha. It should be noted that Mazaheri and colleagues (2009) did not match response times of hits and false alarms. As such, it might be possible that Mazaheri et al. (2009) picked up on general slowing processes after fast responses rather than slowing specific to post-error trials. Alternatively, it might be that MEG is more sensitive to amplitude-amplitude coupling than EEG. This latter explanation seems unlikely however, as orthonormalization and Laplacian transform of our data did not aid capturing the hypothesized negative correlation between midfrontal theta and occipital alpha.

In Chapter 4, the power in different frequency bands was examined for differences between correct and incorrect temporal judgements. For theta (3-6 Hz) band power we consistently (in Experiment 1 and 2) found higher theta power for correct judgements of the long interval compared to incorrect judgements. In addition, higher frontal theta power correlated with shorter response times on correct trials in both experiments and with slower responses in incorrect judgements of the long interval in Experiment 1 (but not in Experiment 2). Van Vugt and colleagues (2012) previously found that 4-9 Hz theta

oscillations were related to the drift rate of the drift diffusion model in perceptual decision making. Importantly, they showed that steeper drift rates were correlated with theta power desynchronization. Although it is tempting to relate temporal and non-temporal decision making it should be pointed out that we did not calculate drift diffusion model parameters in our data. One could argue that the faster response times would be more likely to belong to trials with steeper drift rates. In those trials, the response boundary is reached quicker, which leads to the shorter response times. Interestingly, our data shows the opposite pattern for temporal decision-making compared to the perceptual decision-making findings of van Vugt et al. (2012). Future research would benefit from combining computational modelling of temporal decision making and EEG to further explore these discrepancies.

An alternative explanation of the theta power differences between correct and incorrect judgements of the long intervals might be reflected in a combination of motor preparation and attention-like processes. When participants are paying more attention to the task at hand, they are more aware that the short time interval has elapsed and they start preparing for the button press for long interval judgements. This would explain the negative correlation between theta power and response times. As such, theta power might reflect an urgency to respond (Cisek et al., 2009). Moreover, the theta power differences are accompanied by more pronounced alpha/beta suppression for correct compared to incorrect responses, which might also be indicative of motor preparation. However, this effect in higher frequency ranges did not replicate in Experiment 2. In a follow-up study it would be fruitful to vary response options on a trial-by-trial basis to reduce the possibility of motor preparatory biases in the EEG.

Non-phase locked power

To examine the non-phase-locked power differences between false alarms and hits, the time-frequency representation of the event related potential (ERP) was subtracted from the total power (note that this is identical to subtracting the ERP of the single trial activity in the time domain and then calculating the time-frequency decomposition). In line with previous results (Cohen & Donner, 2013), we found that the ERP had little effect on midfrontal theta. Instead, the ERP was mostly captured by delta activity ~2-3 Hz. Interestingly, we found that oscillatory activity in the alpha band was moderately affected by the subtraction of the ERP. Previous research has suggested an important role for asymmetric alpha oscillations and slow evoked potentials (van Dijk et al., 2010; Mazaheri & Jensen, 2008; Nikulin et al., 2010; Schalk, 2015). It might be that the later part of the ERP reflects asymmetric alpha oscillations and that subtraction of the time-frequency representation affects alpha power. However, it might also be that occipital alpha is a weaker signal than post-error midfrontal theta and that the small N of our sample affected alpha power more than theta power. Moreover, it is important to note that the difference between false alarms and hits was significant if the comparison analysis was performed in a prespecified alpha range after subtraction of the ERP.

Phase-based functional connectivity

To further explore the functional connectivity of the medial frontal cortex to primary sensory regions after commission errors, we examined phase-based connectivity measures in the form of debiased weighted phase-locking index (dwPLI). Functional connectivity from medial frontal cortex was higher after false alarms than hits and this connectivity was

confined to the delta (2-3 Hz) range. Medial frontal cortex was functionally coupled to the left and the right hemisphere. When examining functional connectivity from parieto-occipital electrodes that showed large differences in alpha power between false alarms and hits we found that these electrodes seemed functionally coupled to a centro-parietal region at 4 Hz. Unfortunately, dwPLI does not allow any inferences about directionality. Future research would benefit from intracranial recordings in order to assess how medial frontal cortex activity is related to activity in primary sensory regions after errors.

Climbing neural activity

The final aim of the current thesis was to examine whether slow-evoked potentials like the contingent negative variation (CNV) and the centro-parietal positivity (CPP) were related to temporal decision making. Previous research showed that the CNV might be related to interval timing (Macar et al., 1999), but a straightforward interpretation of this relationship was called into question when Kononowicz & van Rijn (2011) were unable to replicate the original findings and instead showed that the CNV showed habituation over the duration of the task. The CPP was described as a reflection of a decision variable accumulating evidence in a perceptual decision-making task (O'Connell et al., 2012), but it is unknown whether the CPP might reflect evidence accumulation during temporal decisions. The data of Chapter 5 showed a difference over centro-parietal electrodes with higher amplitudes for correct compared to incorrect judgements of the long intervals in Experiment 2. However, we did not replicate this finding in any of the other conditions.

Conclusion

The research presented in the current thesis aimed to identify an internal clock that can be read out with EEG. In addition, we tried to solidify the role of theta oscillations from the medial frontal cortex in performance monitoring and temporal decision making. The presented data does not with certainty identify an internal clock. Future research should be collected from intracranial recordings where different sources of alpha activity can be separated. Moreover, a Laplacian transform should be considered when examining slow-evoked potentials. In the empirical chapters on temporal decision making processes, data was collected in two experiments with an almost identical paradigm that allowed validation of any observed effects across both experiments. Higher theta power was consistently found in long interval trials that were correctly judged as long compared to incorrect judgements and this difference became significant after the short time interval had elapsed. Future research should further address this result, by randomly varying the response options on a trial-by-trial basis to exclude motor preparation as a potential confound.

BIBLIOGRAPHY

Ai, L., & Ro, T. (2014). The phase of prestimulus alpha oscillations affects tactile perception. *Journal of Neurophysiology*, *111*(6), 1300–1307.

Alexander, W. H., & Brown, J. W. (2010). Computational models of performance monitoring and cognitive control. *Topics in Cognitive Science*, *2*(4), 658–677.

Allan, L. G. (1998). The influence of the scalar timing model on human timing research. *Behavioural Processes*, *44*(2), 101–117.

Andersen, P., Andersson, S. A., & Lomo, T. (1968). Thalamo-cortical relations during spontaneous barbiturate spindles. *Electroencephalography and Clinical Neurophysiology*, *24*(1), 90.

Anliker, J. (1963). Variations in alpha voltage of the electroencephalogram and time perception. *Science*, *140*(3573), 1307–1309.

Balcı, F. (2014). Interval Timing, Dopamine, and Motivation. *Timing & Time Perception*, *2*(3), 379–410.

Balcı, F., & Simen, P. (2016). A decision model of timing. *Current Opinion in Behavioral Sciences*, *8*, 94–101.

Bartolo, R., & Merchant, H. (2015). β oscillations are linked to the initiation of sensory-cued movement sequences and the internal guidance of regular tapping in the monkey. *The Journal of Neuroscience: The Official Journal of the Society for Neuroscience*, *35*(11), 4635–4640.

Bartolo, R., Prado, L., & Merchant, H. (2014). Information processing in the primate basal ganglia during sensory-guided and internally driven rhythmic tapping. *The Journal of Neuroscience: The Official Journal of the Society for Neuroscience*, *34*(11), 3910–3923.

Behrmann, M., Geng, J. J., & Shomstein, S. (2004). Parietal cortex and attention. *Current Opinion in Neurobiology*, *14*(2), 212–217.

Bell, A. J., & Sejnowski, T. J. (1995). An information-maximization approach to blind separation and blind deconvolution. *Neural Computation*, *7*(6), 1129–1159.

Benwell, C. S. Y., London, R. E., Tagliabue, C. F., Veniero, D., Gross, J., Keitel, C., & Thut, G. (2019). Frequency and power of human alpha oscillations drift systematically with time-on-task. *NeuroImage*, *192*, 101–114.

Bhattacharyya, B. C. (1943). On an Aspect of Pearsonian System of Curves and a Few Analogies. *Journal of the Indian Society of Agricultural Statistics. Indian Society of Agricultural Statistics*, *6*(4), 415–418.

Block, R. A., & Zakay, D. (1997). Prospective and retrospective duration judgments: A meta-analytic review. *Psychonomic Bulletin & Review*, *4*(2), 184–197.

Boddy, J. (1971). The relationship of reaction time to brain wave period: a re-evaluation. *Electroencephalography and Clinical Neurophysiology*, *30*(3), 229–235.

Bode, S., Sewell, D. K., Lilburn, S., Forte, J. D., Smith, P. L., & Stahl, J. (2012). Predicting perceptual decision biases from early brain activity. *The Journal of Neuroscience: The Official Journal of the Society for Neuroscience*, *32*(36), 12488–12498.

Bogacz, R., Brown, E., Moehlis, J., Holmes, P., & Cohen, J. D. (2006). The physics of optimal decision making: a formal analysis of models of performance in two-alternative forced-choice tasks. *Psychological Review*, *113*(4), 700–765.

Bollimunta, A., Mo, J., Schroeder, C. E., & Ding, M. (2011). Neuronal mechanisms and attentional modulation of corticothalamic α oscillations. *The Journal of Neuroscience: The Official Journal of the Society for Neuroscience*, *31*(13), 4935–4943.

Botvinick, M. M., Braver, T. S., Barch, D. M., Carter, C. S., & Cohen, J. D. (2001). Conflict monitoring and cognitive control. *Psychological Review*, *108*(3), 624–652.

Brainard, D. H. (1997). The Psychophysics Toolbox. *Spatial Vision*, *10*(4), 433–436.

Brown, S. D., & Heathcote, A. (2008). The simplest complete model of choice response time: linear ballistic accumulation. *Cognitive Psychology*, *57*(3), 153–178.

Buhusi, C. V., & Meck, W. H. (2005). What makes us tick? Functional and neural mechanisms of interval timing. *Nature Reviews. Neuroscience*, *6*(10), 755–765.

Busch, N. A., Dubois, J., & VanRullen, R. (2009). The phase of ongoing EEG oscillations predicts visual perception. *The Journal of Neuroscience: The Official Journal of the Society for Neuroscience*, *29*(24), 7869–7876.

Busch, N. A., & VanRullen, R. (2010). Spontaneous EEG oscillations reveal periodic sampling of visual attention. *Proceedings of the National Academy of Sciences of the United States of America*, *107*(37), 16048–16053.

Callaway, E., 3rd, & Yeager, C. L. (1960). Relationship between reaction time and electroencephalographic alpha phase. *Science*, *132*(3441), 1765–1766.

Canolty, R. T., Edwards, E., Dalal, S. S., Soltani, M., Nagarajan, S. S., Kirsch, H. E., … Knight, R. T. (2006). High gamma power is phase-locked to theta oscillations in human neocortex. *Science*, *313*(5793), 1626–1628.

Carp, J., & Compton, R. J. (2009). Alpha power is influenced by performance errors. *Psychophysiology*, *46*(2), 336–343.

Carter, C. S., Braver, T. S., Barch, D. M., Botvinick, M. M., Noll, D., & Cohen, J. D. (1998). Anterior cingulate cortex, error detection, and the online monitoring of performance. *Science*, *280*(5364), 747–749.

Cavanagh, J. F., Cohen, M. X., & Allen, J. J. B. (2009). Prelude to and resolution of an error: EEG phase synchrony reveals cognitive control dynamics during action monitoring. *The Journal of Neuroscience: The Official Journal of the Society for Neuroscience*, *29*(1), 98–105.

Cavanagh, J. F., & Frank, M. J. (2014). Frontal theta as a mechanism for cognitive control. *Trends in Cognitive Sciences*, *18*(8), 414–421.

Cavanagh, J. F., & Shackman, A. J. (2015). Frontal midline theta reflects anxiety and cognitive control: meta-analytic evidence. *Journal of Physiology, Paris*, *109*(1-3), 3–15.

Cecere, R., Rees, G., & Romei, V. (2015). Individual differences in alpha frequency drive crossmodal illusory perception. *Current Biology: CB*, *25*(2), 231–235.

Chen, K. H., Kingyon, J. R., & Cavanagh, J. F. (2014). D1-dependent 4 Hz oscillations and ramping activity in rodent medial frontal cortex during interval timing. *Journal of*. Retrieved from http://www.jneurosci.org/content/34/50/16774.short

Church, R. M., & Broadbent, H. A. (1990). Alternative representations of time, number, and rate. *Cognition*, *37*(1-2), 55–81.

Church, R. M., & Broadbent, H. A. (1991). A connectionist model of timing. *Neural Network of Conditioning and Action. In: Commons, M. , Grossberg, S. , Staddon, J. Eds*. Retrieved

from
https://books.google.co.uk/books?hl=en&lr=&id=oeYcDQAAQBAJ&oi=fnd&pg=PT240&dq
=church+broadbent&ots=eVYW4xVWA6&sig=z_UckMTHAUgsBBoYijOpwgIp5-w

Cohen, J. (1983). The Cost of Dichotomization. *Applied Psychological Measurement*, *7*(3), 249–253.

Cohen, M. X. (2011). Error-related medial frontal theta activity predicts cingulate-related structural connectivity. *NeuroImage*, *55*(3), 1373–1383.

Cohen, M. X. (2014). *Analyzing Neural Time Series Data: Theory and Practice*. MIT Press.

Cohen, M. X. (2014). Fluctuations in oscillation frequency control spike timing and coordinate neural networks. *The Journal of Neuroscience: The Official Journal of the Society for Neuroscience*, *34*(27), 8988–8998.

Cohen, M. X., & Donner, T. H. (2013). Midfrontal conflict-related theta-band power reflects neural oscillations that predict behavior. *Journal of Neurophysiology*, *110*(12), 2752–2763.

Coles, M., & Rugg, M. (1995). *Electrophysiology of mind: event-related potentials and cognition*. New York: Oxford University Press.

Collyer, C. E., Broadbent, H. A., & Church, R. M. (1992). Categorical time production: evidence for discrete timing in motor control. *Perception & Psychophysics*, *51*(2), 134–144.

Collyer, C. E., Broadbent, H. A., & Church, R. M. (1994). Preferred rates of repetitive tapping and categorical time production. *Perception & Psychophysics*, *55*(4), 443–453.

Corcoran, A. W., Alday, P. M., Schlesewsky, M., & Bornkessel-Schlesewsky, I. (2018). Toward a reliable, automated method of individual alpha frequency (IAF) quantification. *Psychophysiology*, *55*(7), e13064.

Coull, J. T., Vidal, F., Nazarian, B., & Macar, F. (2004). Functional anatomy of the attentional modulation of time estimation. *Science, 303*(5663), 1506–1508.

Cravo, A. M., Rohenkohl, G., Wyart, V., & Nobre, A. C. (2011). Endogenous modulation of low frequency oscillations by temporal expectations. *Journal of Neurophysiology*, *106*(6), 2964–2972.

Creelman, C. D. (1960). Detection of Signals of Uncertain Frequency. *The Journal of the Acoustical Society of America*, *32*(7), 805–810.

Cross, Z. R., Santamaria, A., Corcoran, A. W., Alday, P. M., Coussens, S., & Kohler, M. J. (2018). Alpha Oscillations Prior to Encoding Preferentially Modulate Memory Consolidation during Wake Relative to Sleep (p. 202176). https://doi.org/10.1101/202176

Crystal, J. D. (1999). Systematic nonlinearities in the perception of temporal intervals. *Journal of Experimental Psychology. Animal Behavior Processes*, *25*(1), 3–17.

Crystal, J. D., Church, R. M., & Broadbent, H. A. (1997). Systematic nonlinearities in the memory representation of time. *Journal of Experimental Psychology. Animal Behavior Processes*, *23*(3), 267–282.

Debener, S., Ullsperger, M., Siegel, M., Fiehler, K., von Cramon, D. Y., & Engel, A. K. (2005). Trial-by-trial coupling of concurrent electroencephalogram and functional magnetic resonance imaging identifies the dynamics of performance monitoring. *The Journal of Neuroscience: The Official Journal of the Society for Neuroscience*, *25*(50), 11730–11737.

Dehaene, S., Posner, M. I., & Tucker, D. M. (1994). Localization of a Neural System for Error Detection and Compensation. *Psychological Science*, *5*(5), 303–305.

Delorme, A., & Makeig, S. (2004). EEGLAB: an open source toolbox for analysis of single-trial EEG dynamics including independent component analysis. *Journal of Neuroscience Methods*, *134*(1), 9–21.

Delorme, A., Westerfield, M., & Makeig, S. (2007). Medial prefrontal theta bursts precede rapid motor responses during visual selective attention. *The Journal of Neuroscience: The Official Journal of the Society for Neuroscience*, *27*(44), 11949–11959.

Devinsky, O., Morrell, M. J., & Vogt, B. A. (1995). Contributions of anterior cingulate cortex to behaviour. *Brain: A Journal of Neurology*, *118 (Pt 1)*, 279–306.

Donkers, F. C. L., & van Boxtel, G. J. M. (2004). The N2 in go/no-go tasks reflects conflict monitoring not response inhibition. *Brain and Cognition*, *56*(2), 165–176.

Donner, T. H., Siegel, M., Fries, P., & Engel, A. K. (2009). Buildup of choice-predictive activity in human motor cortex during perceptual decision making. *Current Biology: CB*, *19*(18), 1581–1585.

Dubois, J., Hamker, F. H., & VanRullen, R. (2009). Attentional selection of noncontiguous locations: the spotlight is only transiently "split." *Journal of Vision*, *9*(5), 3.1–11.

Dustman, R. E., & Beck, E. C. (1965). PHASE OF ALPHA BRAIN WAVES, REACTION TIME AND VISUALLY EVOKED POTENTIALS. *Electroencephalography and Clinical Neurophysiology*, *18*, 433–440.

Dutilh, G., Forstmann, B. U., Vandekerckhove, J., & Wagenmakers, E.-J. (2013). A diffusion model account of age differences in posterror slowing. *Psychology and Aging*, *28*(1), 64–76.

Dutilh, G., van Ravenzwaaij, D., Nieuwenhuis, S., van der Maas, H. L. J., Forstmann, B. U., & Wagenmakers, E.-J. (2012). How to measure post-error slowing: A confound and a simple solution. *Journal of Mathematical Psychology*, *56*(3), 208–216.

Fell, J., & Axmacher, N. (2011). The role of phase synchronization in memory processes. *Nature Reviews. Neuroscience*, *12*(2), 105–118.

Fiebelkorn, I. C., Saalmann, Y. B., & Kastner, S. (2013). Rhythmic sampling within and between objects despite sustained attention at a cued location. *Current Biology: CB*, *23*(24), 2553–2558.

Forstmann, B. U., Ratcliff, R., & Wagenmakers, E.-J. (2016). Sequential Sampling Models in Cognitive Neuroscience: Advantages, Applications, and Extensions. *Annual Review of Psychology*, *67*, 641–666.

Fu, Z., Wu, D.-A. J., Ross, I., Chung, J. M., Mamelak, A. N., Adolphs, R., & Rutishauser, U. (2019). Single-Neuron Correlates of Error Monitoring and Post-Error Adjustments in Human Medial Frontal Cortex. *Neuron*, *101*(1), 165–177.e5.

Gehring, W. J., Goss, B., Coles, M. G. H., Meyer, D. E., & Donchin, E. (1993). A Neural System for Error Detection and Compensation. *Psychological Science*, *4*(6), 385–390.

Getty, D. J. (1975). Discrimination of short temporal intervals: A comparison of two models. *Perception & Psychophysics*, *18*(1), 1–8.

Gevins, A., Smith, M. E., McEvoy, L., & Yu, D. (1997). High-resolution EEG mapping of cortical activation related to working memory: effects of task difficulty, type of processing, and practice. *Cerebral Cortex* , *7*(4), 374–385.

Gibbon, J. (1977). Scalar expectancy theory and Weber's law in animal timing. *Psychological Review*, *84*(3), 279–325.

Gibbon, J., Church, R. M., & Meck, W. H. (1984). Scalar timing in memory. *Annals of the New York Academy of Sciences*, *423*, 52–77.

Glicksohn, J., Ohana, A. B., Dotan, T. B., Goldstein, A., & Donchin, O. (2009). Time Production and EEG Alpha Revisited. *NeuroQuantology: An Interdisciplinary Journal of Neuroscience and Quantum Physics*, *7*(1). https://doi.org/10.14704/nq.2009.7.1.215

Gold, J. I., & Shadlen, M. N. (2001). Neural computations that underlie decisions about sensory stimuli. *Trends in Cognitive Sciences*, *5*(1), 10–16.

Gold, J. I., & Shadlen, M. N. (2007). The neural basis of decision making. *Annual Review of Neuroscience*, *30*, 535–574.

Gomez, P., Ratcliff, R., & Perea, M. (2007). A model of the go/no-go task. *Journal of Experimental Psychology. General*, *136*(3), 389–413.

Gontier, E., Hasuo, E., Mitsudo, T., & Grondin, S. (2013). EEG investigations of duration discrimination: the intermodal effect is induced by an attentional bias. *PloS One*, *8*(8), e74073.

Green, D. M., Swets, J. A., & Others. (1966). *Signal detection theory and psychophysics* (Vol. 1). Wiley New York.

Grondin, S. (2001). From physical time to the first and second moments of psychological time. *Psychological Bulletin*, *127*(1), 22–44.

Grondin, S. (2014). About the (Non)scalar Property for Time Perception. In H. Merchant & V. de Lafuente (Eds.), *Neurobiology of Interval Timing* (pp. 17–32). New York, NY: Springer New York.

Gu, B.-M., van Rijn, H., & Meck, W. H. (2015). Oscillatory multiplexing of neural population codes for interval timing and working memory. *Neuroscience and Biobehavioral Reviews*, *48*, 160–185.

Haegens, S., Cousijn, H., Wallis, G., Harrison, P. J., & Nobre, A. C. (2014). Inter- and intra-individual variability in alpha peak frequency. *NeuroImage*, *92*, 46–55.

Haegens, S., Nácher, V., Luna, R., Romo, R., & Jensen, O. (2011). α-Oscillations in the monkey sensorimotor network influence discrimination performance by rhythmical inhibition of neuronal spiking. *Proceedings of the National Academy of Sciences of the United States of America*, *108*(48), 19377–19382.

Hajcak, G., McDonald, N., & Simons, R. F. (2003). To err is autonomic: Error-related brain potentials, ANS activity, and post-error compensatory behavior. *Psychophysiology*, *40*(6), 895–903.

Hajcak, G., & Simons, R. F. (2008). Oops!.. I did it again: An ERP and behavioral study of double-errors. *Brain and Cognition*, *68*(1), 15–21.

Hanks, T. D., & Summerfield, C. (2017). Perceptual Decision Making in Rodents, Monkeys, and Humans. *Neuron*, *93*(1), 15–31.

Hanslmayr, S., Pastötter, B., Bäuml, K.-H., Gruber, S., Wimber, M., & Klimesch, W. (2008). The electrophysiological dynamics of interference during the Stroop task. *Journal of Cognitive Neuroscience*, *20*(2), 215–225.

Hass, J., & Durstewitz, D. (2014). Neurocomputational models of time perception. *Advances in Experimental Medicine and Biology*, *829*, 49–71.

Hawkins, G. E., Mittner, M., Forstmann, B. U., & Heathcote, A. (2019). Modeling distracted performance. *Cognitive Psychology*, *112*, 48–80.

Heekeren, H. R., Marrett, S., Bandettini, P. A., & Ungerleider, L. G. (2004). A general mechanism for perceptual decision-making in the human brain. *Nature*, *431*(7010), 859–862.

Heekeren, H. R., Marrett, S., Ruff, D. A., Bandettini, P. A., & Ungerleider, L. G. (2006). Involvement of human left dorsolateral prefrontal cortex in perceptual decision making is independent of response modality. *Proceedings of the National Academy of Sciences of the United States of America*, *103*(26), 10023–10028.

Heekeren, H. R., Marrett, S., & Ungerleider, L. G. (2008). The neural systems that mediate human perceptual decision making. *Nature Reviews. Neuroscience*, *9*(6), 467–479.

Herbst, S. K., & Landau, A. N. (2016). Rhythms for cognition: the case of temporal processing. *Current Opinion in Behavioral Sciences*, *8*, 85–93.

Herrmann, M. J., Römmler, J., Ehlis, A.-C., Heidrich, A., & Fallgatter, A. J. (2004). Source localization (LORETA) of the error-related-negativity (ERN/Ne) and positivity (Pe). *Brain Research. Cognitive Brain Research*, *20*(2), 294–299.

Heskje, J., Heslin, K., De Corte, B. J., Walsh, K. P., Kim, Y., Han, S., … Parker, K. L. (2019). Cerebellar D1DR-expressing neurons modulate the frontal cortex during timing tasks. *Neurobiology of Learning and Memory*, 107067.

Hipp, J. F., Hawellek, D. J., Corbetta, M., Siegel, M., & Engel, A. K. (2012). Large-scale cortical correlation structure of spontaneous oscillatory activity. *Nature Neuroscience*, *15*(6), 884–890.

Hoagland, H. (1933). The Physiological Control of Judgments of Duration: Evidence for a Chemical Clock. *The Journal of General Psychology*, *9*(2), 267–287.

Hoagland, H. (1936a). ELECTRICAL BRAIN WAVES AND TEMPERATURE. *Science*, *84*(2171), 139–140.

Hoagland, H. (1936). PACEMAKERS OF HUMAN BRAIN WAVES IN NORMALS AND IN GENERAL PARETICS. *American Journal of Physiology-Legacy Content*, *116*(3), 604–615.

Hoagland, H. (1936b). Temperature characteristics of the" Berger rhythm" in man. *Science*. Retrieved from https://psycnet.apa.org/record/1936-01878-001

Holroyd, C. B., & Coles, M. G. H. (2002). The neural basis of human error processing: reinforcement learning, dopamine, and the error-related negativity. *Psychological Review*, *109*(4), 679–709.

Hughes, S. W., & Crunelli, V. (2005). Thalamic mechanisms of EEG alpha rhythms and their pathological implications. *The Neuroscientist: A Review Journal Bringing Neurobiology, Neurology and Psychiatry*, *11*(4), 357–372.

Ivry, R. B., & Richardson, T. C. (2002). Temporal control and coordination: the multiple timer model. *Brain and Cognition*, *48*(1), 117–132.

James, W. (1890). The Principles of. *Psychology* , *2*. Retrieved from http://coursecontent.learn21.org/ENG3x-HS-U10/a/unit04/resources/docs/E3HS_4.C_Org Table_Psychology.pdf

Jenkinson, N., & Brown, P. (2011). New insights into the relationship between dopamine, beta oscillations and motor function. *Trends in Neurosciences*, *34*(12), 611–618.

Jensen, O., & Colgin, L. L. (2007). Cross-frequency coupling between neuronal oscillations. *Trends in Cognitive Sciences*, *11*(7), 267–269.

Jensen, O., & Tesche, C. D. (2002). Frontal theta activity in humans increases with memory load in a working memory task. *The European Journal of Neuroscience*, *15*(8), 1395–1399.

Jin, Y., O'Halloran, J. P., Plon, L., Sandman, C. A., & Potkin, S. G. (2006). Alpha EEG predicts visual reaction time. *The International Journal of Neuroscience*, *116*(9), 1035–1044.

Jones, E. G. (2001). The thalamic matrix and thalamocortical synchrony. *Trends in Neurosciences*, *24*(10), 595–601.

Kaiser, S., Unger, J., Kiefer, M., Markela, J., Mundt, C., & Weisbrod, M. (2003). Executive control deficit in depression: event-related potentials in a Go/Nogo task. *Psychiatry Research*, *122*(3), 169–184.

Keitel, C., Benwell, C. S. Y., Thut, G., & Gross, J. (2018). No changes in parieto-occipital alpha during neural phase locking to visual quasi-periodic theta-, alpha-, and beta-band stimulation. *The European Journal of Neuroscience*, *48*(7), 2551–2565.

Kelly, S. P., & O'Connell, R. G. (2013). Internal and external influences on the rate of sensory evidence accumulation in the human brain. *The Journal of Neuroscience: The Official Journal of the Society for Neuroscience*, *33*(50), 19434–19441.

Kim, J., Ghim, J.-W., Lee, J. H., & Jung, M. W. (2013). Neural correlates of interval timing in rodent prefrontal cortex. *The Journal of Neuroscience: The Official Journal of the Society for Neuroscience*, *33*(34), 13834–13847.

Kim, J., Jung, A. H., Byun, J., Jo, S., & Jung, M. W. (2009). Inactivation of medial prefrontal cortex impairs time interval discrimination in rats. *Frontiers in Behavioral Neuroscience*, *3*, 38.

Kleiner, M., Brainard, D., Pelli, D., Ingling, A., Murray, R., Broussard, C., & Others. (2007). What's new in Psychtoolbox-3. *Perception*, *36*(14), 1.

Klimesch, W. (2012). α-band oscillations, attention, and controlled access to stored information. *Trends in Cognitive Sciences*, *16*(12), 606–617.

Klimesch, W., Doppelmayr, M., Schimke, H., & Pachinger, T. (1996). Alpha frequency, reaction time, and the speed of processing information. *Journal of Clinical Neurophysiology: Official Publication of the American Electroencephalographic Society*, *13*(6), 511–518.

Kononowicz, T. W. (2015). Dopamine-dependent oscillations in frontal cortex index "start-gun" signal in interval timing. *Frontiers in Human Neuroscience*, *9*, 331.

Kononowicz, T. W., & Penney, T. B. (2016). The contingent negative variation (CNV): timing isn't everything. *Current Opinion in Behavioral Sciences*, *8*, 231–237.

Kononowicz, T. W., & van Rijn, H. (2011). Slow potentials in time estimation: the role of temporal accumulation and habituation. *Frontiers in Integrative Neuroscience*, *5*, 48.

Kononowicz, T. W., & van Rijn, H. (2014a). Decoupling interval timing and climbing neural activity: a dissociation between CNV and N1P2 amplitudes. *The Journal of Neuroscience: The Official Journal of the Society for Neuroscience*, *34*(8), 2931–2939.

Kononowicz, T. W., & van Rijn, H. (2014b). Decoupling interval timing and climbing neural activity: a dissociation between CNV and N1P2 amplitudes. *The Journal of Neuroscience: The Official Journal of the Society for Neuroscience*, *34*(8), 2931–2939.

Kononowicz, T. W., & van Rijn, H. (2015). Single trial beta oscillations index time estimation. *Neuropsychologia*, *75*, 381–389.

Kononowicz, T. W., & van Wassenhove, V. (2016). In Search of Oscillatory Traces of the Internal Clock. *Frontiers in Psychology*, *7*, 224.

Kulashekhar, S., Pekkola, J., Palva, J. M., & Palva, S. (2016). The role of cortical beta oscillations in time estimation. *Human Brain Mapping*, *37*(9), 3262–3281.

Laming, D. (1979). Choice reaction performance following an error. *Acta Psychologica*, *43*(3), 199–224.

Landau, A. N., & Fries, P. (2012). Attention samples stimuli rhythmically. *Current Biology: CB*, *22*(11), 1000–1004.

Lewis, P. A., & Miall, R. C. (2003). Brain activation patterns during measurement of sub- and supra-second intervals. *Neuropsychologia*, *41*(12), 1583–1592.

Lindbergh, C. A., & Kieffaber, P. D. (2013). The neural correlates of temporal judgments in the duration bisection task. *Neuropsychologia*, *51*(2), 191–196.

Luu, P., Flaisch, T., & Tucker, D. M. (2000). Medial frontal cortex in action monitoring. *The Journal of Neuroscience: The Official Journal of the Society for Neuroscience*, *20*(1), 464–469.

Luu, P., Tucker, D. M., & Makeig, S. (2004). Frontal midline theta and the error-related negativity: neurophysiological mechanisms of action regulation. *Clinical Neurophysiology: Official Journal of the International Federation of Clinical Neurophysiology*, *115*(8), 1821–1835.

Macar, F., & Vidal, F. (2004). Event-Related Potentials as Indices of Time Processing: A Review. *Journal of Psychophysiology*, *18*(2/3), 89–104.

Macar, F., & Vidal, F. (2009). Timing processes: an outline of behavioural and neural indices not systematically considered in timing models. *Canadian Journal of Experimental Psychology = Revue Canadienne de Psychologie Experimentale*, *63*(3), 227–239.

Macar, F., Vidal, F., & Casini, L. (1999). The supplementary motor area in motor and sensory timing: evidence from slow brain potential changes. *Experimental Brain Research. Experimentelle Hirnforschung. Experimentation Cerebrale*, *125*(3), 271–280.

Macar, F., & Vitton, N. (1982). An early resolution of contingent negative variation (CNV) in time discrimination. *Electroencephalography and Clinical Neurophysiology*, *54*(4), 426–435.

MacCallum, R. C., Zhang, S., Preacher, K. J., & Rucker, D. D. (2002). On the practice of dichotomization of quantitative variables. *Psychological Methods*, *7*(1), 19–40.

Macmillan, N. A., & Creelman, C. D. (2004). *Detection theory: A user's guide*. Psychology press.

Maier, M. E., Ernst, B., & Steinhauser, M. (2019). Error-related pupil dilation is sensitive to the evaluation of different error types. *Biological Psychology*, *141*, 25–34.

Makhin, S. A., & Pavlenko, V. B. (2003). EEG Activity in the Process of Measuring-off of Time Intervals by Humans. *Neurophysiology*, *35*(2), 143–148.

Maris, E., & Oostenveld, R. (2007). Nonparametric statistical testing of EEG- and MEG-data. *Journal of Neuroscience Methods*, *164*(1), 177–190.

Matell, M. S., & Meck, W. H. (2004). Cortico-striatal circuits and interval timing: coincidence detection of oscillatory processes. *Brain Research. Cognitive Brain Research*, *21*(2), 139–170.

Matell, M. S., Meck, W. H., & Nicolelis, M. A. L. (2003). Interval timing and the encoding of signal duration by ensembles of cortical and striatal neurons. *Behavioral Neuroscience*, *117*(4), 760–773.

Mathewson, K. E., Gratton, G., Fabiani, M., Beck, D. M., & Ro, T. (2009). To see or not to see: prestimulus alpha phase predicts visual awareness. *The Journal of Neuroscience: The Official Journal of the Society for Neuroscience*, *29*(9), 2725–2732.

Matthews, W. J., & Meck, W. H. (2016). Temporal cognition: Connecting subjective time to perception, attention, and memory. *Psychological Bulletin*, *142*(8), 865–907.

Mazaheri, A., & Jensen, O. (2008). Asymmetric amplitude modulations of brain oscillations generate slow evoked responses. *The Journal of Neuroscience: The Official Journal of the Society for Neuroscience*, *28*(31), 7781–7787.

Mazaheri, A., & Jensen, O. (2010). Rhythmic pulsing: linking ongoing brain activity with evoked responses. *Frontiers in Human Neuroscience*, *4*, 177.

Meck, W. H. (2006). Frontal cortex lesions eliminate the clock speed effect of dopaminergic drugs on interval timing. *Brain Research*, *1108*(1), 157–167.

Mento, G. (2013). The passive CNV: carving out the contribution of task-related processes to expectancy. *Frontiers in Human Neuroscience*, *7*, 827.

Merchant, H., & de Lafuente, V. (Eds.). (2014). *Neurobiology of Interval Timing*. Springer, New York, NY.

Miall, C. (1989). The Storage of Time Intervals Using Oscillating Neurons. *Neural Computation*, *1*(3), 359–371.

Miall, C. (1996). Models of neural timing. In M. A. Pastor & J. Artieda (Eds.), *Advances in Psychology* (Vol. 115, pp. 69–94). North-Holland.

Mierau, A., Klimesch, W., & Lefebvre, J. (2017). State-dependent alpha peak frequency shifts: Experimental evidence, potential mechanisms and functional implications. *Neuroscience*, *360*, 146–154.

Milton, A., & Pleydell-Pearce, C. W. (2016). The phase of pre-stimulus alpha oscillations influences the visual perception of stimulus timing. *NeuroImage*, *133*, 53–61.

Mita, A., Mushiake, H., Shima, K., Matsuzaka, Y., & Tanji, J. (2009). Interval time coding by neurons in the presupplementary and supplementary motor areas. *Nature Neuroscience*, *12*(4), 502–507.

Moran, R. J., Campo, P., Maestu, F., Reilly, R. B., Dolan, R. J., & Strange, B. A. (2010). Peak frequency in the theta and alpha bands correlates with human working memory capacity. *Frontiers in Human Neuroscience*, *4*, 200.

Morita, V. C., Sato, J. R., Caetano, M. S., & Cravo, A. M. (2019). Dissociating decisional and temporal information in interval categorisation (p. 659375). https://doi.org/10.1101/659375

Mueller, E. M., Makeig, S., Stemmler, G., Hennig, J., & Wacker, J. (2011). Dopamine effects on human error processing depend on catechol-O-methyltransferase VAL158MET genotype. *The Journal of Neuroscience: The Official Journal of the Society for Neuroscience*, *31*(44), 15818–15825.

Muller, T., & Nobre, A. C. (2014). Perceiving the passage of time: neural possibilities. *Annals of the New York Academy of Sciences*, *1326*, 60–71.

Nakazono, T., Sano, T., Takahashi, S., & Sakurai, Y. (2015). Theta oscillation and neuronal activity in rat hippocampus are involved in temporal discrimination of time in seconds. *Frontiers in Systems Neuroscience*, *9*, 95.

Narayanan, N. S., Cavanagh, J. F., Frank, M. J., & Laubach, M. (2013). Common medial frontal mechanisms of adaptive control in humans and rodents. *Nature Neuroscience*, *16*(12), 1888–1895.

Narayanan, N. S., Land, B. B., Solder, J. E., Deisseroth, K., & DiLeone, R. J. (2012). Prefrontal D1 dopamine signaling is required for temporal control. *Proceedings of the National Academy of Sciences of the United States of America*, *109*(50), 20726–20731.

Navarro-Cebrian, A., Knight, R. T., & Kayser, A. S. (2013). Error-monitoring and post-error compensations: dissociation between perceptual failures and motor errors with and without awareness. *The Journal of Neuroscience: The Official Journal of the Society for Neuroscience*, *33*(30), 12375–12383.

Nelli, S., Itthipuripat, S., Srinivasan, R., & Serences, J. T. (2017). Fluctuations in instantaneous frequency predict alpha amplitude during visual perception. *Nature Communications*, *8*(1), 2071.

Notebaert, W., Houtman, F., Van Opstal, F., Gevers, W., Fias, W., & Verguts, T. (2009). Post-error slowing: an orienting account. *Cognition*, *111*(2), 275–279.

O'Connell, R. G., Dockree, P. M., & Kelly, S. P. (2012). A supramodal accumulation-to-bound signal that determines perceptual decisions in humans. *Nature Neuroscience*, *15*(12), 1729–1735.

Oehrn, C. R., Hanslmayr, S., Fell, J., Deuker, L., Kremers, N. A., Do Lam, A. T., … Axmacher, N. (2014). Neural communication patterns underlying conflict detection, resolution, and adaptation. *The Journal of Neuroscience: The Official Journal of the Society for Neuroscience*, *34*(31), 10438–10452.

Oostenveld, R., Fries, P., Maris, E., & Schoffelen, J.-M. (2011). FieldTrip: Open source software for advanced analysis of MEG, EEG, and invasive electrophysiological data. *Computational Intelligence and Neuroscience*, *2011*, 156869.

Oprisan, S. A., & Buhusi, C. V. (2011). Modeling pharmacological clock and memory patterns of interval timing in a striatal beat-frequency model with realistic, noisy neurons. *Frontiers in Integrative Neuroscience*, *5*, 52.

Osipova, D., Hermes, D., & Jensen, O. (2008). Gamma power is phase-locked to posterior alpha activity. *PloS One*, *3*(12), e3990.

Overbeek, T. J. M., Nieuwenhuis, S., & Ridderinkhof, K. R. (2005). Dissociable components of error processing: On the functional significance of the Pe vis-à-vis the ERN/Ne. *Journal of Psychophysiology*, *19*(4), 319–329.

Palva, S., & Palva, J. M. (2007). New vistas for alpha-frequency band oscillations. *Trends in Neurosciences*, *30*(4), 150–158.

Parker, K. L., Chen, K.-H., Kingyon, J. R., Cavanagh, J. F., & Narayanan, N. S. (2015). Medial frontal ~4-Hz activity in humans and rodents is attenuated in PD patients and in rodents with cortical dopamine depletion. *Journal of Neurophysiology*, *114*(2), 1310–1320.

Parker, K. L., Ruggiero, R. N., & Narayanan, N. S. (2015). Infusion of D1 Dopamine Receptor Agonist into Medial Frontal Cortex Disrupts Neural Correlates of Interval Timing. *Frontiers in Behavioral Neuroscience*, *9*, 294.

Paton, J. J., & Buonomano, D. V. (2018). The Neural Basis of Timing: Distributed Mechanisms for Diverse Functions. *Neuron*, *98*(4), 687–705.

Paul, I., Le Dantec, C., Bernard, C., Lalonde, R., & Rebaï, M. (2003). Event-related potentials in the frontal lobe during performance of a visual duration discrimination task. *Journal of Clinical Neurophysiology: Official Publication of the American Electroencephalographic Society*, *20*(5), 351–360.

Paulsen, J. S., Zimbelman, J. L., Hinton, S. C., Langbehn, D. R., Leveroni, C. L., Benjamin, M. L., … Rao, S. M. (2004). fMRI biomarker of early neuronal dysfunction in presymptomatic Huntington's Disease. *AJNR. American Journal of Neuroradiology*, *25*(10), 1715–1721.

Perrin, F., Pernier, J., Bertrand, O., & Echallier, J. F. (1989). Spherical splines for scalp potential and current density mapping. *Electroencephalography and Clinical Neurophysiology*, *72*(2), 184–187.

Petter, E. A., Lusk, N. A., Hesslow, G., & Meck, W. H. (2016). Interactive roles of the cerebellum and striatum in sub-second and supra-second timing: Support for an initiation, continuation, adjustment, and termination (ICAT) model of temporal processing. *Neuroscience and Biobehavioral Reviews*, *71*, 739–755.

Pfeuty, M., Ragot, R., & Pouthas, V. (2003). When time is up: CNV time course differentiates the roles of the hemispheres in the discrimination of short tone durations. *Experimental Brain Research. Experimentelle Hirnforschung. Experimentation Cerebrale*, *151*(3), 372–379.

Pfeuty, M., Ragot, R., & Pouthas, V. (2005). Relationship between CNV and timing of an upcoming event. *Neuroscience Letters*, *382*(1-2), 106–111.

Pfurtscheller, G., & Lopes da Silva, F. H. (1999). Event-related EEG/MEG synchronization and desynchronization: basic principles. *Clinical Neurophysiology: Official Journal of the International Federation of Clinical Neurophysiology*, *110*(11), 1842–1857.

Philiastides, M. G., Ratcliff, R., & Sajda, P. (2006). Neural representation of task difficulty and decision making during perceptual categorization: a timing diagram. *The Journal of Neuroscience: The Official Journal of the Society for Neuroscience*, *26*(35), 8965–8975.

Polanía, R., Krajbich, I., Grueschow, M., & Ruff, C. C. (2014). Neural oscillations and synchronization differentially support evidence accumulation in perceptual and value-based decision making. *Neuron*, *82*(3), 709–720.

Pouthas, V., George, N., Poline, J.-B., Pfeuty, M., Vandemoorteele, P.-F., Hugueville, L., … Renault, B. (2005). Neural network involved in time perception: an fMRI study comparing long and short interval estimation. *Human Brain Mapping*, *25*(4), 433–441.

Rabbitt, P. M. (1966). Error correction time without external error signals. *Nature*, *212*(5060), 438.

Rabbitt, P., & Rodgers, B. (1977). What does a Man do after he Makes an Error? An Analysis of Response Programming. *The Quarterly Journal of Experimental Psychology*, *29*(4), 727–743.

Rammsayer, T. (1990). Temporal discrimination in schizophrenic and affective disorders: evidence for a dopamine-dependent internal clock. *The International Journal of Neuroscience*, *53*(2-4), 111–120.

Ratcliff, R. (1978). A theory of memory retrieval. *Psychological Review*, *85*(2), 59.

Ratcliff, R. (2001). [Review of *Putting noise into neurophysiological models of simple decision making*]. *Nature neuroscience*, *4*(4), 336–337. nature.com.

Ratcliff, R., Huang-Pollock, C., & McKoon, G. (2018). Modeling individual differences in the go/no-go task with a diffusion model. *Decisions*. Retrieved from https://psycnet.apa.org/journals/dec/5/1/42/

Ratcliff, R., & McKoon, G. (2008). The diffusion decision model: theory and data for two-choice decision tasks. *Neural Computation*, *20*(4), 873–922.

Ratcliff, R., Philiastides, M. G., & Sajda, P. (2009). Quality of evidence for perceptual decision making is indexed by trial-to-trial variability of the EEG. *Proceedings of the National Academy of Sciences of the United States of America*, *106*(16), 6539–6544.

Ratcliff, R., & Rouder, J. N. (1998). Modeling Response Times for Two-Choice Decisions. *Psychological Science*, *9*(5), 347–356.

Ratcliff, R., & Smith, P. L. (2004). A comparison of sequential sampling models for two-choice reaction time. *Psychological Review*, *111*(2), 333–367.

Ratcliff, R., Smith, P. L., Brown, S. D., & McKoon, G. (2016). Diffusion Decision Model: Current Issues and History. *Trends in Cognitive Sciences*, *20*(4), 260–281.

Ratcliff, R., & Tuerlinckx, F. (2002). Estimating parameters of the diffusion model: approaches to dealing with contaminant reaction times and parameter variability. *Psychonomic Bulletin & Review*, *9*(3), 438–481.

Re, D., Inbar, M., Richter, C. G., & Landau, A. N. (2019). Feature-Based Attention Samples Stimuli Rhythmically. *Current Biology: CB*, *29*(4), 693–699.e4.

Reppert, S., & Moore, R. (1991). *Suprachiasmatic Nucleus: The Mind's Clock*. Oxford University Press.

Ridderinkhof, K. R., Ullsperger, M., Crone, E. A., & Nieuwenhuis, S. (2004a). The role of the medial frontal cortex in cognitive control. *Science*, *306*(5695), 443–447.

Ridderinkhof, K. R., Ullsperger, M., Crone, E. A., & Nieuwenhuis, S. (2004b). The role of the medial frontal cortex in cognitive control. *Science*, *306*(5695), 443–447.

Rivest, F., & Bengio, Y. (2011). Adaptive Drift-Diffusion Process to Learn Time Intervals. Retrieved from http://arxiv.org/abs/1103.2382

Robertson, I. H., Manly, T., Andrade, J., Baddeley, B. T., & Yiend, J. (1997). Oops!': performance correlates of everyday attentional failures in traumatic brain injured and normal subjects. *Neuropsychologia*, *35*(6), 747–758.

Rohenkohl, G., & Nobre, A. C. (2011). Alpha Oscillations Related to Anticipatory Attention Follow Temporal Expectations. *The Journal of Neuroscience: The Official Journal of the Society for Neuroscience*, *31*(40), 14076–14084.

Roitman, J. D., & Shadlen, M. N. (2002). Response of neurons in the lateral intraparietal area during a combined visual discrimination reaction time task. *The Journal of Neuroscience: The Official Journal of the Society for Neuroscience*, *22*(21), 9475–9489.

Ronconi, L., & Melcher, D. (2017). The Role of Oscillatory Phase in Determining the Temporal Organization of Perception: Evidence from Sensory Entrainment. *The Journal of Neuroscience: The Official Journal of the Society for Neuroscience*, *37*(44), 10636–10644.

Rushworth, M. F. S., Buckley, M. J., Behrens, T. E. J., Walton, M. E., & Bannerman, D. M. (2007). Functional organization of the medial frontal cortex. *Current Opinion in Neurobiology*, *17*(2), 220–227.

Rushworth, M. F. S., Walton, M. E., Kennerley, S. W., & Bannerman, D. M. (2004). Action sets and decisions in the medial frontal cortex. *Trends in Cognitive Sciences*, *8*(9), 410–417.

Ruzzoli, M., Torralba, M., Morís Fernández, L., & Soto-Faraco, S. (2019). The relevance of alpha phase in human perception. *Cortex; a Journal Devoted to the Study of the Nervous System and Behavior*, *120*, 249–268.

Samaha, J., Bauer, P., Cimaroli, S., & Postle, B. R. (2015). Top-down control of the phase of alpha-band oscillations as a mechanism for temporal prediction. *Proceedings of the National Academy of Sciences of the United States of America*, *112*(27), 8439–8444.

Samaha, J., & Postle, B. R. (2015). The Speed of Alpha-Band Oscillations Predicts the Temporal Resolution of Visual Perception. *Current Biology: CB*, *25*(22), 2985–2990.

Sauseng, P., Klimesch, W., Heise, K. F., Gruber, W. R., Holz, E., Karim, A. A., … Hummel, F. C. (2009). Brain oscillatory substrates of visual short-term memory capacity. *Current Biology: CB*, *19*(21), 1846–1852.

Savitzky, A., & Golay, M. J. E. (1964). Smoothing and Differentiation of Data by Simplified Least Squares Procedures. *Analytical Chemistry*, *36*(8), 1627–1639.

Schafer, R. W., & Others. (2011). What is a Savitzky-Golay filter. *IEEE Signal Processing Magazine*, *28*(4), 111–117.

Schalk, G. (2015). A general framework for dynamic cortical function: the function-through-biased-oscillations (FBO) hypothesis. *Frontiers in Human Neuroscience*, *9*. https://doi.org/10.3389/fnhum.2015.00352

Schlichting, N., de Jong, R., & van Rijn, H. (2018). Performance-informed EEG analysis reveals mixed evidence for EEG signatures unique to the processing of time. *Psychological Research*. https://doi.org/10.1007/s00426-018-1039-y

Schroder, H. S., Nickels, S., Cardenas, E., Breiger, M., Perlo, S., & Pizzagalli, D. A. (2019). Optimizing assessments of post-error slowing: A neurobehavioral investigation of a flanker task. *Psychophysiology*, *5*, 141.

Schulz, K. P., Fan, J., Magidina, O., Marks, D. J., Hahn, B., & Halperin, J. M. (2007). Does the emotional go/no-go task really measure behavioral inhibition? Convergence with

measures on a non-emotional analog. *Archives of Clinical Neuropsychology: The Official Journal of the National Academy of Neuropsychologists*, *22*(2), 151–160.

Schwartze, M., Rothermich, K., & Kotz, S. A. (2012). Functional dissociation of pre-SMA and SMA-proper in temporal processing. *NeuroImage*, *60*(1), 290–298.

Shenhav, A., Botvinick, M. M., & Cohen, J. D. (2013). The expected value of control: an integrative theory of anterior cingulate cortex function. *Neuron*, *79*(2), 217–240.

Simen, P., Balci, F., de Souza, L., Cohen, J. D., & Holmes, P. (2011). A model of interval timing by neural integration. *The Journal of Neuroscience: The Official Journal of the Society for Neuroscience*, *31*(25), 9238–9253.

Simen, P., Rivest, F., Ludvig, E. A., Balci, F., & Killeen, P. (2013). Timescale Invariance in the Pacemaker-Accumulator Family of Timing Models. *Timing & Time Perception*, *1*(2), 159–188.

Smith, P. L., Ratcliff, R., & McKoon, G. (2014). The diffusion model is not a deterministic growth model: comment on Jones and Dzhafarov (2014). *Psychological Review*, *121*(4), 679–688.

Solís-Vivanco, R., Jensen, O., & Bonnefond, M. (2018). Top-Down Control of Alpha Phase Adjustment in Anticipation of Temporally Predictable Visual Stimuli. *Journal of Cognitive Neuroscience*, *30*(8), 1157–1169.

Staddon, J. E. R., & Higa, J. J. (1999). Time and memory: Towards a pacemaker-free theory of interval timing. *Journal of the Experimental Analysis of Behavior*, *71*(2), 215–251.

Stam, C. J., Nolte, G., & Daffertshofer, A. (2007). Phase lag index: assessment of functional connectivity from multi channel EEG and MEG with diminished bias from common sources. *Human Brain Mapping*, *28*(11), 1178–1193.

Stanislaw, H., & Todorov, N. (1999). Calculation of signal detection theory measures. *Behavior Research Methods, Instruments, & Computers: A Journal of the Psychonomic Society, Inc*, *31*(1), 137–149.

Stevens, M. C., Kiehl, K. A., Pearlson, G., & Calhoun, V. D. (2007). Functional neural circuits for mental timekeeping. *Human Brain Mapping*, *28*(5), 394–408.

Surwillo, W. W. (1961). Frequency of the "alpha"rhythm, reaction time and age. *Nature*, *191*(4790), 823–824.

Surwillo, W. W. (1966a). On the relation of latency of alpha attenuation to alpha rhythm frequency and the influence of age. *Electroencephalography and Clinical Neurophysiology*, *20*(2), 129–132.

Surwillo, W. W. (1966b). Time perception and the "internal clock": some observations on the role of the electroencephalogram. *Brain Research*, *2*(4), 390–392.

Tracy, J. I., Monaco, C., McMichael, H., Tyson, K., Chambliss, C., Christensen, H. L., & Celenza, M. A. (1998). Information-processing characteristics of explicit time estimation by patients with schizophrenia and normal controls. *Perceptual and Motor Skills*, *86*(2), 515–526.

Treisman, M. (1963). Temporal discrimination and the indifference interval: Implications for a model of the" internal clock." *Psychological Monographs: General and Applied*, 77(13), 1.

Treisman, M. (1984). Temporal rhythms and cerebral rhythms. *Annals of the New York Academy of Sciences*, *423*, 542–565.

Treisman, M. (2013). The Information-Processing Model of Timing (Treisman, 1963): Its Sources and Further Development. *Timing & Time Perception*, *1*(2), 131–158.

Treisman, M., Cook, N., Naish, P. L., & MacCrone, J. K. (1994). The internal clock: electroencephalographic evidence for oscillatory processes underlying time perception. *The Quarterly Journal of Experimental Psychology. A, Human Experimental Psychology*, *47*(2), 241–289.

Trillenberg, P., Verleger, R., Wascher, E., Wauschkuhn, B., & Wessel, K. (2000). CNV and temporal uncertainty with "ageing"and "non-ageing"S1--S2 intervals. *Clinical Neurophysiology: Official Journal of the International Federation of Clinical Neurophysiology*, *111*(7), 1216–1226.

Tsujimoto, T., Shimazu, H., & Isomura, Y. (2006). Direct recording of theta oscillations in primate prefrontal and anterior cingulate cortices. *Journal of Neurophysiology*, *95*(5), 2987–3000.

Turek, F. W. (1985). Circadian neural rhythms in mammals. *Annual Review of Physiology*, *47*, 49–64.

Twomey, D. M., Murphy, P. R., Kelly, S. P., & O'Connell, R. G. (2015). The classic P300 encodes a build-to-threshold decision variable. *The European Journal of Neuroscience*, *42*(1), 1636–1643.

Ullsperger, M. (2010). Genetic association studies of performance monitoring and learning from feedback: the role of dopamine and serotonin. *Neuroscience and Biobehavioral Reviews*, *34*(5), 649–659.

Ullsperger, M., Danielmeier, C., & Jocham, G. (2014). Neurophysiology of performance monitoring and adaptive behavior. *Physiological Reviews*, *94*(1), 35–79.

Ulrich, R., Mattes, S., & Miller, J. (1999). Donders's assumption of pure insertion: an evaluation on the basis of response dynamics. *Acta Psychologica*, *102*(1), 43–76.

Usher, M., & McClelland, J. L. (2001). The time course of perceptual choice: the leaky, competing accumulator model. *Psychological Review*, *108*(3), 550–592.

Üstün, S., Kale, E. H., & Çiçek, M. (2017). Neural Networks for Time Perception and Working Memory. *Frontiers in Human Neuroscience*, *11*, 83.

Valadez, E. A., & Simons, R. F. (2018). The power of frontal midline theta and post-error slowing to predict performance recovery: Evidence for compensatory mechanisms. *Psychophysiology*, *55*(4). https://doi.org/10.1111/psyp.13010

van den Brink, R. L., Wynn, S. C., & Nieuwenhuis, S. (2014). Post-error slowing as a consequence of disturbed low-frequency oscillatory phase entrainment. *The Journal of Neuroscience: The Official Journal of the Society for Neuroscience*, *34*(33), 11096–11105.

van den Broek, S. P., Reinders, F., Donderwinkel, M., & Peters, M. J. (1998). Volume conduction effects in EEG and MEG. *Electroencephalography and Clinical Neurophysiology*, *106*(6), 522–534.

van Diepen, R. M., Cohen, M. X., Denys, D., & Mazaheri, A. (2015). Attention and temporal expectations modulate power, not phase, of ongoing alpha oscillations. *Journal of Cognitive Neuroscience*, *27*(8), 1573–1586.

van Dijk, H., Schoffelen, J.-M., Oostenveld, R., & Jensen, O. (2008). Prestimulus oscillatory activity in the alpha band predicts visual discrimination ability. *The Journal of Neuroscience: The Official Journal of the Society for Neuroscience*, *28*(8), 1816–1823.

van Dijk, H., van der Werf, J., Mazaheri, A., Medendorp, W. P., & Jensen, O. (2010). Modulations in oscillatory activity with amplitude asymmetry can produce cognitively relevant event-related responses. *Proceedings of the National Academy of Sciences of the United States of America*, *107*(2), 900–905.

van Driel, J., Ridderinkhof, K. R., & Cohen, M. X. (2012). Not all errors are alike: theta and alpha EEG dynamics relate to differences in error-processing dynamics. *The Journal of Neuroscience: The Official Journal of the Society for Neuroscience*, *32*(47), 16795–16806.

van Rijn, H., Kononowicz, T. W., Meck, W. H., Ng, K. K., & Penney, T. B. (2011). Contingent negative variation and its relation to time estimation: a theoretical evaluation. *Frontiers in Integrative Neuroscience*, *5*, 91.

van Vugt, M. K., Beulen, M. A., & Taatgen, N. A. (2019). Relation between centro-parietal positivity and diffusion model parameters in both perceptual and memory-based decision making. *Brain Research*, *1715*, 1–12.

van Vugt, M. K., Simen, P., Nystrom, L. E., Holmes, P., & Cohen, J. D. (2012). EEG oscillations reveal neural correlates of evidence accumulation. *Frontiers in Neuroscience*, *6*, 106.

VanRullen, R. (2016). Perceptual Cycles. *Trends in Cognitive Sciences*, *20*(10), 723–735.

VanRullen, R. (2018). [Review of *Attention Cycles*]. *Neuron*, *99*(4), 632–634. Elsevier.

VanRullen, R., Carlson, T., & Cavanagh, P. (2007). The blinking spotlight of attention. *Proceedings of the National Academy of Sciences of the United States of America*, *104*(49), 19204–19209.

Vanrullen, R., & Dubois, J. (2011). The psychophysics of brain rhythms. *Frontiers in Psychology*, *2*, 203.

VanRullen, R., & Koch, C. (2003). Is perception discrete or continuous? *Trends in Cognitive Sciences*, *7*(5), 207–213.

VanRullen, R., & Thorpe, S. J. (2001). The time course of visual processing: from early perception to decision-making. *Journal of Cognitive Neuroscience*, *13*(4), 454–461.

Verleger, R., Wascher, E., Arolt, V., Daase, C., Strohm, A., & Kömpf, D. (1999). Slow EEG potentials (contingent negative variation and post-imperative negative variation) in schizophrenia: their association to the present state and to Parkinsonian medication

effects. *Clinical Neurophysiology: Official Journal of the International Federation of Clinical Neurophysiology*, *110*(7), 1175–1192.

Vinck, M., Oostenveld, R., van Wingerden, M., Battaglia, F., & Pennartz, C. M. A. (2011). An improved index of phase-synchronization for electrophysiological data in the presence of volume-conduction, noise and sample-size bias. *NeuroImage*, *55*(4), 1548–1565.

Wagenmakers, E.-J., Steyvers, M., Raaijmakers, J. G. W., Shiffrin, R. M., van Rijn, H., & Zeelenberg, R. (2004). A model for evidence accumulation in the lexical decision task. *Cognitive Psychology*, *48*(3), 332–367.

WALTER, & G, W. (1964). Contingent negative variation : an electric sign of sensori-motor association and expectancy in the human brain. *Nature*, *230*, 380–384.

Wearden, J. H. (1999). "Beyond the fields we know...": exploring and developing scalar timing theory. *Behavioural Processes*, *45*(1), 3–21.

Weisz, N., Hartmann, T., Müller, N., Lorenz, I., & Obleser, J. (2011). Alpha rhythms in audition: cognitive and clinical perspectives. *Frontiers in Psychology*, *2*, 73.

Werboff, J. (1962). Time judgment as a function of electroencephalographic activity. *Experimental Neurology*, *6*, 152–160.

Wessel, J. R. (2018). Prepotent motor activity and inhibitory control demands in different variants of the go/no-go paradigm. *Psychophysiology*, *55*(3). https://doi.org/10.1111/psyp.12871

White, P. A. (2018). Is conscious perception a series of discrete temporal frames? *Consciousness and Cognition*, *60*, 98–126.

Wiemers, E. A., & Redick, T. S. (2019). The influence of thought probes on performance: Does the mind wander more if you ask it? *Psychonomic Bulletin & Review*, *26*(1), 367–373.

Wiener, M., Kliot, D., Turkeltaub, P. E., Hamilton, R. H., Wolk, D. A., & Coslett, H. B. (2012). Parietal influence on temporal encoding indexed by simultaneous transcranial magnetic stimulation and electroencephalography. *The Journal of Neuroscience: The Official Journal of the Society for Neuroscience*, *32*(35), 12258–12267.

Wiener, M., Parikh, A., Krakow, A., & Coslett, H. B. (2018). An Intrinsic Role of Beta Oscillations in Memory for Time Estimation. *Scientific Reports*, *8*(1), 7992.

Wong, A. S. W., Cooper, P. S., Conley, A. C., McKewen, M., Fulham, W. R., Michie, P. T., & Karayanidis, F. (2018). Event-Related Potential Responses to Task Switching Are Sensitive to Choice of Spatial Filter. *Frontiers in Neuroscience*, *12*, 143.

Woodruff, D. S. (1975). Relationships among EEG alpha frequency, reaction time, and age: a biofeedback study. *Psychophysiology*, *12*(6), 673–681.

Wyart, V., de Gardelle, V., Scholl, J., & Summerfield, C. (2012). Rhythmic fluctuations in evidence accumulation during decision making in the human brain. *Neuron*, *76*(4), 847–858.

Xu, M., Zhang, S.-Y., Dan, Y., & Poo, M.-M. (2014). Representation of interval timing by temporally scalable firing patterns in rat prefrontal cortex. *Proceedings of the National Academy of Sciences of the United States of America*, *111*(1), 480–485.

Young, M. E., Sutherland, S. C., & McCoy, A. W. (2018). Optimal go/no-go ratios to maximize false alarms. *Behavior Research Methods*, *50*(3), 1020–1029.

Zakay, D., & Block, R. A. (1996). The role of attention in time estimation processes. In M. A. Pastor & J. Artieda (Eds.), *Advances in Psychology* (Vol. 115, pp. 143–164). North-Holland.

Zakay, D., & Block, R. A. (2004). Prospective and retrospective duration judgments: an executive-control perspective. *Acta Neurobiologiae Experimentalis*, *64*(3), 319–328.

Zumer, J. M., Scheeringa, R., Schoffelen, J.-M., Norris, D. G., & Jensen, O. (2014). Occipital alpha activity during stimulus processing gates the information flow to object-selective cortex. *PLoS Biology*, *12*(10), e1001965.